EXPERIMENTAL INVESTIGATION INTO ELECTROCHEMICAL DISCHARGE MICRO-GROOVING ON GLASS

Thesis submitted
by

MD NIAMOT ALI

DOCTOR OF PHILOSOPHY (ENGINEERING)

DEPARTMENT OF PRODUCTION ENGINEERING
FACULTY COUNCIL OF ENGINEERING & TECHNOLOGY
JADAVPUR UNIVERSITY
KOLKATA-700032
INDIA

2025

JADAVPUR UNIVERSITY

KOLKATA-700032

Index No. 15/18/E

Registration No. 1021816008

TITLE OF THE Ph. D. (Engg.) THESIS:

Experimental Investigation into Electrochemical Discharge Micro-Grooving on Glass

NAME, DESIGNATION & INSTITUTION OF THE SUPERVISORS:

DR. BISWANATH DOLOI
Professor,
Department of Production Engineering,
Jadavpur University,
Kolkata-700032, India.

DR. BIPLAB RANJAN SARKAR
Professor,
Department of Production Engineering,
Jadavpur University,
Kolkata-700032, India.

LIST OF PUBLICATIONS

International Journal:

1. Ali, M.N., Sarkar, B.R., Doloi, B., Bhattacharyya, B., (2023). Micro-Channel Cutting on Glass in Electrochemical Discharge Machining Process Using Different Electrolytes and Tool Polarity. ASME Journal of Micro & Nano-Manufacturing Vol. 11/031002 pp.1-14 Doi:10.1115/1.4065326, (Web of Science. Scopus Indexed)

International Proceedings Journal:

1. Ali, M.N., Sarkar, B.R., Doloi, B., (2019), Electrochemical Discharge Machining Technology applied for Turning Operation. IOP Conference Series: Materials Science and Engineering 653(1), 012029. Doi:10.1088/1757-899X/653/1/012029, (Scopus Indexed)

International Conferences:

(i) Ali, M.N., Sarkar, B.R., Doloi, B., Bhattacharyya B. (2024) "Experimental Investigation on electrochemical discharge micro-grooving of glass "presented in 13th International Conference on Precision, Meso, Micro and Nano Engineering, (COPEN 13), organised by NIT Calicut during December 13-15, 2024.

(ii) Santra, S., Singh, D.P., Ali, M.N., Doloi, B., Sarkar, B.R., "Experimental Investigation into Electrochemical Discharge Turning of Cylindrical Glass", presented in 9th International and 30th All India Manufacturing Technology, Design and Research Conference (AIMTDR 2023) organised by IIT BHU, Varanasi, India during December 08-10, 2023 and published in Advances and Futuristic Trends in Machining Volume-I, Lecture Notes in Mechanical Engineering, AIMTDR-2023.

(iii) Ali, M.N., Sarkar, B.R., Doloi, B., (2019) "Electrochemical Discharge Machining Technology applied for Turning Operation" presented in International Conference on Advances in Materials and Manufacturing Engineering (ICAMME 2019), organised by KIIT, Bhubaneshwar during March 15- 17, 2019.

PROFORMA-1

"Statement of Originality"

I, Md Niamot Ali registered on 7th June, 2018 do hereby declare that this thesis entitled "**EXPERIMENTAL INVESTIGATION INTO ELECTROCHEMICAL DISCHARGE MICRO-GROOVING ON GLASS**" contains literature survey and original research work done by the undersigned candidate as part of Doctoral studies.

All information in this thesis have been obtained and presented in accordance with existing academic rules and ethical conduct. I declare that, as required by these rules and conduct, I have fully cited and referred all materials and results that are not original to this work.

I also declare that I have checked this thesis as per the "Policy on Anti Plagiarism, Jadavpur University, 2019", and the level of similarity as checked by iThenticate software is 6%

Md. Niamot Ali

Signature of Candidate:

Date: 22/05/2025

Certified by Supervisor(s): 22/05/25 22/05/25

(Signature with date, seal)

Professor
Production Engineering Department
Jadavpur University
Kolkata - 700 032

Professor
Production Engineering Department
Jadavpur University
Kolkata - 700 032

JADAVPUR UNIVERSITY

FACULTY OF ENGINEERING AND TECHNOLOGY

DEPARTMENT OF PRODUCTION ENGINEERING

CERTIFICATE FROM THE SUPERVISORS

This is to certify that the thesis entitled ***"EXPERIMENTAL INVESTIGATION INTO ELECTROCHEMICAL DISCHARGE MICRO-GROOVING ON GLASS"*** *submitted by Mr. Md Niamot Ali, who got his name registered on 7th June, 2018 for the award of Ph.D. (Engg.) degree of Jadavpur University is absolutely based upon his own work under the supervision of Prof. Biswanath Doloi and Prof. Biplab Ranjan Sarkar and that neither his thesis nor any part of the thesis has been submitted for any degree/diploma or any other academic award anywhere before.*

22/05/2025

(Signature of the Supervisor with date and official seal)

Professor
Production Engineering Department
Jadavpur University
Kolkata - 700 032

22/05/25

(Signature of the Supervisor with date and official seal)

Professor
Production Engineering Department
Jadavpur University
Kolkata - 700 032

ACKNOWLEDGEMENT

The insight presented in this thesis is undoubtedly a result of the contributions made by numerous outstanding individuals. The author expresses sincere gratitude to the Ph.D. (Engg.) thesis supervisors, Dr. Biswanath Doloi, Professor and Dr. Biplab Ranjan Sarkar, Professor in the Production Engineering Department at Jadavpur University, Kolkata for their unwavering guidance, helpful suggestions, continuous association, support, encouragement, and valuable advice throughout every stage of this research work. The author recognizes that without constructive and timely advice of supervisors, the thesis would not have progressed as smoothly as it did.

The author also extends appreciation for the cooperation and encouragement received from Dr. Bijoy Bhattacharyya, Dr. Shankar Chakrabarty, and the Head of the Department, Dr. Bijan Sarkar and all the faculty members of the Production Engineering Department at Jadavpur University during the research work. Special thanks go to Mr. Bishwajit Pathak and other technical staff of our department for their consistent support during my research work.

The author expresses gratitude to fellow colleagues, Mr. Sudip Santra, Dr. Mohit Pandey, Dr. Bijan Mallick, Dr. Santosh Kumar, Dr. Himadri Sekhar Panda, Mr. Arindam Maity, Mr. Dwarika Pratap Singh, Mr. Kailash Roy and existing research scholars for their constant cooperation, useful assistance, and support during the research work. Special thanks are extended to the FET office and Research section for their cordial assistance and administrative support. The author gratefully acknowledges the co-operation and encouragement received from all the faculty members and staff members of Production Engineering Department, Jadavpur University for carrying out research work successfully.

Md. Niamot Ali

Md Niamot Ali

PREFACE

The limitations of conventional machining process in the area of complex shapes, miniature sizes, three dimensional (3D) complex parts and the need of machining of brittle harder and newer materials lead to the development and establishment of non-conventional machining processes in the industry as efficient and economic alternatives to conventional machining processes. Demand and need of research in these areas are also growing to develop precise understanding and knowledge of different aspects. The fast-paced development of advanced manufacturing technology requires the creation of innovative machining processes that can satisfy the high precision and efficiency requirements of numerous industries. Recently, micromachining and nano-finishing has gained an importance as reduction of workpiece size and dimensions to cover the miniaturization of components. Micro-grooving on electrically non-conducting materials with electrochemical discharge micro-grooving (μ-ECDG) process has drawn a momentous attention in manufacturing field as compared to other existing non-traditional machining processes.

Micro-grooving on glass with conventional methods can induce mechanical stresses that may lead to cracks or fractures. Some non-conventional processes like ECM (Electrochemical Machining) and EDM (Electrical Discharge Machining) are also ineffective to machined glass material as it a non-conductive material. But μ-ECDG avoids direct mechanical contact between the tool and the glass, reducing the risk of damage and allowing for smoother grooving, especially on delicate or thin glass components. This operation offers high precision, control, and the ability to create specific geometries like narrow and shallow channels and this process is more suitable for applications involving microfabrication, microfluidics, optics, and electronic components, where precise and delicate features are required. This process provides the control needed to achieve those dimensions with high accuracy. Electrochemical Discharge micro-Grooving (μ-ECDG) is a newly developed machining process that can be used for grooving and micro-profile generation of any hard and brittle, electrically non-conducting material of cylindrical shape. μ-ECDG is a hybrid machining process that effectively combines the fundamentals of ECM and EDM to achieve precise and excellent surface quality. The fundamental concept of μ-ECDG process is similar to the Electrochemical Discharge Machining (ECDM) process. In this process, two forms of energy namely chemical and thermal are utilised with the continuous rotation of workpieces.

In μ-ECDG process, workpiece is rotated with an angular speed against a micro-tool which is fitted to a XZ stage. Both longitudinal and cross feed can be given to tool by means of a spring feed mechanism.

While electrochemical discharge machining has been widely explored in various research domains, its application for micro-level grooving on non-conducting materials remains limited. There is a strong need for in-depth studies and experimental investigations into the micromachining process, particularly focusing on electrochemical discharge micro-grooving of different engineering materials. Significant research efforts and technical advancements are required to enhance this technology, making it more efficient and widely accepted for successful integration into modern micro-manufacturing industries.

The thesis is systematically divided into six chapters, with a brief summary of each chapter given below:

Chapter 1 provides an overview of electrochemical discharge micro-machining processes, highlighting the importance of micro-grooving and explaining the basic principles of electrochemical discharge micro-grooving. It outlines the applications of this technology in various engineering fields and discusses both the mechanisms of material removal and tool wear. Additionally, this chapter includes a literature review of previous research in the field, covering recent developments in electrochemical discharge micro-machining. The chapter also outlines different approaches suggested by researchers to improve the effectiveness and output of this process.

Chapter 2 focuses on design and development of the electrochemical discharge micro-grooving setup, along with its various subsystems. It discusses two different types of setups used for micro-grooving operations on cylindrical and flat surfaces. It highlights about the power supply and specifications of the newly developed experimental setup.

Chapter 3 highlights the materials and methods used in this research. It discusses the selection of all input parameters including their maximum and minimum ranges as well as the choice of different machining characteristics such as MRR, Width of Groove (WG), Depth of Groove (DG) etc. The chapter also explains how the responses are measured. It outlines the detailed criteria for selecting workpiece and tool electrode materials. Various experimental design methods, such as One Factor at a Time (OFAT) and Response Surface Methodology (RSM) along with their respective input parameter settings are presented here.

Chapter 4 presents the experimental investigation of producing micro-grooves on the flat surface of glass materials using the μ-ECDG process. It discusses the experimental conditions including variations in different parametric settings and presents the corresponding outcomes. A detailed analysis of how different process variables affect the results is provided with the help of graphs and photographic views. SEM images of the micro-grooves are also analyzed and the findings are presented in this chapter.

Chapter 5 highlights the experimental investigation of producing micro-grooves on the cylindrical surface of glass materials. This chapter includes the analysis of experimental result based on OFAT and RSM method. The outcomes are examined based on graph and photographic view obtained using Leica microscope. Mathematical model and ANOVA test for all the responses have been presented in this chapter.2D contour plot and 3D surface plot have been generated to study the effects of various process parameters on responses. Both single-objective and multi-objective optimization of responses have been carried out to determine the optimal set of process variables that produce the best possible response values.

Chapter 6 presents the general conclusions drawn based on the results and discussions derived from various experiments conducted throughout the study. It provides a comprehensive overview of the main findings and emphasizing how various process parameters affect the machining performance and micro-groove quality on both flat and cylindrical surface. Finally, suggestions for future scopes of research work are also included in this chapter.

VITA

The author, Md Niamot Ali, son of Md Kajem Ali and Sabila Bibi, was born on December 20, 1988 in Birbhum, West Bengal. He passed the Secondary Examination from Santoshpur J.M. Vidyapith under WBBSE and Higher Secondary Examination from Rampurhat High School under WBCHSE, both with a first division.

The author was graduated with Production Engineering degree in the year 2012 from Jadavpur University, Kolkata, West Bengal with First class. The author qualified GATE (Graduate Aptitude Test in Engineering) and received AICTE approved post graduate fellowship for a period of two years i.e. 2012-2014. The author completed his M.E. in Production Engineering in the year 2014 from Production Engineering Department, Jadavpur University, Kolkata. The author has published two research papers in international journals and presented two research papers in reputed international conference to advance micro-machining process during his tenure of research in Production Engineering Department, Jadavpur University. The author is currently affiliated as a lecturer in Mechanical Engineering Department at Kaliachak Govt. Polytechnic.

Dedicated to my parents and teachers, who have been my pillars of strength and unwavering sources of inspiration, providing endless love, support, and encouragement.

TABLE OF CONTENTS

LIST OF THE FIGURES

LIST OF THE TABLE

CHAPTER 1: INTRODUCTION

1.1 INTRODUCTION

The limitations of conventional machining in handling complex shapes, miniature sizes, and hard or brittle materials have led to the rise of nonconventional machining processes. These advanced techniques use mechanical, electrical, chemical, thermal, or hybrid energy sources to achieve precise material removal. Nonconventional machining is essential for industries like aerospace, biomedical, and electronics, where high precision and intricate geometries are required. The growing need for micromachining and nano-machining has further driven research and innovation in this field. As manufacturing demands become more complex, these methods have become indispensable in modern industrial applications. There is a growing demand for research focused on the production of miniature components, complex 3D parts, and the machining of advanced hard and brittle materials, as well as newly developed materials, to gain a deeper understanding of their various aspects. The newest manufacturing technology requires the creation of innovative machining techniques that can satisfy the high precision and efficiency requirements of several industries. Recently, micromachining and nano-finishing has gained an importance as reduction of workpiece size and dimensions to cover the miniaturization of components. Micromachining on electrically non-conducting materials has drawn a momentous attention in manufacturing sector. Electrochemical discharge micro-grooving (μ-ECDG) is one such hybrid machining technique that can be used for creating micro-grooves and micro-channels on glass. Conventional methods are unsuitable for this purpose, as they can induce mechanical stresses, potentially leading to cracks or fractures. This method avoids direct mechanical contact between the tool and the glass, reducing the risk of damage and allowing for smoother grooving, especially on delicate or thin glass components. This newly developed technique offers high precision, control, and the ability to create specific geometries like narrow and shallow channels where precise and delicate features are required. The core principle of the μ-ECDG technique is comparable to that of Electrochemical Discharge Machining (ECDM) process. This method combines chemical and thermal energy sources to remove materials from the continuously rotating workpieces. During the μ-ECDG operation, the workpiece rotates at an angular velocity against a micro-tool attached to an XZ stage. The tool can be moved both longitudinally and laterally using a spring feed mechanism.

1.2 NEED OF ELECTROCHEMICAL DISCHARGE MICRO-GROOVING (μ-ECDG) PROCESS

The μ-ECDG process is essential for creating intricate micro-grooves in hard, brittle, and non-conductive materials such as glass and ceramics, which are difficult to machine using conventional methods. By combining electrochemical and thermal energy, μ-ECDG enables precise material removal while mechanical stress. This process is particularly important for applications in microfluidics, biomedical devices, and electronics, where high precision and complex microstructures are in demand.

i. μ-ECDG process is especially beneficial for machining non-conductive materials such as ceramics, glass, quartz, and composites, which are generally difficult to machine using conventional methods.

ii. Micro-grooving on glass material with traditional techniques can lead to mechanical stresses, potentially causing cracks or breakage. Due to its non-conductive nature, glass cannot be effectively machined by unconventional methods like ECM or EDM. However, the μ-ECDG process avoids direct mechanical contact with the glass, reducing the risk of damage and allowing for smoother grooving, especially on thin or fragile glass pieces.

iii. In certain applications, μ-ECDG is a more economical choice due to its lower tool wear and energy consumption when compared to other thermal-based processes like laser machining or EDM process.

iv. μ-ECDG process has potential for producing microstructures like micro-channels, micro-grooves, and holes. Micro-grooving is particularly well-suited for microfabrication, microfluidics, optics, electronic components, and MEMS (Micro-Electro-Mechanical Systems) applications, where precise, delicate features are needed. This process provides high accuracy, control, and the ability to create specific geometries, such as narrow and shallow channels.

v. Micro-grooves created by μ-ECDG process can improve the surface texture of a component, enhancing its performance. For example, these grooves can be designed to optimize fluid flow.

1.3 FUNDAMENTALS OF ELECTROCHEMICAL DISCHARGE MICRO-GROOVING (μ-ECDG) PROCESS

The μ-ECDG method has several variations that are intended to solve distinct machining problems and enhance productivity, precision, or flexibility for diverse materials and applications. These processes differ in their specific setups, electrode layouts, and operational parameters. μ-ECDG processes are adaptable and beneficial for manufacturing hard-to-machine and intricate materials in a range of industries, addressing specific machining requirements. This process can be applied for machining of both flat and cylindrical surfaces

1.3.1 Electrochemical Discharge Micro-Grooving on Flat Surface

Electrochemical Discharge Micro-Grooving (μ-ECDG) is an advanced machining process designed to efficiently machine hard and brittle materials that are difficult to machine with conventional turning techniques. This process combines ECM and EDM processes, making it a versatile option for various applications. μ-ECDG integrates the material removal mechanisms of electrochemical dissolution, electrical discharge erosion, and mechanical turning, making it a more complex setup than traditional turning operations. Fig.1.1 shows the schematic diagram of μ-ECDG setup used for micro-grooving on any flat surface. To achieve consistent performance, proper control of electrical parameters such as voltage, current, and pulse duration, electrolyte flow, and tool feed is necessary. Like other electrochemical processes, the electrolyte flow and its concentration must be carefully varied in order to achieve higher efficiency and effectiveness of the material removal process. This variant is highly specialized technique that holds great promise for complex geometries and demanding precision requirements. As research and development in μ-ECDG progress, its capabilities are expected to expand, opening up a wider array of industrial applications.

.

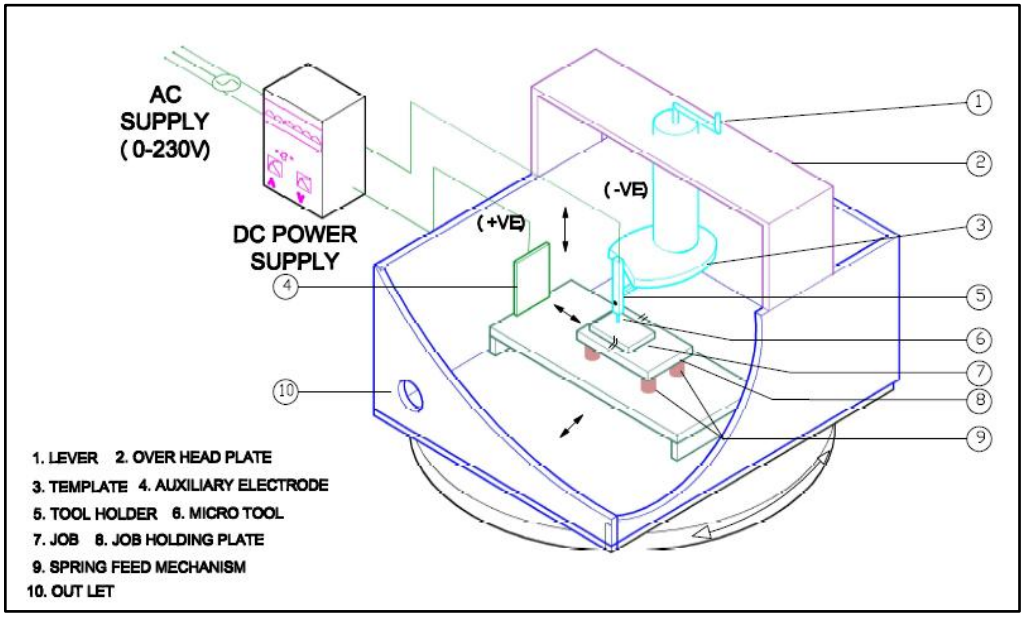

Fig. 1.1 Schematic diagram of μ-ECDG setup used for flat surface

1.3.2 Electrochemical Discharge Micro-Grooving on Cylindrical Surface

The newest manufacturing technology requires the creation of innovative machining technique that can satisfy the high precision and efficiency requirements of several industries. Electrochemical discharge micro-grooving (μ-ECDG) is one such hybrid machining technique that can be used for creating micro-grooves and micro-profiles on any cylindrical shape workpieces. Conventional methods are unsuitable for this purpose, as they can induce mechanical stresses, potentially leading to cracks or fractures. This method avoids direct mechanical contact between the tool and the glass, reducing the risk of damage and allowing for generation of micro-grooves, especially on delicate cylindrical glass components. This electrochemical discharge micro-grooving system offers high precision, control, and the ability to create specific geometries like narrow and shallow micro-grooves on glass. During the μ-ECDG operation on cylindrical surface of workpieces rotates at different RPM. The micro-tool can be moved both longitudinally and laterally using a spring feed mechanism.

.

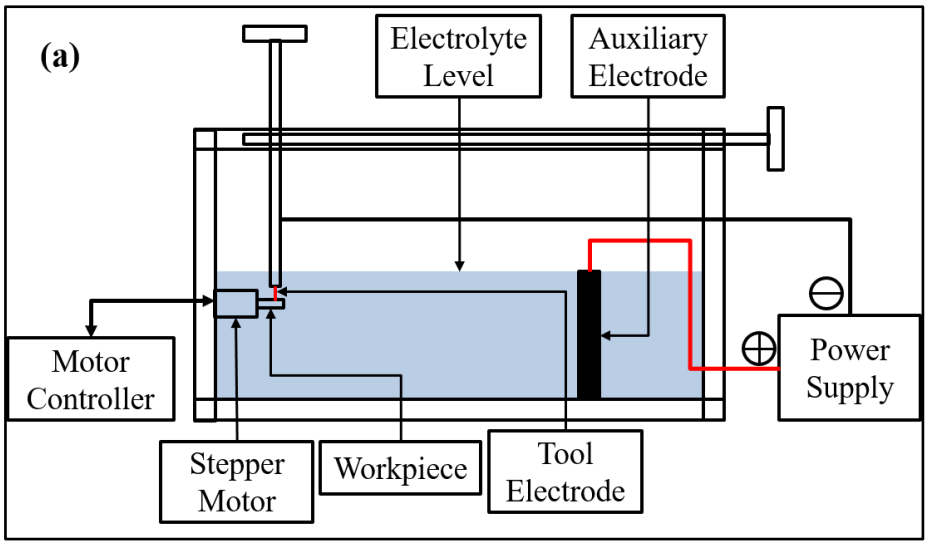

Fig. 1.2 Schematic diagram of μ-ECDG setup used for cylindrical surface

1.4 MATERIAL REMOVAL MECHANISM OF μ-ECDG PROCESS

Electrochemical Discharge Micro-Grooving (μ-ECDG) is a machining process that can be used for grooving and micro-profile generation of any hard and brittle, electrically non-conducting material of cylindrical shape. This hybrid machining process is the combination of principle of material removal mechanism of ECM and EDM to achieve precise and excellent surface quality. The fundamental concept of μ-ECDG process is similar to the ECDM process. The electrode tool typically functions as a cathode and is placed near the machining location. A DC voltage is applied to the cell, and the potential difference across the double layer triggers the electrolytic decomposition of water, resulting in H_2 evolution at the cathode and O_2 evolution at the anode. When bubble size increases, the buoyancy force surpasses the adhesive force, causing the bubbles to detach and creating a region of high current density that initiates further bubble formation. At a critical voltage (about 30 V), bubble formation occurs at a faster rate than bubble detachment, causing the bubbles to coalesce into a gas film that covers and insulates the electrode, leading to resistive or Joule heating. This heating vaporizes neighbouring water molecules, and the overheated gas film aids in current transport, resulting in electrical discharges across the gas film. The discharges, in conjunction with the Joule heating, cause intense local heating of workpiece material. In μ-ECDG process, three forms of energy namely chemical, thermal and mechanical are utilised with the continuous rotation of workpieces. When μ-ECDG process is used for machining of cylindrical workpiece, the workpiece is rotated with an angular speed against a micro-tool which is fitted to a XZ stage. Both longitudinal and cross feed can be given to tool by means of a spring feed mechanism.

1.4.1. Bubbles Generation Mechanism

In μ-ECDG process, the gas bubbles generated during the electrochemical reaction are positively charged due to their low ionic nature. As the voltage supply increases, the formation of bubbles also increases and at a threshold voltage, sparking occurs in the gap between the tool and the workpiece within the electrolyte, which is across a layer of hydrogen or steam bubbles. The critical voltage required for sparking to begin depends on the electrolyte's conductivity and concentration, as well as the tool's geometry. A high voltage DC power supply of 30 V is applied between the tool (or cathode) and the auxiliary electrode (or anode), with the tool positioned about 2 to 3 mm below the upper level of the electrolytic solution. As soon as the proper voltage is established between the interelectrode gap of the machining zone, the distinct cathode and anode reactions occur.

Reactions at the cathode (or tool):

The usual types of reactions at the cathode are:
(i) plating of metal ions; and (ii) evolution of hydrogen gas
The reaction for metal plating is: $M^{+}+e^{-} \rightarrow M$, where M represents any anode material.
The reaction for hydrogen evolution is:
$2H^{+}+2e^{-} \rightarrow H_2$ (in acidic electrolytic solution)
$2H_2O+ 2e^{-} \rightarrow 2(OH)^{-} +H_2$(in alkaline solution)

Reaction at anode (auxiliary electrode):

There will be two types of anodic reactions: (i) dissolution of metal ions in the electrolytic solution; and (ii) evolution of oxygen gas at the auxiliary electrode surface

The anodic dissolution reaction is:

$M \rightarrow M^{+} + e^{-}$ (in acidic electrolyte solution)

The oxygen evolution reaction is:

$H_2+O \rightarrow O_2+4H^{+} +4e^{-}$ (.in acidic electrolyte solution)

$4(OH)^{-} \rightarrow 2H_2O+O_2+4e-$ (in alkaline electrolyte solution

The micro-gaps contain an electrolyte that is responsible for generating gas bubbles and steam. Specifically, the rate of hydrogen gas bubble formation is quite high in the area near the tool. When the electrolyte is heated, some of it evaporate and steam is produced.

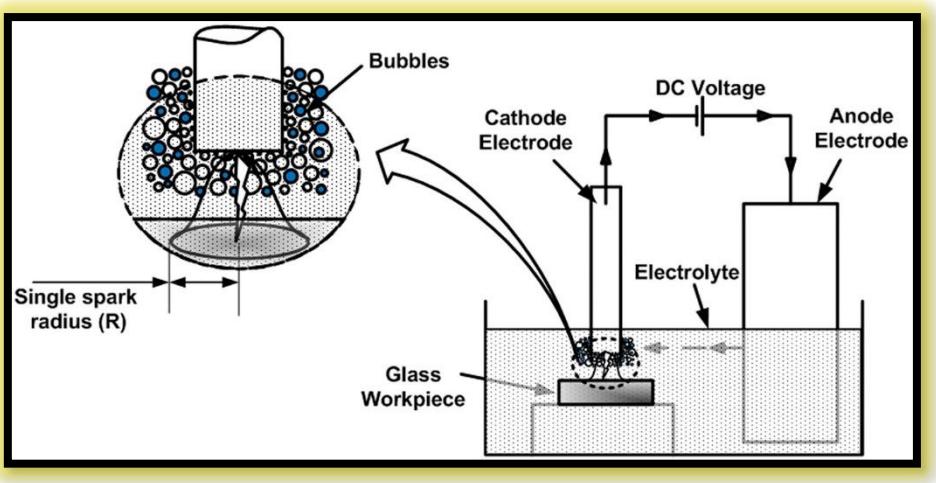

Fig.1.3 Bubble formation and sparking phenomena in µ-ECDG Process [70]

1.4.2 Spark Generation Mechanism

In the cell of µ-ECDG, electrolysis reactions are initiated when a DC voltage greater than the required threshold is applied, leading to the production of discharge and the evolution of hydrogen gas bubbles. These bubbles accumulate at the cathode tip immersed in the electrolyte. As bubble generation increases, the bubbles combine to form a single large bubble, which isolates the tip from the electrolyte. When the cathode tip is covered by a gaseous layer of hydrogen gas bubbles, a large dynamic resistance is present, and the current through the circuit becomes almost zero. This creates a local electric field gradient between the tool and the electrolyte interface, resulting in an arc discharge. At the moment of discharge, a significant number of electrons are ionized, causing them to flow towards the anode. Consequently, a large current spike flows through the highly conducting spark channel for a very short duration, typically a few milliseconds. If the voltage is increased further, violent sparking will occur. The process of spark generation, plasma channel formation and material removal is repeated several times per second, depending on the voltage, current and other process parameters. When the gap reaches the critical value, the electric field is stronger than the penetration force. The dielectric then breaks through and the spark is created. When the electrons hit the anode and the positive ions reach the cathode, their kinetic energy is converted into heat.

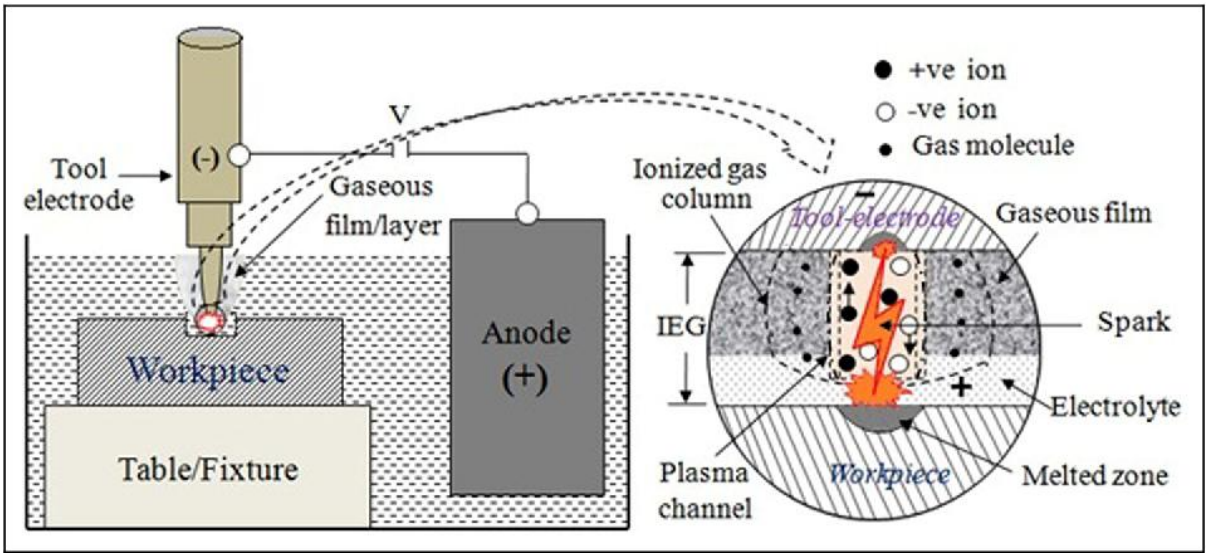

Fig.1.4 Bubble formation and sparking phenomena [71]

1.4.3 Material Removal Mechanism

It is well-known that the combination of electrochemical (EC) reaction and electrical spark discharge (ESD) is responsible for removing material from the workpiece. The EC reaction occurs at the metal-electrolyte interface and involves the transfer of ions in electrolytic solution. This process takes place through three mechanisms: (i) diffusion, (ii) migration in an electric field, and (iii) convection in the flow process. In case of auxiliary electrode, the material removal rate is quite low because only a small amount of current passes through a large inter-electrode gap in μ-ECDG process, which has a much larger inter-electrode gap compared to the electrochemical machining (ECM) process. When the voltage gradient is high enough to break down the gas bubble layer between the tool and workpiece, a conductive path is created for spark discharge due to the ionization of gas bubbles, allowing a large amount of current to flow. When an electric discharge occurs, a high-velocity and accelerated stream of electrons moves from the cathode (or tool) towards the workpiece, creating compressive shock waves on the workpiece surface. This process occurs rapidly, taking only a few microseconds and the temperature at the spot hit by the electrons can rise to a very high value. This high temperature is sufficient to melt the workpiece material. The high pressure of the compressive shock waves produces a blast, causing metallic vapors to form wear products in the shape of metallic globules, leaving craters on the workpiece surface. The rate at which material is removed from the surface of a workpiece during electrical spark discharge is proportional to the energy of the spark which is generated as heat during the machining process. Some researchers have suggested that instead of melting hard and brittle ceramics, the heat generated by the spark may

cause the material to spall due to a phenomenon known as thermal spalling. This occurs when the material is removed due to mechanical failure rather than melting. The sudden temperature change in the machining area of the ceramic material creates a complex temperature gradient, which results in internal stresses that may be sufficient to overcome the bond strength of the ceramic grains leading to mechanical erosion. Additionally, the mechanism of material removal in the μ-ECDG process is highly complex and is influenced by a variety of process parameters that are not yet fully understood by researchers. In order to achieve effective and controlled material machining, it is necessary to thoroughly investigate and optimize the dominant input variables of μ-ECDG process.

1.4.4 Tool Wear Mechanism

In μ-ECDG process, an electrically non-conducting workpiece is placed below the tool electrode and it is immersed in an electrolyte solution in the machining chamber maintaining about 2 to 3 mm above the tool tip. Due to the much smaller area of the tool electrode compared to the auxiliary electrode, electrochemical reactions cause bubbles to form around the tool, creating a bubble layer. When the voltage exceeds the breakdown voltage of the gas layer, a spark is initiated at the tool tip, emitting light and releasing heat energy. A portion of this energy is absorbed by the tool electrode through conduction heat transfer, raising the tool's temperature. If this temperature surpasses the tool material's melting point, the tool begins to melt and may even vaporize. The process of material removal from the tool is similar to the removal of material from the workpiece. If the tool's current density rises, meaning that the tool's area is smaller, then tool wear will be more significant. Additionally, if the applied voltage and electrolyte concentration are increased, tool wear will also increase.

1.5 APPLICATIONS OF μ-ECDG PROCESS

Electrochemical Discharge Micro-Grooving is a specialized machining technique that combines the principles of electrochemical machining (ECM) and electrical discharge machining (EDM) to perform grooving operations at the micro-scale level. It finds use in a variety of industries where exact machining of small components is necessary. The following are some particular uses of μ-ECDG process

i) Microfluidic Instruments:

- **Lab-on-chip instruments:** μ-ECDG is used to cut complex micro-channels and grooves in glass or polymer surfaces, which are necessary for fluid manipulation in lab-on-a-chip instruments for biological and chemical experiments.
- **Micro-mixers and Micro-pumps**: μ-ECDG is used in the fabrication of the precise channels and grooves needed in these devices to mix fluids at the micro-scale, guaranteeing precision and functioning.

ii) Bio-Medical Instruments:

- **μ-channels in Biochips:** Utilising this technology, biochips with the required channels and grooves may be made, which is essential for applications like medication administration, cell sorting, and DNA sequencing.
- **Surgical instruments and micro-implants:** By creating microscopic grooves on biocompatible materials (such as glass, ceramics etc.) used in implants and surgical equipment, μ-ECDG can enhance the functionality and performance of these devices.

iii) Optoelectronics:

- **Micro-lenses and Waveguides:** In optoelectronic devices, such as micro-lenses, optical waveguides, and other light-guiding structures, fine structuring is made possible by μ-grooves on optical materials like glass.
- **Fiber Optic Connectors:** In order to improve signal transmission and efficiency, this process can be utilised to produce exact grooves for fibre optic cables to align in connectors.

iv) MEMS:

- **Micro-sensors and Micro-actuators:** Micro-grooving is vital for the production of various Micro-Electro-Mechanical Systems (MEMS) devices as these devices require detailed microstructuring including actuators, sensors and resonators.

v) μ-machining of Glass and Ceramics:

- **Precision Engineering:** μ-ECDG process can be utilized to create fine grooves and intricate patters on ceramics material that are broadly applied in micro-engineering domains such as high-performance electronics, automotive and aerospace.
- **Glass Machining for Displays and Lenses**: This technique can be used to create the micro-grooves on glass that are utilised in optical lenses and display technologies such as smartphones, tablets and other electronic gadgets.

vi) Aerospace and Defence:

- **Precision Grooving on Hard Materials**: The process can be widely used to create fine grooves and channels on glass and ceramic materials used in aerospace parts including thermal protection systems, sensors and high-temperature parts.
- **Stealth Technology**: This process can be used to manufacture of various microgrooves and microchannel in advanced materials that absorb radar waves, contributing to stealth capabilities.

vii) Artful Engravings and Jewellery:

- **Decorative Micro-grooving:** μ-ECDG can be utilised for complex ornamental grooving on jewellery, glass ornaments, and other unique creative product imparting high accuracy with precise detailing.

viii) Photovoltaic and Solar Cells

- **Glass Structuring for Solar Panels:** μ-ECDG process can be employed to shape glass surfaces in photovoltaic cells, thereby enhancing light trapping and energy conversion efficiency.
- **Solar Power Systems:** In certain concentrated solar power systems, μ-ECDG is utilized to create precise grooves on glass reflectors or lenses, which focus sunlight onto a precise area, thereby enhancing the system's efficiency.

1.6 LITERATURE REVIEW OF PAST RESEARCH

Over the last few decades, researchers have attempted to elucidate the physical and chemical mechanisms underlying electrode electrical spark discharge in electrolyte solution. Concurrently, many scientists and production engineers have been working to address the challenges of applying the ECDM technique for grooving operations, aiming to make it viable for use in contemporary manufacturing industries. A significant number of investigators have focused on μ-ECDG process, exploring various possibilities related to micro-holes, micro-channel and micro-grooving operations. The following is a compilation of previous research investigations conducted by different researchers:

Basak and Ghosh [1] investigated the process of discharge generation during ECDM technique and found that spark discharge occurred across the gas bubble layers at the bottom edge of the smaller electrode. In order to investigate the possibilities of improving the process's capability, a basic model was developed to forecast the features of the material removal rate for changing input parameters. The critical voltage and current needed to start a discharge between the electrode and electrolyte were calculated with the aid of the model. The rate at which bubbles generated also rose, according to the observations, when the voltage between the electrode was increased. It was described that the electro discharge phenomena were due to switching process between the tool and the electrolyte. The theoretically expected values of critical voltage using a mathematical model were compared and it was found that the critical voltage was increased marginally with tool diameter.

Ghosh [2] discussed the principles and possibilities of ECDM process and stated that electric discharges were primarily occurred due to a switching phenomenon rather than gas breakdown in the blanket of gas bubble. The author explained the ECDM mechanism as an electrochemical discharge phenomenon, where a resistant layer was formed around the cathode (tool), and hydrogen evolves as fine bubbles. Discharge began when the applied voltage reached a critical level, which varied with electrolyte type and concentration. The author emphasized that blanketing, influenced by hydrogen evolution and vapor production through boiling, was vital to electrochemical discharge. By controlling the heat source, the workpiece shape can be tailored. Experimental results showed spherical bubbles covering the surface and the breakdown of the insulating layer was likened to a switching phenomenon. The process capability of ECDM was also analyzed.

Bhattacharyya *et al.* [3] investigated the effects of various process parameters including the applied voltage, the concentration and type of electrolyte and the shape, size and material of the electrodes. In ECDM process. The fundamental material removal mechanism in ECDM process was discussed for the efficient machining of non-conducting ceramic materials and it was concluded that the effect of electrical spark discharge and electrochemical reaction were responsible for the removal of the material. The rate of material removal was raised when the applied voltage was increased for varying electrolyte concentrations. It was found that over-cut was occurred more frequently at higher applied voltages for varying electrolyte concentrations due to the increased possibility of stray sparking at the tool tip's side wall. The material removal rate and over-cut criterion in ECDM process were significantly impacted by the geometry of the tool tip. It was concluded that despite the low machining rate of ceramic materials during ECDM process, the technology was more efficient in cutting non-conductive materials since it could machine intricate profiles.

Jain *et al.* [4**]** documented that the Electrochemical Spark Machining (ECSM) process can be used to machine high-strength, electrically non-conductive materials with low machinability. With the help of a developed model, experimental results were explained based on circuit and arc discharge valve characteristics. A proposed valve theory was applied to estimate the spark energy and the approximate size of hydrogen gas bubbles. The authors showed the theory's ability to model the discharge phenomenon in ECSM process. The authors attempted to determine the material removal rate by treating the problem as a 3D unsteady-state heat conduction issue. The volume of the melted material was multiplied by its density to get the amount of material taken per spark, and the isotherms at temperatures above and equal to the melting temperature were used to calculate the volume of the material. The finite element method was utilized to compute temperature distribution and also to estimate the material removal per discharge.

Kulkarni *et al.* [5] studied the fundamental mechanism of material removal in ECDM process through experimental measurements of time-varying current using copper tool as cathode and graphite plate as anode electrode. The authors analyzed the SEM images of a spot struck by a single spark to illustrate the material removal process. During this experiment, a D.C. supply voltage of 155V and an electrolyte content of 30 weight percent of HCl were maintained. It was found that near the cathode tip a high electric field of around 107 V/m was generated which created an arc discharge within the gas layers surrounding the tip. The authors observed that the electrons were flowing in the direction of the workpiece that was kept close to the cathode

tip. This electron flow was manifested as a brief spike in current, lasting a few milliseconds, and measuring at least 20 A. The area impacted by the discharge was observed as a circular area.

Skrabalak *et al.* [6] reported that the electrochemical breakdown and discharges striking the workpiece's surface were the cause behind ECDM process. The authors applied Fuzzy-logic control to illustrate the process of developing a simpler model for current estimate of electrochemical discharge machining (ECDM) process and described the process as current-voltage dependences. An effort was made to develop a fuzzy-logic controller for this process where both voltage and current were considered as input parameters by the controller. The appropriate movement of the electrode was produced by the controller's output signal. The authors proposed that surface roughness parameters and the frequency of microcracks might be decreased by using fuzzy-logic, and specifically adaptive fuzzy-logic control systems. It was concluded that the ECDM process might be applied in fields like aviation and medical surgery where high levels of machining accuracy and efficiency are necessary.

Peng *et al.* [7] reported that ECDM process has potential for machining high-strength non-conductive materials and introduced a new technique called Traveling Wire Electrochemical Discharge Machining (TW-ECDM) for cutting small optical glass and quartz bars of 10 to 30 mm in diameter. They found that copper wire generated more sparks due to its lower surface contact resistance and greater stability, while stainless steel wire could withstand higher voltages and exhibited stronger erosive capabilities. The authors optimized the frequencies and duty cycles for machining glass and quartz, suggesting that voltage and frequency should align with the bubble formation rate to achieve optimal energy intensity. The material removal rate (MRR) of 0.9 mm^3/min for optical glass and quartz was achieved for duty factor of 0.53, frequency of 200 Hz, and voltage of 65 V. For ceramic materials, the MRR was about 0.06 mm^3/min for duty factor of 0.23, frequency of 300 Hz, KOH electrolyte, and voltage of 85 V. It was concluded that ion translation rate, electrolyte immersion depth, and alkali concentration were key factors that affected bubble reactions.

Kozak *et al.* [8] studied pulsed electrochemical micromachining (ECMM) process to produce highly accurate complex and potentially 3-dimensional microcomponents. Based on the fundamentals of the process mechanism, a mathematical model was created and then experimentally validated using an ECMM system that was designed and developed. The authors reported that the ECMM process performance was influenced by various input

variables like duty factor, frequency, voltage, and feed rate. Compared to the results at 250 KHz, the higher frequency (1 MHz) results showed smaller side and frontal gaps with sharper edges. A frontal and side gap prediction mathematical model was created and validated through experimentation. At the frontal gap, there was a strong agreement between the experimental and theoretically estimated values. Likewise, for applied voltage pulses below 8 V, a near agreement for side gap values was noted, confirming the applicability of the model at low voltages.

Mediliyegedara *et al.* [9] investigated the ECDM process's performance and suggested a control system namely tool position control system (TPCS). It was found that ECDM overall performance could be improve by fixing the electrode gap at its ideal value. The authors stated that TPCS was made up of eight main subsystems namely supervisory controller, tool position control system, security control system, flushing control system, gap estimation system, man machine interface, graphical user interface and pulse parameter control system. It was reported that desired machining rate and good surface finish could be achieved by proper controlling of gap width i.e. the distance between the tool and the workpiece, electrolyte flow rate, temperature, concentration, and pulse parameters. It was concluded that the major benefit of ECDM over ECM or EDM is that its combination of metal removal methods provides a much greater machining rate.

Wuthrich and Fascio [10] conducted experiments on machining various electrically non-conductive materials using electrochemical discharge phenomena and demonstrated that a wide range of materials such as glass, quartz, and different ceramics could be machined, not only into simple structures like holes but also into more intricate forms such as threads. It was reported that the machining mechanism in the ECDM process was a combination of thermal and chemical effects, with the thermal effect being predominant. The authors documented that electrochemical discharges were influenced by the geometry and concentration of the electrolyte used, and that the surface roughness of the machined workpiece was affected by both the electrolyte and the applied voltage. It was reported for micro-machining applications, reproducibility needed to be within a few microns, and one of the key challenges to achieving this was controlling the gas film formed around the tool-electrode, where the discharges occur. It was concluded that for successful machining, not only a thin gas film but also its stability and dynamic conditions significantly impacted the machining process, particularly in terms of resolution and reproducibility.

Bhondwe *et al.* [11] developed a thermal model to calculate the MRR during the electro-chemical spark machining process and discussed about finite element prediction of MRR due to ECSM. Using the finite element method (FEM), the temperature distribution within the single spark's zone of influence was determined. It was found that the developed FEM-based thermal model fell within an acceptable range of accuracy when compared to the experimental results under the same machining conditions. Two different types of material namely soda lime glass and alumina were chosen as workpiece materials and the effect of duty factor and energy partition on MRR were studied. The researchers demonstrated that the MRR of soda lime glass workpiece material increased from 10% to 30% electrolyte concentration, surpassing that of alumina. MRR increased with an increase in duty factor for both the workpiece materials but the variation in MRR with duty factor for the alumina workpiece material was found to be less than that of the soda lime glass, and MRR enhanced with an increase in energy partition.

Sarkar *et al.* [12] investigated the impact of various process parameters in ECDM process and developed a second-order nonlinear mathematical model to establish the relationship between input process parameters like applied voltage, electrolyte concentration and machining criteria including MRR, radial overcut, and HAZ area during machining of silicon nitride. Stainless steel as tool material and an aqueous NaOH solution as electrolyte were used due to its high electrical conductivity. The parametric analysis based on the mathematical model revealed that applied voltage had a more pronounced effect on MRR, radial overcut, and HAZ area. The authors demonstrated that MRR was increased with a rise in applied voltage across various NaOH concentrations, and at 25% concentration, the radial overcut was lower compared to the 20% concentration. The ANOVA test results were presented to confirm the validity and accuracy of the developed model. It was concluded that optimal machining rates and high accuracy could be achieved by selecting the appropriate combination of parameters in this process.

Kim *et al.* [13] conducted experiments on ECDM to study the effects of voltage, pulse frequency and duty ratio on micro-drilling of glass wafers. It was observed that one drawback of ECDM process was HAZ area left on the surface during micro-drilled operation. The electrolyte used in the experiment was 25 wt% KOH at room temperature, with a cylindrical copper and three cylindrical graphite tools serving as the negative electrode and a platinum plate as the positive electrode. It was revealed that by increasing the frequency and reducing the duty ratio led to less thermal damage to the micro-drilled holes. Conversely, a higher duty

ratio increased the material removal rate due to longer discharge times. It was recommended to use a series of rectangular voltage pulses rather than rectified or full-wave DC voltage to reduce the HAZ area. It was found that tool wear and clearance enhanced with smaller diameter tools, while surface roughness increases with a higher duty ratio and lower voltage pulse frequency. The study also confirmed that higher duty ratio increased the MRR but result in rougher drilled surfaces.

Maillard *et al.* [14] created a qualitative model on SACE process using gravity feed mechanism. It was found that the characteristics of micro-hole drilling via gravity feed with spark-assisted chemical depended on the depth of the hole and the machining voltage. The authors showed that diameter changed from 15 µm to 100 µm when the applied voltage was increased. Relative roundness error increased from 10% to 20% with drilling depth and was independent of machining voltage. The optimal drilling results were achieved at voltages just above the critical level, during which the discharge activity entered the transition phase.

Zheng *et al.* [15] examined how tool geometry and pulse-off time of pulse voltage affect the electrochemical discharge micro-drilling process in Pyrex glass. The authors designed two types of tool geometries namely cylindrical tool and flat sidewall–straight front tool, with the goal of enhancing the quality micro-holes generated by ECDM process. It was found that the flat sidewall–straight front tool was more effective in reducing accuracy losses by minimizing the impact of discharge around the tool's sidewall. The study revealed that discharge occured not only at the tool's end but also along its sidewall. By using the flat sidewall–straight front tool, the distance between the tool's sidewall and the hole increased, reducing the discharge influence. The researchers also explored the effects of using rectangular pulse voltage and found that higher frequencies and smaller duty ratio decreased deviations in the form and dimensions of the micro-holes. It was concluded that combining the straight sidewall–flat front tool with pulse voltage significantly improved machining accuracy while maintaining the machining rate.

Han *et al.* [16] developed a new method to enhance surface integrity in ECDM process by incorporating conductive particles into the electrolyte and using powder-mixed fluids to enhance the quality of the machining. The experimental results showed that both the breakdown voltage and peak current were reduced by ten percent. The researchers explained the role of the particles in the electrolyte using two models: the hydrogen film model and the

single conductive particle charge model. These models demonstrated that conductive particles decreased the dielectric strength of the gas film. The reduction in breakdown strength was attributed to two types of particle behavior: i) particles attaching to the tool electrode, which intensified the local electric field, making discharge easier and more stable, and ii) dynamic particle movements due to electrostatic or gravitational forces. It was concluded that, while conventional ECDM processes could cause irregularities in the machined surface due to micro-cracks, local fractures, and breakage, the use of conductive particles significantly reduced these issues.

Jain and Adhikary [17] investigated the material removal mechanisms in ECSM process of quartz materials using two polarity conditions, using both cathode and anode as tools. It was found that while direct polarity led to increased sparking, the material removal rate, penetration rate, overcut, and tool wear rate were higher with reverse polarity. The authors proposed that material removal in ECSM with reverse polarity involved not only melting and vaporization of the workpiece material but also additional mechanisms. It was revealed that a deep crater was formed on the tool when it functioned as the anode, whereas there was almost no crater when it served as the cathode. The magnified view of the machined surface showed distinct differences in the material removal modes between ECSM with direct and reverse polarity. It was recommended that using a small tool electrode in the ECSM process, with the auxiliary electrode being either small or large, effective machining could occur even with a small auxiliary electrode.

Coteata *et al.* [18] explored the creation of small-diameter holes in metallic workpieces using ECDM process. It was reported that material removal in this process involved two main mechanisms one was electrochemical dissolution of the material and another one was thermal erosion due to electrical discharges between the electrodes. The researchers used an aqueous sodium silicate solution as the working liquid to improve control over electrochemical dissolution. The experimental results demonstrated that the density of the working liquid significantly impacted the wear rate of the electrode tool, along with factors such as working voltage, diameter, and capacity. It was found that electrode tool wear increased as the tool diameter decreased, and as electric capacity, voltage between electrodes, and working liquid density increased. The researchers also observed numerous micro-cavities on the lateral sides of the electrode tool, which they examined using a digital microscope. In this research, an optimized system was also identified for both mechanical and electrical equipment.

Chak and Rao *et al.* [19] investigated experimental study of ECDM process for drilling operation on aluminium oxide material with a rotating abrasive electrode. The researchers employed two distinct tool configurations i.e. Spring-fed cylindrical hollow brass tool of 1.5 mm diameter as fixed electrode and spring-fed cylindrical abrasive tool with same diameter but as a rotating electrode with a rotational speed of 20 rpm. The researchers measured and compared the MRR under various machining conditions such as pulsed DC supply voltage, duty factor, and electrolyte conductivity. The experimental results showed that the volume of material removed was increased with higher supply voltage and duty factor. The study suggested that a mixed electrolyte solution of NaOH & KOH achieved higher conductivity, which could only be reached by heating each electrolyte individually. A second-order mathematical model and a regression equation were developed to examine how each parameter affected the volume of material removed. The rotary tool abrasive was found to be a more efficient electrode arrangement for ceramic hole drilling.

Furutani and Maeda [20] demonstrated the effectiveness of ECDM process to machine any cylindrical workpieces made up of insulating materials by rotating it against a tungsten tool electrode. In this study, a soda lime glass rod was immersed in NaCl electrolyte solution which was used as the working fluid, while a tool electrode touched the workpiece surface with a light pressure and the workpiece was rotated to ensure a continuous supply of fresh working fluid into the gap between the tool electrode and the workpiece. The applied voltage was varied up to 40 V, while the rotation speeds were set at 0, 0.3, 3, and 30 revolutions per minute. Discharge was detected with an applied voltage of 30 V. As the applied voltage increased, both the width and depth of the machined grooves, as well as the surface roughness at the bottom of these grooves, also increased. It was found that when the rotation speed increased, the thickness of vaporization around the tool electrode decreased resulting in a narrower machined groove.

Han *et al.* [21] explored the enhancement of geometric precision in electrochemical discharge micro-drilling by utilizing an electrolyte subjected to ultrasonic vibrations. In this research work, ultrasonic electrolyte vibrations were applied to improve the machining depth of μ-drilling using ECDM process by ensuring proper electrolyte flow that helped to maintain steady spark generation. Additionally, side-insulated tools, pulse voltages, and ultrasonic waves were applied to enhance the performance of ECDM micro-hole drilling. The researchers demonstrated that the use of a side-insulated electrode and a pulse-power generator improved both the stability of gas film formation and the surface quality at the entrance of the hole. It was reported that by applying a cooling effect, maintaining a constant active tool surface and

with the use of pulse voltage minimized overcut and taper were minimized. The authors concluded that in comparison to traditional drilling outcomes, with the technique used in this process, the diameter of the machined hole was decreased from 426 µm to 328 µm, and the machining depth was increased from 320 µm to 550 µm.

Coteata *et al.* [22] aimed to assess the weight factor in electrochemical discharge drilling. The weight factor of the electric discharge as the ratio of the time for one complete rotation of the crank around the rotation axis to the total number of electrical discharges occurring during that time period. In order to carry out the experiment, a device for electrochemical discharge drilling was created and constructed. It was based on the workshop milling machine's slotter ram and used a crank mechanism to convert the milling machine's main shaft's rotational motion into a linear alternative motion. There was the impact of the input parameters on tool wear and axial electrode. It was concluded that MRR was dependent upon the features of motion and specific dimensions of the crank mechanism's constituent parts.

Liu *et al.* [23] developed a model to show the electric field acting on a hydrogen bubble in the electrochemical discharge machining process and examined the discharge mechanism in this process. The researchers tried to simulate the discharge mechanism, with a particular focus on estimating the hydrogen bubble's critical breakdown voltage. The researchers examined the electric field at the surface of the hydrogen bubble and noted that the peak field strength was observed at an angle of 90 degrees to the vertical line drawn between the two electrodes. The model was able to predict the breakdown voltage of a discharge within the range of 26.2 to 34.2V, while the actual experimental breakdown voltage was ranged from 26 to 30V, aligning closely with the predicted values. The researchers analyzed the XRD patterns for both ECDM and EDM specimens and concluded Al_4C_3 was found on the EDM but not on ECDM.

Yang *et al.* [24] reported that ECDM process combined the two different phenomena one was high temperature melting and another one was accelerated chemical etching. Wire electrical discharge grinding was used to fabricate a tool electrode with a diameter of 200 mm and it was found that the discharge was dependent on the electrode's tool material. The researchers explored how the shape of the tool electrode end and the diameter of the tool affect the machining stability, particularly in relation to gas film formation and the wettability of the tool electrode. It was found that the corner of the electrode end experienced the highest current density and the most significant wear. Different levels of surface roughness were observed

while machining with various tool electrode materials such as stainless steel, tungsten carbide and tungsten. It was concluded that tungsten carbide exhibited the best machining stability and the least tool wear, followed by tungsten and stainless steel.

Cheng *et al.* [25] defined ECDM process as an alternative spark based μ-machining technique for producing μ-holes and μ-grooves on nonconducting materials. A gas film was utilized on the electrode surface that acted as dielectric medium necessary for generating discharge and noted that the quality of this gas film was a crucial and decisive factor in determining machining criteria like geometric accurateness, reliability, and surface roughness. Experiment results indicated that a steady and compact gas film could be obtained when the applied voltage reached a certain level after surpassing the critical value. In this study, the machined contours and current indications were used as indicators of the quality of the gas layer. The authors noted that while the shear stress between the gas film and the rotating tool could be ignored, variations in the tool's rotational speed had no effect on the quality of the gas film. It was concluded that the lowest dimensions of the machining profiles were obtained when the applied voltage reached the transition voltage, which enabled the production of a stable electrochemical discharge current.

Wüthrich and Allagui [26] studied on the behavior of current density in electrochemical discharge (ECD) events from large-scale to small-scale perspectives. The authors discussed the various applications of this process in the medical research field for micromachining and the manufacturing of nanomaterials. In this research study, an attempt was made to review the material removal mechanisms and the latest advancements in process control. While the electrons in the discharges and the subsequent chemical reactions were useful for various uses, such as wastewater cleansing and nanoparticle production, the heat produced during the process was primarily utilized for micro-machining applications. The authors suggested that the sparks produced in ECD phenomena could be compared to the energy radiation chemistry in water base solutions. It was concluded that ECD held great promise for applications in nanoscience and micromachining.

Yang *et al.* [27] Investigated the machining efficiency and level of wear on tool material during gravity feeding of μ-drilling. It was shown that the surface roughness of the tool material impacted the wettability of the tool electrodes, which subsequently influenced the coalescence of the gas film, precision in machining and the size of the micro-holes produced. Gas bubbles on the electrode with poor wettability had higher surface tension, which led to the formation

of a thicker gas layer and the biggest hole diameter. It was observed that Various tool materials needed different optimal voltages, influencing the formation of the gas film, the size of the holes created, and the average current achieved. It was also shown that different types of tool materials led to variations in the speed at which the machining process could be carried out. It was concluded that the optimal voltage level for different tool electrodes influenced the performance of the machining process.

Sankar *et al.* [28] successfully machined on electrode plates using ECDM process and discussed the influence of gold coated layer on enhancement of a quad beam capacitance accelerometer's functionality to deal with the interconnected relationship between sensitivity and damping ratio in capacitive accelerometers. It was observed that with a fixed damping ratio, the sensor's prime-axis sensitivity was enhanced by damper holes, while an electroplated gold layer boosted not only the prime-axis sensitivity but also the cross-axis sensitivity. The efficiency of acceleration sensors was calculated by Performance Index. It was observed that gold coated hole's Prime-axis sensitivity compared instrument with damper hole was enhanced by 5 hundred times whereas cross axis sensitivity was decreased by tenth times. It was concluded that the combined effect of electroplating technique and utilizing ECDM technique, different sensitivity measuring parameters were improved surprisingly.

Yang *et al.* [29] proposed to use a spherical-shaped tool instead of a cylindrical one and demonstrated how machining was improved with the proposed tool. It was noted that the front end of the cylindrical tool electrode fully contacted the job material, preventing the electrolyte from reaching the front end and generation of a gas bubble layer. However, using a spherical tool would decrease the contact area between the tool and the job due to its curved surface, enabling the electrolyte to reach the end point more easily and leading to faster formation of the gas bubble layer. Compared to traditional cylindrical tool, the proposed tool offered lower hole diameter but minimize the machining time by sixty-five percentage. It was noted that machining to make a hole in quartz with a cylindrical tool caused fracture, whereas the use of a spherical tool prevented them.

Wei *et al.* [30] introduced a model based on finite elements method for ECDM inside the spark regime and identified many attributes and procedure of removing materials in spark regime for different dimensions of machining depth. The researchers utilized ANSYS10 to anticipate material removal from a single discharge, and a sensor was used to gauge the depth of the drilled hole. The authors created a 2D axisymmetric thermal model using finite element

analysis to simulate material removal caused by a single spark. It was observed that the spark duration was approximately 100 μs with constant DC power; durations longer than 100 μs lead to significant energy dissipation due to material transfer between electrodes. The model effectively forecast the drilling depth in the discharge regime, matching the experimental data. It was determined that 29.1% of the thermal energy was transferred to the workpiece, achieving a machinable depth of 303 μm.

Wei *et al.* [31] introduced a newly dressing process *i.e.* electrochemical discharge dressing (ECDD) and reported that this technique was mainly based on electrochemical discharge phenomenon. For the experimentation, NaOH electrolyte concentration was varied between 30% and 32 wt%. The DC pulsed voltage was adjusted from 0 to 60V, and a micro-grinding tool, measuring 850 μm in diameter and bonded with sintered nickel and copper was used. It was found that dressing process was highly influenced by electrochemical discharge phenomenon and various dressing characteristics such as tool's surface structure, grinding stress and surface roughness were investigated. It was found that after the tool was dressed, the abrasive grains on the tool were seen to stick out without any visible damage. Additionally, both the normal grinding force and the surface roughness of the workpiece decreased by 50% as a result of the dressing process. It was concluded that ECDD process was straightforward and cost-effective, offering many advantages over traditional dressing process.

Ziki *et al*. [32] revealed that spark assisted chemical engraving (SACE) process had the ability to modify the surface characteristic of μ-channels in glass material. The investigation explored how various factors, including electrolyte viscosity, tool-workpiece gap, machining voltage, and tool travel speed, affected channel surface characteristic during operations. The study identified electrolyte viscosity as the most crucial factor in determining surface characteristic. The researchers found that channels machined at a lower speed exhibited uniform surface characteristic and straight walls compared to those machined at higher speeds. It was found higher electrolyte concentrations i.e. upto 40 wt% NaOH could lead to damage of the surface of the channel. It was proposed that the damage occurred at higher electrolyte concentrations might be due to the increasing of thermal conductivity. It was concluded that SACE technique could be used to manufacture advanced microfluidic and biomedical devices with high accuracy.

Cao *et al.* [33] explored a combined approach of ECDM and Micro-Grinding using polycrystalline diamond (PCD) tools to enhance performance and surface texture in glass

machining. The researchers demonstrated that intricate 3D microstructures with superior surface finish could be effectively produced in glass by integrating ECDM and PCD grinding. A time comparison between traditional grinding and this hybrid method revealed significantly reduced machining duration for the latter. This innovative technique showed potential for fabricating complex, high-quality glass structures. The study also examined machining feed rate to boost MRR. It was found that when feed rates were exceeded 0.75 μm/s, setbacks increased rapidly, while average MRR remained relatively constant. It was reported that a good surface finish (Ra-0.05 μm) was obtained through grinding with PCD tools (10 μm grit size) with the help of a capacitance of 400 pF and 100 V voltage.

Jiang *et al.* [34] introduced a stochastic model based on experiments to evaluate spark energy in ECDM process. The authors utilized a tungsten tool electrode of 250 μm diameter, a 30 wt% NaOH solution and tapered tool electrodes to enhance spark generation uniformity. The researchers demonstrated that these tapered tools increased the spark generation regularity and reduced minimal discharges. A finite element model was also developed to link spark energy with the geometry of removed material, concluding that material removal occurred through heat applied to the region and chemical reactions. The study explained gas layer generation using the current output of a DC power supply, with experiments setting the minimum pulse width above 30 ms. It was proposed that material removal could be simulated by addressing heat transfer problems, as the transferred electrical energy transformed into a heat source acting on the workpiece during machining.

Huang *et al.* [35] implemented the ECDM process for drilling μ-holes on 304 grade SS metal. The researchers employed tungsten carbide μ-tool electrodes ranging from 250 μm to 400 μm in diameter, which were operated at high rotational speeds. Tool wear was examined before and after the machining of μ-holes on workpiece. With the help of scanning SEM images, the authors tried to analyze the shape and surface characteristics of the drilled μ-holes, revealing minimal burrs and stray current corrosion at the hole edges. The researchers developed a mathematical model based on the results obtained from the experiments. It was concluded that machining voltage significantly impacted tool electrode wear, while the increase in tool electrode rotation speed, tool electrode diameter, and machining voltage led to diminish the wear of the tool electrode.

Singh *et al.* [36] explored a comprehensive review on different variants of ECDM process and also identifying future research opportunities of this technique. The authors classified various

ECDM variants such as electrochemical discharge drilling (ECDD), milling, turning (ECDT), dressing, wire ECDM (WECDM), and die-sinking ECDM. The researchers analyzed ECDM-based triplex hybrid process that incorporate a third energy source to enhance performance of this techniques. These methods include rotary ECDM (R-ECDM), powder mixed ECDM (PM-ECDM), electrochemical discharge grinding (ECDG), magnetic field assisted ECDM (MAECDM), and vibration assisted ECDM (VAECDM). This research study highlighted the limited research conducted on machining metal matrix and polymer matrix composite materials using these techniques. It was reported that these processes might be applied to create micro-level products like lab-on-chips and MEMs using superior-strength advanced composites.

Furutani *et al.* [37] presented a lathe-style ECDM process utilizing a rod made up of glass material as the workpiece, tungsten as the tool electrode, and a graphite rod as the anode. The authors used the apparatus that employed a forced sensor to control the normal force in the radial direction between 0.06 and 0.08 N, while strain gauges measured both normal and tangential forces. It was found that the machined area had a workpiece diameter of 2.82 mm, with the machined length extending 0.02 mm beyond, and groove bottom corner radii under 0.1 mm. The researchers also conducted a comparative analysis of electro feeding systems in traditional ECDM versus ECDM based on lathe, examining machined surfaces using a scanning electron microscope. It was observed that although electrode feeding with constant stress yielded a higher material removal rate than constant velocity feeding, achieving precise shapes without breakage required supplying the electrode at a steady speed with firm support for the electrode

Guo et al. [38] introduced a novel method for creating 3D micro & nanostructures to develop various micro or nano electromechanical devices. This technique combined the focused ion beam and chemical vapor deposition for microelectrode fabrication with ECDM process. The experiments were conducted using a custom-built electrochemical micromachining system. The researchers utilized microelectrodes created on polished stainless needle tips, measuring 10 µm in diameter and 28 µm in height. It was observed that for 304 austenite SS, both the hole diameter and unilateral discharge gap were increased as the applied voltage was enhanced. The authors also produced various types of 3D nano-electrode including pillar, horn, corner, and array configurations, demonstrating the benefits of using ion beam chemical vapor deposition for micro & nano-electrode fabrication in µ-ECDM process. It was concluded that the µ-ECDM

process showed promise for manufacturing complex 3D components using 3D micro-nano electrodes.

Lie et al. [39] demonstrated a novel wire-ECDM apparatus utilizing a rotating helical tool with a 105 µm diameter. The authors made an arrangement of equipment & tools to generate a deep cut/groove in a piece of glass that was 1000µm thick. The effect of different input parameters such as applied voltage (30-42V), frequency (0-100KHz), duty ratio (50-90%), rotating speed (3000-15000rpm), and feed velocity (0.5-2.5 µm/s) were studied. It was observed that side gap increased with higher applied voltage and duty factor, while it was decreasing with increased frequency, spindle speed, and feed rate. The study also demonstrated that narrower grooves could be produced using lower voltage and duty factor, combined with higher frequency, spindle speed, and feed rate. The researchers successfully created a series of grooves measuring 138 µm in width and generated microstructures. It was concluded that this wire-ECDM process with a rotating helical tool was effective in creating detailed, high-aspect-ratio microstructures in tough, non-conductive materials.

Mehrabi *et al.* [40] explored the use of a hollow electrode system for injecting electrolyte under high pressure to enhance the performance of ECDM process for deep hole drilling on optical glass. The researchers tried to improve the ECDM performance in mesoscale drilling operations by ensuring adequate electrolyte delivery to the deeper sections of the hole. The experiments utilized hollow brass tools with varying outer diameters (1, 1.4, and 1.7mm) and internal diameters (0.3, 0.5, and 0.8 mm), while a steel plate served as the anode, positioned 10 cm from the cathode. The researchers examined the effects of injection pressure (0-0.03 MPa), DC voltage (45-75 V), and machining time (1-5 min) on drilling depth in terms of MRR, hole diameter, and entrance shape. It was found that injecting electrolyte through the deep hole drilling area led to increased material removal rate and drilling speed. A larger hole diameters and conical hole shapes were also observed with increased electrode diameter and injection pressure. It was concluded that the injection pressure should be as low as possible to attain the target hole diameter.

Xu *et al.* [41] conducted a critical analysis of the impact of magnetohydrodynamics (MHD) in ECDM process. It was revealed that MHD effect led to quicker drilling and deeper holes, attributed to the additional bubble movement it induced, which resulted in improved electrolyte flow and enhanced machining performance. It was observed that with the application of a magnetic field, more the bubbles generated during the process to move in a circular pattern

around the tool. This movement was influenced by a Lorentz force component, which acted on the bulk bubbles, driving them circumferentially. An analytical model was also used to explain that MHD increased electrolyte circulation in the narrow gap, preventing bubble accumulation at the μ-hole entrance, thus leading to increase the depth of holes and improved machining performance. It was concluded that combining a magnetic field with counter resistant feeding method not only improved machining performance and finishing precision hole but also enabled the creation of through holes.

Arya *et al*. [42] introduced a pressurized flow-ECDM (PF-ECDM) technique where a tubular electrode was used that allowed for accurate control over the electrolyte flow rate to inject new electrolyte into the machining region. The researchers examined how factors such as electrolyte flow rate, applied voltage, pulse on time, and electrolyte concentration influenced the depth and entrance diameter of holes. A comparative analysis of material removal in ECDM without electrolyte injection versus PF-ECDM was conducted and it was revealed that the pressurized flow system offered enhanced control and precision compared to traditional ECDM technique. The researchers observed that replenishing vaporized electrolyte at the machining region maintained the discharge process and enhanced machining outcomes. It was found that lower thermal energy inputs required a low electrolyte flow to replenish vaporized electrolyte. The authors successfully improved the performance of machining μ-hole by 61.2% over traditional ECDM process. It was concluded that the PE-ECDM method might be used to create μ-holes in borosilicate glass for use in MEMs, lab-on-a-chip, and microfluidics applications.

Arab *et al.* [43] showed how the ECDM process can be used to produce numerous small through-holes of diameter about 300 μm in non-conductive materials. The authors examined how various factors, including voltage, duty cycle, tip length of tool, electrolyte type and pulse frequency affected machining outcomes like entrance hole size, HAZ area and overcut. The researchers also explored how the creation and trapping of hydrogen gas bubbles between tool tips were regulated by the length of the tool tips. It was discovered from the experiments that a lengthy tool tip does not allow hydrogen bubbles to become trapped, leading to continuous sparking. The researchers compared different types of electrolytes, such as NaOH, KOH, and H_2SO_4, and showed that KOH offers good quality through holes due to its lower viscosity and higher ion mobility. It was reported that this process achieved a higher rate of performance compared to plasma etching and laser drilling method. It was concluded that TGV links, 3D

wrapping, miniature channels for microfluidics, and bio-MEMS technologies could all gain advantages from this experimental work.

Singh et al. [44] investigated a vertical Wire-ECDM process using a textured wire electrode for micro-slit fabrication on glass. The effects of input process parameters like applied voltage, pulse on time, electrolyte concentration and feed rate were analyzed in relation to kerf overcut and slit straightness. It was revealed that the textured wire enhanced localized electric field intensity that enabled uniform spark discharges. The mechanism MRR was also examined using COMSOL Multiphysics and regression models were developed using Design Expert software. It was observed that a lower electrochemical discharge energy reduced kerf overcut but compromised slit straightness due to edge chipping, while a lower feed rate increased kerf overcut while reducing straightness. It was found that the optimal machining parameters were determined to be an applied voltage of 48V, a pulse on time of 3ms, a feed rate of 3mm/min, and an electrolyte concentration of 15% resulting in a minimal kerf overcut of 105μm and a straightness of 94.42%. It was concluded that using textured wire electrodes improved the machining efficiency and precision in W-ECDM technique that enhanced micro-slit fabrication in glass materials.

Ji *et al.* [45] revealed that specific conditions could restrict discharges to the end of the tool electrode in Spark Assisted Chemical Engraving (SACE) process when machining Zirconium dioxide (ZrO_2). It was suggested that employing a cylindrical notched tool electrode with additional sharp edges could improve discharge control. The significance of sharp square edges on the tool electrode in facilitating end discharges was emphasized. Experimental work involving the creation and assessment of microgrooves demonstrated that this notched tool electrode enhanced both precision and efficiency in ZrO_2 ceramic machining by better confining discharges at the electrode's end. The study also introduced an accurate method for setting the electrode immersion depth, utilizing a liquidometer and workpiece surface alignment. Through basic experiments, crucial parameters such as voltage, electrode immersion depth, and NaOH electrolyte concentration were optimized. It was concluded that SACE scanning experiments on ZrO_2 ceramics validated the substantial improvement in machining performance achieved by the proposed tool electrode.

Singh *et al.* [46] demonstrated an improved ECDM technique for creating micro-holes in Yttria-stabilized zirconia (Y-SZ) by combining electrolyte flow and pressurized feeding. It was found that main material removal mechanism was due to thermal spalling, with minimal

chemical etching, setting Y-SZ apart from other glass-based ceramics. It was observed that introduction of electrolyte flow substantially enhanced machining performance, resulting in a 42% increase in hole depth and a 33% reduction in hole diameter for identical processing times. It was revealed that this enhancement was attributed to the increased frequency of electrochemical discharges (ECDs) facilitated by electrolyte supply, enabling controlled material removal and producing crack-free micro-holes without edge fractures. The process achieved a maximum penetration speed of 126 μm/min that allowed for the production of deep micro-holes reaching 630 μm diameter. It was concluded that this method can enhance both productivity and precision in Y-SZ machining, offering an efficient and reliable approach for producing high-quality micro-holes in this challenging ceramic material.

Kang *et al.* [47] introduced finite element models (FEM) to forecast material removal in ECDM process. The models focused on single-pulse discharge with a tapered electrode and continuous discharge with a cylindrical electrode. It was showed that 30.5% of the discharge energy was transmitted to the workpiece and the simulated crater shapes closely matched the experimental for single-pulse discharge. It was found that material removal initiated at the projected contour of the electrode edge and progressed inward with an effective discharge ratio of 10.1% for material removal within a 37–43 V range. The model's accuracy was verified by comparing simulated crater morphologies with experimental results. The FEM was employed to predict hole drilling depths at various voltages, showing strong correlation with experimental data. The proposed FEM was aimed at being validated for accurately simulating and comprehending the material removal process in ECDM, offering insights into energy transfer, discharge efficiency, and material removal behaviour. The model's capability to enhance ECDM process predictability and precision was emphasized in the study.

Arab et al. [48] investigated the effect of initial tool-workpiece (T-W) gap, machining duration, and electrolyte concentration on micro-hole formation and tool wear in Electrochemical Discharge Drilling (ECDD) process on glass. A new numerical model, utilizing inverse heat flux reduction was developed to forecast micro-hole formation and the results were confirmed through finite element simulations. It was observed that micro-hole size increased up to a critical T-W gap of 20 μm for NaOH and 10 μm for KOH before decreasing. The greatest micro-hole depth was occurred at a zero-gap condition which also resulted in significant tool wear. It was revealed that a maximum depth of 175 μm was achieved with 30 wt% NaOH after 60 seconds of machining and tool wear decreased as the T-W gap increased with the lowest wear of 9 μm. It aws concluded that the traditional gravity-feed mechanism

was unsuitable due to excessive tool wear but maintaining an optimal T-W gap of 10 to 30 μm for NaOH and 5 to 20 μm for KOH was effective for improving process efficiency and tool durability.

Bhargav et al. [49] examined the creation of microholes in a glass fiber-reinforced polymer (GFRP) composite utilizing a custom-built electrolyte-sonicated micro-electrochemical discharge machining (ES-μ-ECDM) system. The study focused on voltage (V), electrolyte concentration (wt%), and feed rate (μm/s) as process parameters, with material removal rate (MRR) and overcut (OC) as the measured responses. It was revealed that higher voltage and electrolyte concentration led to increased MRR and OC. The OC was initially increasing with feed rate up to 4 μm/s before decreasing. Voltages of 55 V or more and concentrations of 17.5 wt% or higher resulted in surface damage and bump formation. SEM analysis was done to confirm the smoother surfaces at lower voltage and electrolyte concentration levels. The MOJAYA algorithm was employed for multi-objective optimization to derive Pareto-optimal solutions. It was found that a 5 μm/s feed rate optimally balanced MRR and OC. For maximum MRR, optimal parameters were 59.57 V, 17.42 wt%, and 4.60 μm/s, while minimum OC was achieved at 50 V, 15.89 wt%, and 4.32 μm/s. It was concluded that this process was suitable for microhole fabrication in GFRP composites, with potential applications in circuit boards and biomedical filters.

Appalanaidu et al. [50] tried to estimate the depth of thermal damage under specific energy conditions and bonded glass wafers of equal thickness to glass material. A specialized tool feeding setup with a dial gauge was created to measure machining depth in real-time, providing data for calculating energy applied to each material layer. It was found that lower applied voltages produced insufficient thermal energy for significant material removal, resulted in inadequate hole depth. Whereas, higher voltages increased material removal and hole depth but damaged the sacrificial layer. Lower pulse ratios were observed to enhance heat dissipation through the electrolyte that reduced the machining depth while minimizing thermal damage. A multi-criteria optimization technique was employed to maximize hole depth while minimizing heat-affected zones and defects. The optimal machining settings resulted in a 71.5% reduction in heat-affected zone and improved hole quality, although the glass wafer application decreased hole depth by 39% due to energy consumption by the wafer rather than direct machining of the work material.

Santra et al. [51] introduced a side feeding technique to overcome the problem of machining inefficiencies due to gas bubbles escaping from the tool tip in electrochemical discharge milling process. A copper tool-electrode and 20 wt% NaOH electrolytes were used to investigate the influence of voltage range from 30V to 40V and feed rate range from 40–80 μm/sec on different responses such as channel width, surface roughness, and machining depth in glass. It was observed that largest channel width of 579.6 μm was obtained at 40V and 40 μm/sec feed rate whereas smallest channel width of 478.86 μm was found at 30V and 80 μm/sec feed rate. It was revealed that lowest roughness of 0.222 μm was obtained at 35V with upward tool movement. It was observed that machining depth was increased with higher voltage and lower feed rate and maximum depth of 384.54 μm was recorded at 40V and 40 μm/sec. It was stated that the side feeding method allowed gas bubbles to stay at the machining zone, enhancing material removal. It was concluded that the side feeding technique effectively improved the machining efficiency by retaining gas bubbles at the tool tip, leading to better material removal, smoother surfaces and deeper channels.

Nawaz et al. [52] introduced a new technique in micro-ECDM process where a spindle integrating a flexure hinge and a high-resolution micro-force sensor was developed for real-time servo control of micro contact force. The spindle was designed with two special hinges, one that is highly flexible in axial direction and another that is rigid in radial direction that allowed it to quickly adapt to sudden force changes. Thus, it prevented the tool bending and ensuring stable machining operation. In this study, a new method was used that combined two different techniques: μ-EDM and wire-electro discharge grinding, for the fabrication of μ-tools with a diameter of less than 200 μm that helped in accurately shaping the tiny electrodes with high precision. The authors used a new feed technique i.e. servo control of flexible micro force (SCFMS) was proposed to maintain consistent depth by monitoring tool position and contact force in real time, effectively reducing overcutting errors and achieving a machining depth accuracy of ±2 μm. It was found that using this method different shape of 3D microstructures like S-shape and square was fabricated on quartz glass with high precision.

Mandal et al. [53] demonstrated the feasibility of the powder-mixed micro-electrochemical discharge machining (PMECDM) process and compared this process with the conventional micro-electrochemical discharge machining (MECDM) process for fabricating micro-holes in C103 niobium-based alloy. It was observed that unlike MECDM process which involved only spark erosion and chemical etching, PMECDM incorporated an additional mechanism by introducing powder into the electrolyte. It was found that powder-mixed technique enhanced

the material removal rate and improved the surface quality. It was revealed that PMECDM yield in a higher material removal rate (MRR) of 2.8 mg/min and a lower surface roughness (Ra) of 0.61 mm, whereas an MRR of 2.01 mg/min with an Ra of 1.11 mm was achieved using MECDM. The applied voltage (V) was identified as the most influential parameter in both the processes, compared to electrolyte concentration (C) and duty factor (D). The transfer of tungsten from the tool to the workpiece and aluminum from Al_2O_3 particles was confirmed through energy-dispersive spectroscopy (EDS) for both the machining approaches.

Lu et al. [54] investigated the discharge behaviour in Jet-ECDM with anodic discharge by manipulating electrical and chemical conditions and evaluating plasma region temperature. It was found that discharges primarily occurred in areas of high current density, influenced by pulse cycle and electric field distribution. It was proposed that a gas ionization-dominated anodic discharge model to illustrate how discharge type and electrolyte choice affect material removal. It was revealed that using a DC power supply produce a maximum machining rate of 1.44 mm/min, while high-frequency AC of 1000 Hz, produced a better surface finish of Ra 170 nm. It was noted that a time delay in plasma ignition during pulse due to dielectric layer formation, and high-frequency pulses regulated discharge duration, preventing excessive discharge. It was concluded that NaCl electrolyte resulted in more localized discharges while NaOH achieved nearly three times higher MRR and material removal was found to be dependent on plasma formation with increased discharge improving MRR and machining performance.

Wang et al. [55] introduced a novel machining technique called Electrochemical Discharge Milling and Grinding (ECDM-G) for creating microchannel structures on glass. KH_2PO_4 solution was utilized as an electrolyte and applied voltage, duty ratio, and rotation speed were chosen as other input variables. A comparative analysis was conducted between ECDM-G, traditional grinding, and ECDM processes. It was revealed that ECDM-G significantly enhanced machining performance. It achieved a 35.1% reduction in overcut compared to mechanical grinding and a 49.1% reduction compared to ECDM. Furthermore, edge damage was decreased by 42.2% and 56.6% relative to grinding and ECDM, respectively. Surface quality was also enhanced, with ECDM-G reducing surface roughness by 47.7% compared to grinding and 74.9% compared to ECDM. It was stated that this process effectively eliminated edge collapse, breakage, thermal defects and heat-affected zones, establishing itself as a highly effective and reliable machining approach. It was exhibited that ECDM-G offered minimal tool electrode wear, even when machining complex structures with long paths. It was concluded

that this technique showed considerable promise for industrial applications, particularly in the production of biological and medical equipments.

Chen *et al.* [56] developed a novel method called Ultrasonic Assisted Electrochemical Discharge Milling (UAECDM) and demonstrated that incorporating ultrasonic vibration into the ECDM process enhanced film thickness and sustained current signal stability. The researchers investigated the process mechanism and refined the technique. It was reported that precise control of the system and accurate parameter settings enabled the successful creation of a micro-channel complex structure and a stepped pentagram with approximately 0.2 surface roughness. It was confirmed that UAECDM significantly improved machining precision, stability, and surface quality. Intricate 2D and 3D micro-structures with 0.2 μm surface roughness were fabricated on glass using this technique. It was concluded that this innovative technique was an ideal method for producing micro-channels on glass, with promising potential for widespread industrial applications in the future.

Zou *et al.* [57] investigated problem of creating uniform and high-quality micro-hole arrays in glass with ECDM process which was frequently hampered by an unstable gas film. A non-Newtonian fluid (non-NTF) electrolyte was introduced to enhance precision and consistency through its damping and confinement effects. Different sizes micro-holes were created with an average entrance diameter of 343.8 ± 3.47 μm and a heat-affected zone (HAZ) width of 18.01 ± 1.52 μm in 300-μm-thick glass. In comparison to conventional KOH electrolyte, the entrance overcut and HAZ width were decreased by 43.84% and 64.81%, respectively, while repeatability was improved by 67.92%. The concentration of the non-NTF electrolyte and tool rotation speed were identified as crucial factors affecting hole quality. It was emphasized that utilizing a non-NTF electrolyte improves gas film stability and enhances the precision and reliability of ECDM for micro-holes, making it a promising technique for industrial applications.

Kong *et al.* [58] presented a technique for controlling machining behavior, shifting from electrochemical machining (ECM) to electrochemical discharge machining (ECDM), by manipulating the inter-electrode gap (IEG). A new sinking push method for electrochemical milling of TC4 alloy was introduced to boost the MRR and reduce unwanted corrosion. It was reported that deliberately triggering electrochemical discharges by narrowing the IEG to further enhanced the MRR. The transition in machining behavior from ECM to ECDM was also studied while the IEG was decreased. These insights led to the development of an innovative

hybrid ECDM-ECM approach for effective recast layer removal. It was concluded that this approach efficiently eliminated the coarse recast layer and ensured the removal of both the recast layer and heat-affected zone (HAZ) while achieved a smooth finished surface.

Mhahe *et al.* [59] aimed to determine optimal parameters for minimizing tool wear, thermal damage, and overcut deviation in ECDM process for creating micro-holes in molybdenum. Experiments were conducted to evaluate the effects of various electrolytes, including $NaNO_3$, NaCl, NaOH, KOH, and a mixture of NaOH and KOH, on MRR, Tool Wear Rate (TWR), overcut (OC), HAZ, and surface quality. In comparison to neutral electrolytes, mixed electrolytes showed better material removal, lower tool wear rates, and improved surface quality, but with a bigger HAZ. It was also shown that NaCl had a greater MRR than $NaNO_3$ and KOH. It was revealed that alkaline solutions, particularly the mixed electrolyte, outperformed KOH and NaOH used individually or neutral solutions in terms of higher MRR and HAZ, lower TWR, and production of micro-holes with minimal overcut, while also improving surface quality. It was concluded that tools used with KOH and mixed electrolytes showed less wear and material erosion than those used with NaOH and neutral solutions, according to a subsequent analysis of brass tools exposed to various electrolytes using Scanning Electron Microscopy (SEM) images and Energy-Dispersive Spectroscopy (EDS).

Li *et al.* [60] examined the process of μ-channel creation on alumina ceramic surfaces using ECDM process. The volt-ampere characteristics of 20 wt% NaOH electrolyte at different tool immersion depths was studied and it was found that deeper immersion led to thicker gas films, reduced spark energy and higher critical voltage requirements. A thermal removal finite element model (FEM) was also developed to indicate that heat accumulation and intermittent cooling were the primary drivers of material removal. The research identified key factors affecting microchannel precision and bottom surface quality, including the Gaussian heat source, gas film formation, and temperature distribution. The impact of various parameters such as discharge frequency, applied voltage, duty ratio, and tool feed rate on microchannel performance was also investigated. It was showed that lower duty cycles and frequencies, coupled with higher voltages and feed rates, enhanced dimensional accuracy and surface smoothness but decreased MRR. Complex 3D structures and zigzag arrays with varying depths were successfully produced, achieving minimal surface roughness and shape deviations. It was concluded that ECDM was capable of precise microchannel machining on alumina ceramics with minimal tool wear.

Shen *et al.* [61] explored the influence of discharge thermal effects on electrochemical corrosion in ECDM process. The researchers aimed to correlate discharge heat with solution temperature. An attempt was made to correlate discharge heat with solution temperature. A mathematical model was developed to demonstrate that solution temperature was directly proportional to discharge energy. It was observed that with the increase of voltage a gradual temperature raised in machining area with higher temperatures at closer measuring points. The researchers employed X-ray photoelectron spectroscopy (XPS) and electrochemical impedance spectroscopy (EIS) to analyze passive films which were found to contain FeO, Fe_2O_3, and Cr_2O_3. It was revealed that recast layer films offered greater density and corrosion resistance due to Cr enrichment. It was shown that while higher electrolyte temperatures led to thicker films, it also reduced corrosion resistance because of looser structures. Electrochemical corrosion morphologies of the matrix material and its recast layer over various corrosion periods were also examined. It was revealed that matrix materials corroded faster than recast layers. It was noted that discharge thermal action increased current density, decreased solution viscosity and improved surface quality and efficiency.

Bahar *et al.* [62] illustrated the micro-scale machining of glass composite utilizing the Rotary Magnetic field-ECDM technique. It was emphasized in the study that the use of a magnetic stirrer in μ-ECDM process, combined with a rise in electrolyte temperature, resulted in attainment of the desired quality characteristics in the glass epoxy composite material. Metaheuristic algorithms was used to enhance the quality attributes of micro holes drilled in the composite material. A Machine Learning (ML) algorithm based on Bayesian regularization was utilized to verify the reliability of the optimal results obtained from metaheuristic algorithms. The optimal process parameters were identified as approximately 48 V, 48 C, 3.56 ms, and 550 rpm, resulting in optimal outcomes of around 35% smoothness and 20% deviation in micro holes. The ML model employing Bayesian regularization confirmed the optimal results with minimal deviation ranging from 0.45 to 2.87%. It was concluded that the enhancement in quality characteristics under optimal conditions suggests the industrial viability of this process for micro drilling glass composite materials.

1.7 RESEARCH GAPS IDENTIFIED

Despite advancements in Electrochemical Discharge Micro-Grooving (μ-ECDG) process, significant challenges remain in its application for micro-machining various glass surfaces, particularly flat and cylindrical ones. The majority of studies concentrate on macro-scale machining, neglecting micro-scale precision. There is very little research on micro-machining cylindrical glass surfaces using μ-ECDG process. Developing an experimental setup of μ-ECDG for such studies presents a valuable opportunity. Key challenges include a limited understanding of how various parameters such as voltage, electrolyte concentration, pulse duration, pulse frequency, and rotational speed of workpiece interact each other and influence different micro-groove geometry e.g., depth of groove, width of groove and surface quality. Additionally, most studies do not consider differences in glass composition such as silica and soda-lime glass which limits the ability to optimize the process universally. Another research gap is the lack of investigation into how different tool polarities affect machining performance. Finally, developing a mathematical model and optimizing process parameters could enhance the efficiency and precision of μ-ECDG process. In the μ-ECDG process, achieving a high Material Removal Rate (MRR) often necessitates increasing discharge energy, which can cause significant thermal effects on the workpiece surface. These thermal effects may lead to micro-cracks and an enlarged Heat-Affected Zone (HAZ), thus compromising surface integrity. Although a higher MRR boosts productivity, it usually results in diminished surface quality and dimensional accuracy. Recurring issues such as micro-cracks, heat-affected zones (HAZ) and inadequate dimensional control are common. Although there is an increasing focus on sustainable manufacturing, there is still limited research on eco-friendly or biodegradable electrolytes, such as those derived from plants or ionic liquids. μ-ECDG systems frequently depend on trial-and-error for parameter selection.

After thoroughly reviewing past research on electrochemical discharge machining and related studies, it is observed that very few studies have focused on micro-machining of cylindrical components composed of brittle, hard, and non-conductive materials. In particular, micro-grooving on glass has received little attention despite its considerable importance in various industrial applications. Therefore, it is essential to explore and develop machining techniques for this purpose.

1.8 THE OBJECTIVES OF THE PRESENT RESEARCH WORK

Literature survey done so far reveals that enough scope of research exists in the area of ECDG process. Hence, exhaustive experimentations are urgently needed to investigate thoroughly on various aspects of μ-ECDG process.

The objectives of the proposed research work are given as below:

(i) To develop an experimental set-up of Electrochemical Discharge Micro-Grooving (μ-ECDG)) process.

(ii) To investigate the effects of various process parameters such as applied voltage, types of electrolyte concentrations, duty ratio, pulse frequency, mixing ratio of electrolyte, and tool polarity etc. on different responses such as heat affected zone area, Overcut, material removal rate, geometrical accuracy etc. on flat workpiece of glass materials.

(iii) To explore the effects of various process parameters such as applied voltage, types of electrolyte concentrations, rotational speed of workpiece, tool polarity etc. on different responses such as material removal rate, width of groove and depth of groove on cylindrical workpiece of glass materials.

(iv) To establish mathematical models showing the relationship between different input process parameters and machining responses of μ-ECDG for grooving operation on cylindrical surface of glass and also to perform the optimal analysis of responses for finding suitable parametric condition for grooving operations by μ-ECDG process.

CHAPTER 2: DEVELOPMENT OF ELECTROCHEMICAL DISCHARGE MICRO-GROOVING (µ-ECDG) SYSTEMS

2.1 DETAILS OF µ-ECDG SETUP FOR MICRO-GROOVING ON FLAT SURFACE

To perform micro-grooving operation on flat surface of glass, an experimental set up is used which has been developed indigenously with lower cost and higher accuracy. The µ-ECDG experimental set up consists of three sub-units: (a) Mechanical hardware unit, (b) Electrolyte supply unit and (c) DC power source.

2.1.1 Mechanical hardware unit

One of the most vital parts of the µ-ECDG setup is the mechanical hardware unit. It consists of the main components such as (i) machine chamber, (ii) workpiece and tool holding units and (iii) workpiece feeding arrangement. The machining chamber is made up of Perspex as it is a transparent material and also possesses the shock resistance property.

The tool holder is made up of mild steel and at the end a screw-nut system is used to hold the micro-tool. The schematic diagram and photographic views of µ-ECDG setup are shown in Fig. 2.1.

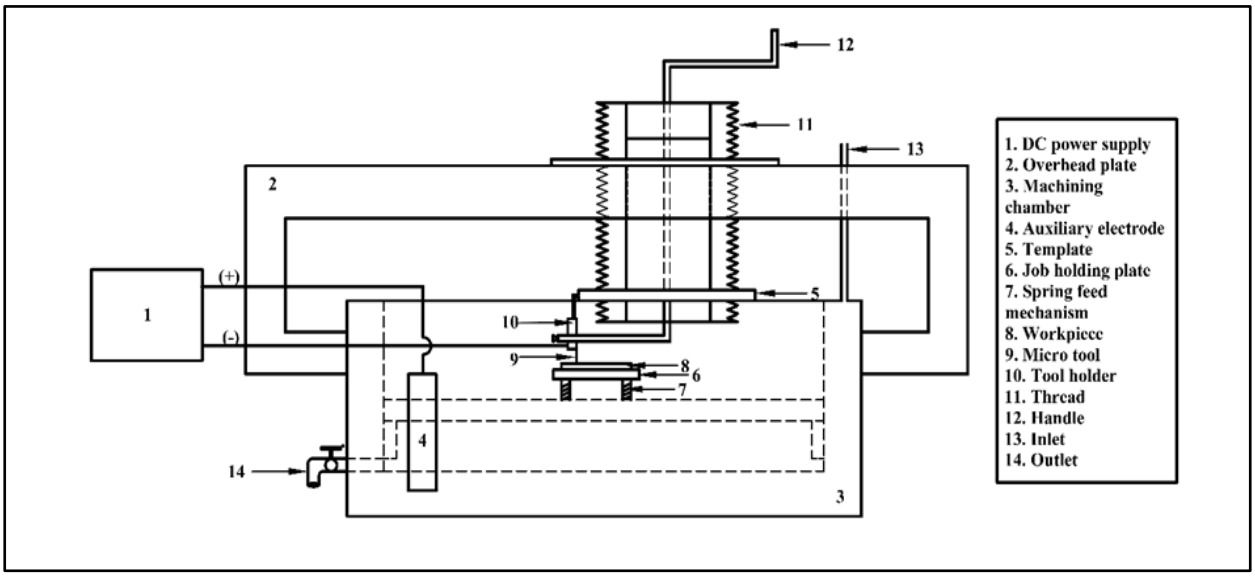

Fig. 2.1: Schematic diagram of developed µ-ECDG setup used for flat surface

A curved profile is created on the outer periphery of a template, which is attached to the tool holding unit in such a way that the tool holder can move around the same profile. A rotational motion is fed to the µ-tool through the tool holder with a hand operated lever. The feed motion is given to a job material by means of spring-feed mechanism in which the workpiece holding

unit is placed on four springs to keep the workpiece always in touch with the micro-tool electrode during machining.

2.1.2 Electrolyte supply unit

To achieve improved machining performance, such as a high material removal rate and minimal overcut, the generation of gas bubbles resulting from the electrochemical reaction between the tool and electrolyte play a crucial role. These bubbles should form at the bottom edge of the tool electrode. To maximize bubble generation, a stagnant electrolyte is used; otherwise, the bubbles would disperse from the machining zone. Therefore, the electrolyte level is carefully maintained by regulating the flow control valve, which is connected to the supply line from the electrolyte supply unit.

2.1.3 DC power source

In an electrical power system, a DC power supply is utilized, incorporating a voltmeter and an ammeter with a digital display unit to regulate the applied voltage in µ-ECDG process. This DC power supply ensures a constant polarity during machining. For micro-grooving operations using a cylindrical tool, the required voltage ranges from 20 to 55 V, with a machining current of less than 2 amps. To meet these requirements, a three-phase AC supply ranging from 0 to 200 V is employed and rectified using a silicon diode-controlled rectifier unit. A digital oscilloscope is connected to the power supply unit to adjust and record process parameters such as voltage, pulse frequency, and duty ratio. The oscilloscope enables real-time observation of varying signal voltages, typically displayed as a two-dimensional plot of one or more signals over time. Fig. 2.2 presents a photographic view of the µ-ECDG setup, including the power supply and digital oscilloscope, used for generating micro-grooves on a flat glass surface.

2.1.4 Specification of µ-ECDG setup used for flat surface

The detailed specifications for the various subsystems of newly developed µ-ECDG setup are as follows:

Maximum workpiece dimension:	60 mm X 60 mm X 5mm.
Maximum IEG:	50 mm.
Size of machining chamber:	250 mm X 200 mm X 180 mm.
Maximum horizontal movement:	170 mm.
Auxiliary electrode material:	Graphite plate (100 mm X 100 mm X 10 mm)
Capacity of reservoir tank:	8 lit

Workpiece feeding arrangement: Spring feed.

Tool material: Stainless steel Diameter (300-400µm)

2.1.5 Specification details of electrical power supply unit

Main input power supply: 3 phase 440 V A.C.

Power supply: Pulsed D.C.

Voltage range: 0 to 200 V

Range of current: 0 to 5 A

Range of pulse frequency: 50 Hz to1.2kHz

Range of duty ratio: 30% to 80%

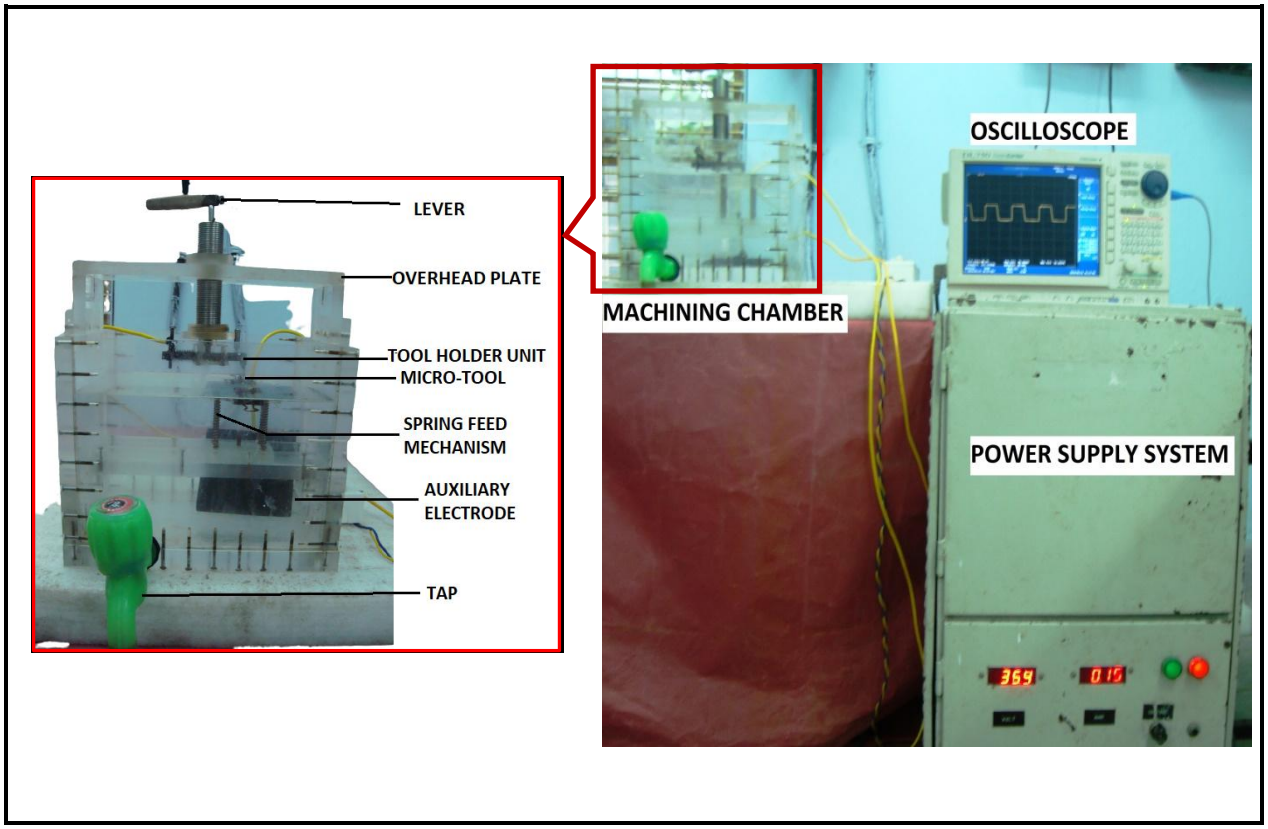

Fig. 2.2: Photographic view of µ-ECDG setup with power supply system

2. 2 DETAILS OF μ-ECDG SETUP DEVELOPMENT FOR MICRO-GROOVING ON CYLINDRICAL SURFACE

The experimental setup for the μ-ECDG process includes several mechanical and electrical components, such as a main machine chamber, a job holding and rotating unit, a tool holding unit, an auxiliary electrode unit, an electrolyte supply system, and a tool feeding arrangement.

2.2.1 Mechanical Hardware System

To achieve the objectives of the current research work, a custom-designed μ-ECDG setup has been developed. The mechanical hardware system of the μ-ECDG setup, developed indigenously, includes the following subsystems a) Main Machining Chamber, b) Job holding and rotating unit c) Tool Holding unit d) Auxiliary electrode unit and e) Job feeding arrangement

Fig. 2.3 shows the 3D view of the newly developed μ-ECDG setup. The main machining chamber is constructed from Perspex, chosen for its transparency and shock-resistant properties. In this process, a flat rectangular graphite plate serves as the auxiliary electrode, submerged in the electrolyte solution and connected to the DC power supply's positive terminal. A stepper motor rotates the cylindrical workpiece at a specific spindle speed and the speed of the workpiece can be regulated though a spindle speed controller. The tool electrode, mounted on an XZ table, is fed using a spring feed mechanism for linear movement. The rotational movement of job materials draws fresh electrolyte solution into the Inter-electrode Gap (IEG). μ-ECDG involves numerous factors, and selecting these through trial-and-error is crucial. Key parameters influencing machining responses such as Material Removal Rate (MRR), accuracy, overcut, and surface finish include applied voltage, electrolyte concentration, pulse frequency, duty ratio, tool polarity, spindle speed RPM, and the IEG between tool and workpiece. These parameters are identified using the trial-and-error method. The workpiece's rotational speed is a critical process parameter, and controlling it presents a significant challenge. Fig. 2.3 shows the 3D model of μ-ECDG setup used for cylindrical surface while the photographic view is illustrated in Fig. 2.4. The setup comprises several subsystems, which are discussed individually in the following sections.

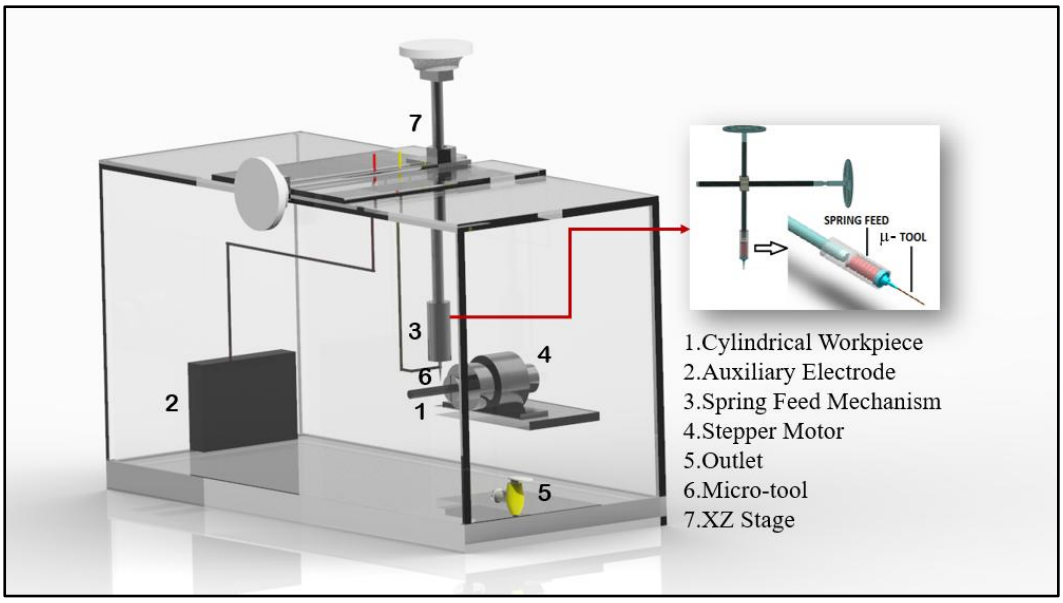

Fig. 2.3 3D Model of μ-ECDG setup used for cylindrical surface

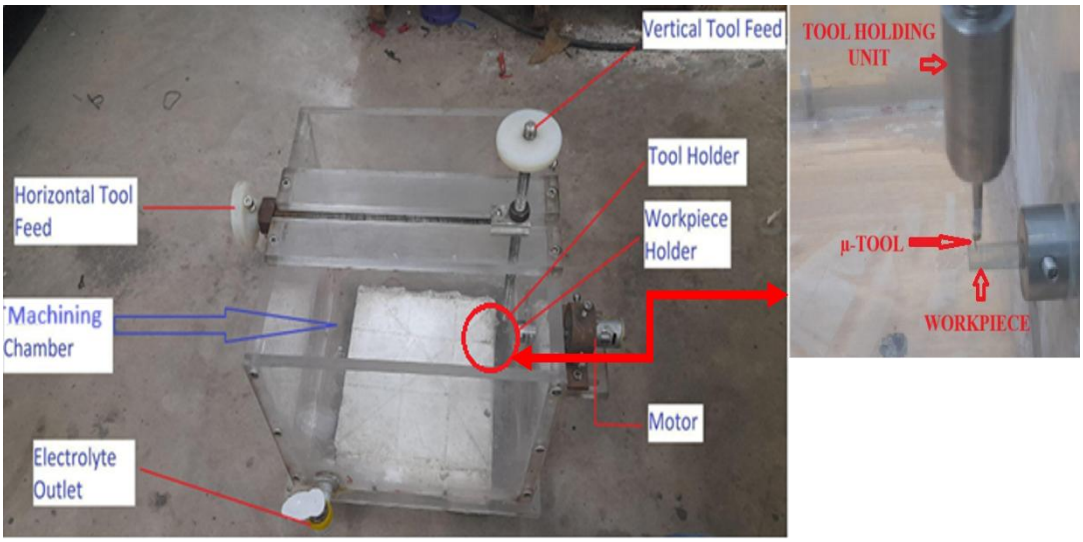

Fig. 2.4 Photographic view of μ-ECDG setup

2.2.1.1 Main machining chamber

Fig. 2.5 illustrates the 3D CAD drawing of the main machining chamber of μ-ECDG setup. The primary components of the machining system in a μ-ECDG setup are enclosed within the main machine chamber. This chamber is intended for housing the rotational workpiece, tool, and auxiliary electrode. It is constructed from Perspex, a non-conductive, corrosion-resistant polymer that is compatible with the electrolyte. The workpiece rotates horizontally, while the tool is positioned vertically. The auxiliary electrode is situated at a fixed distance from the workpiece inside the chamber. To stop the electrolyte from leaking during micro-machining operation, the chamber is carefully constructed. An oil seal was used to prevent the leakage of

electrolyte through the hole where the spindle is inserted into the chamber to control the rotating speed of the workpiece. It features an open top for direct electrolyte input and a bottom valve for draining post-operation. The chamber's dimensions are determined by the workpiece and tool specifications. The newly developed chamber measures 25X25X20 cubic centimeters, with 10 mm thick side walls. The chamber has a 6 litres capacity to hold electrolyte for the micro-grooving operations.

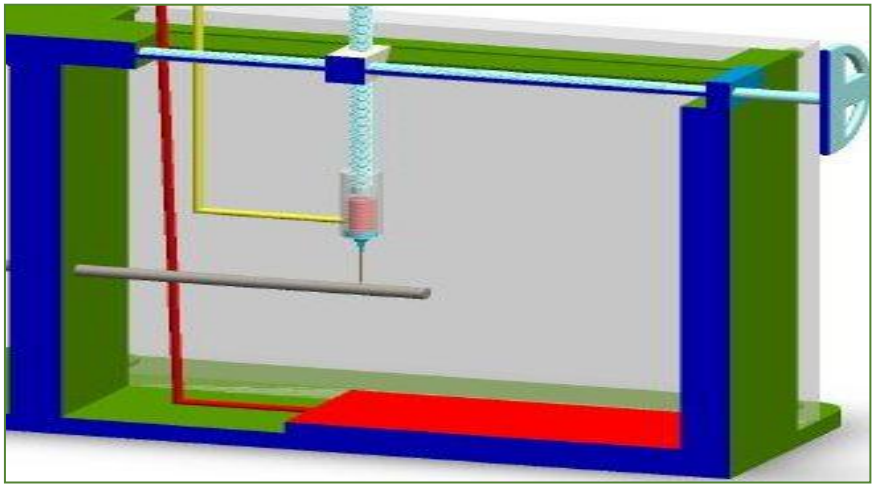

Fig. 2.5 3D CAD drawing of the main machining chamber with tool holding arrangement

2.2.1.2 Job holding and rotating unit

In order to secure and rotate the workpiece during the combined electrochemical and spark discharge machining, the μ-ECDG method makes use of a specialized component. Smooth finishing and uniform material removal are made possible by proper controlling the speed of workpiece. Accurate regulation of rotational velocity and orientation is crucial for ensuring that manufactured components meet the specified requirements, including the necessary level of intricacy, surface quality, and dimensional precision. The job holding and rotating unit, which safely holds and rotates the workpiece during machining, is an important component of the μ-ECDG setup. The cylindrical workpiece is rotated at a precise spindle speed using a stepper motor, and the spindle speed can be adjusted using a spindle speed controller. 3D CAD model of job holding unit is shown in Fig. 2.6. This unit provides controlled rotational movement and can be motor-driven or manually operated. In the developed setup, a 12 V input motor is utilized for workpiece rotation. The rotation speed and direction can be modified to suit particular machining needs.

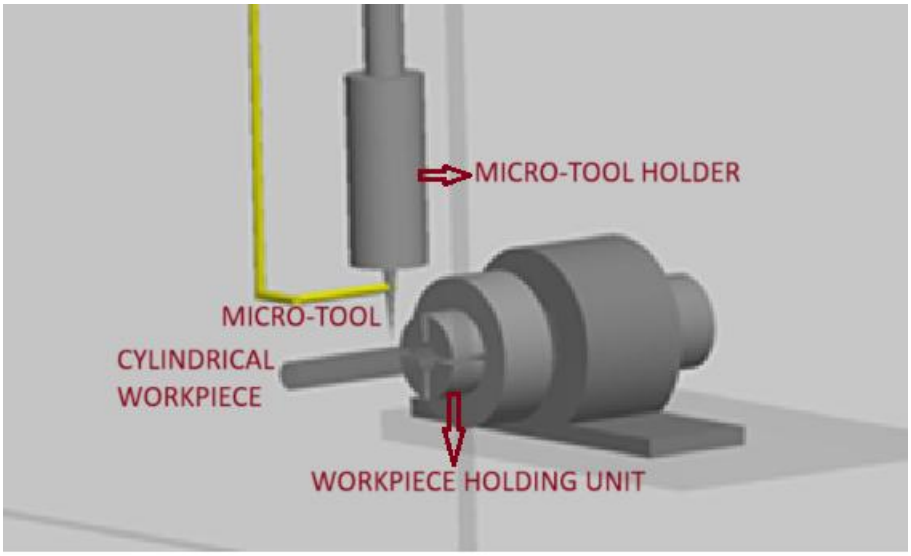

Fig 2.6 3D CAD drawing of job holding and tool holding unit

2.2.1.3 Tool holding unit

Fig.2.6 shows the tool holding unit along with micro-tool. In µ-ECDG setup, a tool holding unit featuring a spring feed mechanism offers an effective approach for precise tool feed control, especially in sensitive or high-precision machining like micro-grooving operation. The combination of its straightforward design and ability to sustain consistent tool pressure makes it a first choice for various applications. Implementing a spring feed mechanism streamlines the control system by naturally adjusting the feed rate according to spring tension and tool resistance. In this research study, a mild steel tool holder, along with a screw-nut system at the end of the tool holding unit, is used to secure the micro-tool. It was designed to accommodate any cylindrical tool for creating micro-grooves or channels on the workpiece.

2.2.1.4 Auxiliary electrode unit

The auxiliary electrode unit plays an important role in µ-ECDG setup. It comprises a graphite plate in rectangular shape positioned parallel to the machining electrode as illustrated in Fig. 2.7. The large surface area of this graphite plate enhances the machining process efficiency. Being an excellent electrical conductor, the graphite plate offers a low-resistance pathway for electricity. Additionally, it helps narrow the electrical discharge gap between the machining electrode and workpiece, resulting in reduced machining time and improved surface quality. Essentially, the auxiliary electrode unit plays a crucial role in improving the machining performance and productivity of the µ-ECDG setup.

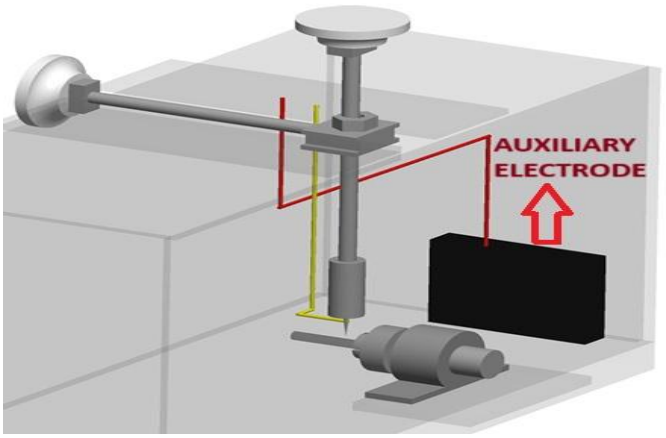

Fig. 2.7 3D CAD drawing showing auxiliary electrode

2.2.1.5 Tool feeding arrangement

Tool feed arrangement is also an important aspect of µ-ECDG process. It involves precisely controlling the tool electrode's movement relative to the workpiece to achieve the desired material removal and shape during micro-grooving process. The specific setup and machining requirements determine the tool feed arrangement in µ-ECDG process. The tool feeding arrangement in µ-ECDG process should be meticulously designed and controlled to meet machining objectives. It must consider factors such as dimensional accuracy, surface finish requirements, material removal rate, and workpiece material properties. Optimal tool feeding arrangements, combined with suitable feed rates and control mechanisms, contribute to efficient and precise µ-ECDG operations. The overhead plate of the chamber is attached to the tool holding unit using a screw-nut mechanism, allowing for adjustable tool positioning as needed. This setup enables vertical movement of the tool holding unit. For horizontal motion, the tool electrode is mounted on an XZ table, with a spring feed mechanism providing the necessary feed. The tool holding unit is guided by springs, which supply the feed for the tool's vertical movement during cross feed and horizontal movement during longitudinal feed. Fig. 2.8 illustrates the tool holder unit with the micro-tool.

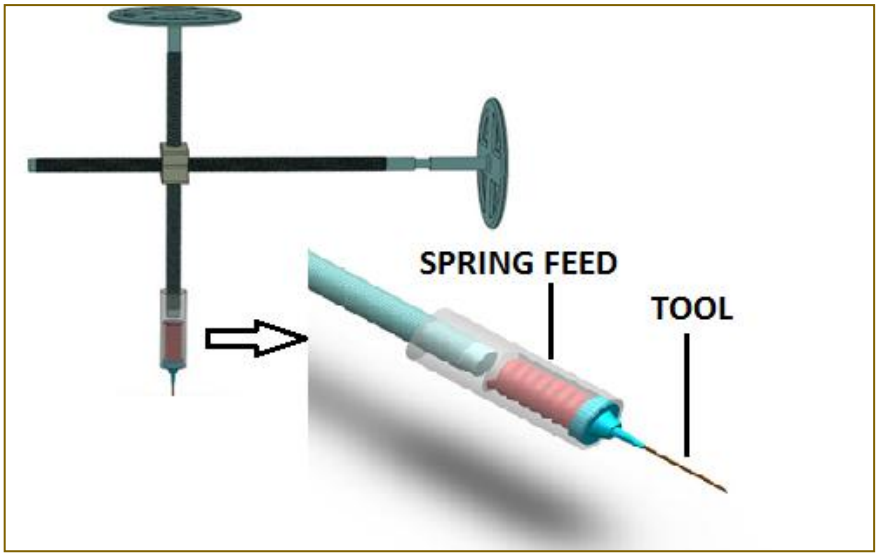

Fig. 2.8 3D CAD drawing of tool holding unit with μ-tool

2.2.2 Electrolyte Supply and Control Unit

To achieve superior machining results, characterized by high MRR and minimal overcut, it is essential to generate gas bubbles through the electrochemical reaction between the tool and electrolyte. These bubbles should form at the cathode tool's bottom edge. A stagnant electrolyte is employed to promote high gas bubble generation, preventing the bubbles from dispersing away from the machining area. The electrolyte's upper level is carefully regulated using a flow control valve connected to the electrolyte supply unit.

The electrolyte supply system plays a vital role in μ-ECDG setup. Depending on the circumstances, the electrolyte either circulates through the workpiece and tool during machining or submerges both components. Selecting the appropriate electrolyte is critical, considering the workpiece material and desired post-turning quality. Fig. 2.9 presents different types of electrolytes that can be used in μ-ECDG process. The electrolyte's concentration significantly impacts machining performance. In the developed setup, the electrolyte is directly poured into the open-top turning chamber from above. Upon completion of the micro-grooving operation, the electrolyte can be drained through a valve installed at the bottom corner.

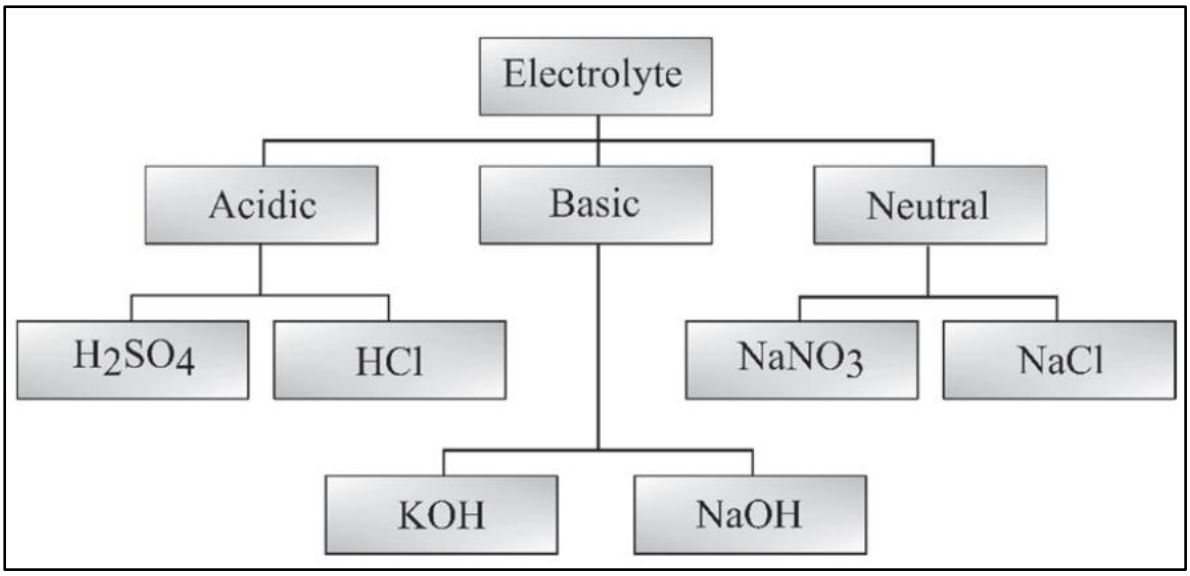

Fig. 2.9 Different types of electrolytes

2.2.3 Power Supply and Control Unit

A DC power supply unit is employed to supply the electrical energy needed to produce discharges and regulate process variables such as voltage, current, duty factor, and frequency. A digital multimeter and an oscilloscope are measurement devices that can be incorporated into the μ-ECDG setup to enhance efficiency and accuracy by monitoring process parameters and performance. μ-ECDG process involves the use of high voltage, which can pose significant risks during both setup and operation. Therefore, it's crucial to implement appropriate safety measures to protect operators and equipment. It should be ensured that all electrical components are properly insulated to prevent accidental contact with live parts, and emergency shutdown systems must be in place to quickly cut off power for stopping the machining operation. The control unit handles the input voltage and current, adjusts pulse frequency and duration, and keeps an eye on the system for any problems, alerting the operator if needed. A pulse generator creates pulses that control the rate at which material is removed. In electrochemical discharge applications, pulse power supplies are often used because they can precisely control electrical discharge and briefly produce high peak currents. For low-current tasks, DC power supplies are typically used, while AC power supplies are preferred for high-frequency pulsing. The choice of power supply and control unit depends on the specific needs of the experimental setup. In experiments, selection is guided by what is available, practical, and capable of meeting the set objectives.

In μ-ECDG process, a DC power supply with a voltmeter unit is used to regulate the applied voltage. This DC power supply maintains constant polarity during ECDM machining. Micro-

grooving cutting with a cylindrical tool requires a voltage range of 20 to 55 V and a machining current below 2 amps. To meet these specifications, a three-phase AC supply ranging from 0 to 200V is utilized and rectified by a silicon diode-controlled rectifier unit. In µ-ECDG process, a rectifier transformer is commonly employed to convert the input AC voltage to the required DC voltage for electrochemical discharge machining operations. This rectifier transformer is essential in providing the necessary power supply to the µ-ECDG setup. The power supply device may be used with a digital oscilloscope to record and modify process parameters such as voltage, pulse frequency, and duty ratio. The oscilloscope enables observation of continuously varying signal voltages, typically as a two-dimensional plot of one or more signals over time.

2.2.4 Tool Electrode Development

The design and manufacturing of the cathode, referred to as the tool electrode, are essential for the fabrication of ECDM tools. This component must generate electrical discharge with minimal wear to achieve the desired machining dimensions. For the electrode material to withstand the high temperatures and current density generated during the process, it must have excellent wear resistance in addition to good electrical and thermal conductivity. In µ-ECDG process, materials such as copper, brass, tungsten, stainless steel, etc. are commonly used as tool electrodes. For this study, a copper tool was selected as micro-tool based on preliminary experiments comparing copper and stainless-steel tool electrode. Copper is more widely available and showed less wear. The tool is secured using a spring-based arrangement, as illustrated in Fig. 2.10.

The shape and dimensions of the tool electrode are determined by specific machining requirements, including the desired workpiece shape, size, and surface finish. In applications such as micro-machining, the development of small-scale tools is needed, as tool precision directly affects the end product's quality. The final form and surface qualities of the grooved produced on workpiece are influenced by the shape of the tool. Considering the workpiece material and the necessary level of accuracy and precision, a cylindrical tool electrode with a diameter of 280µm was chosen in this research work.

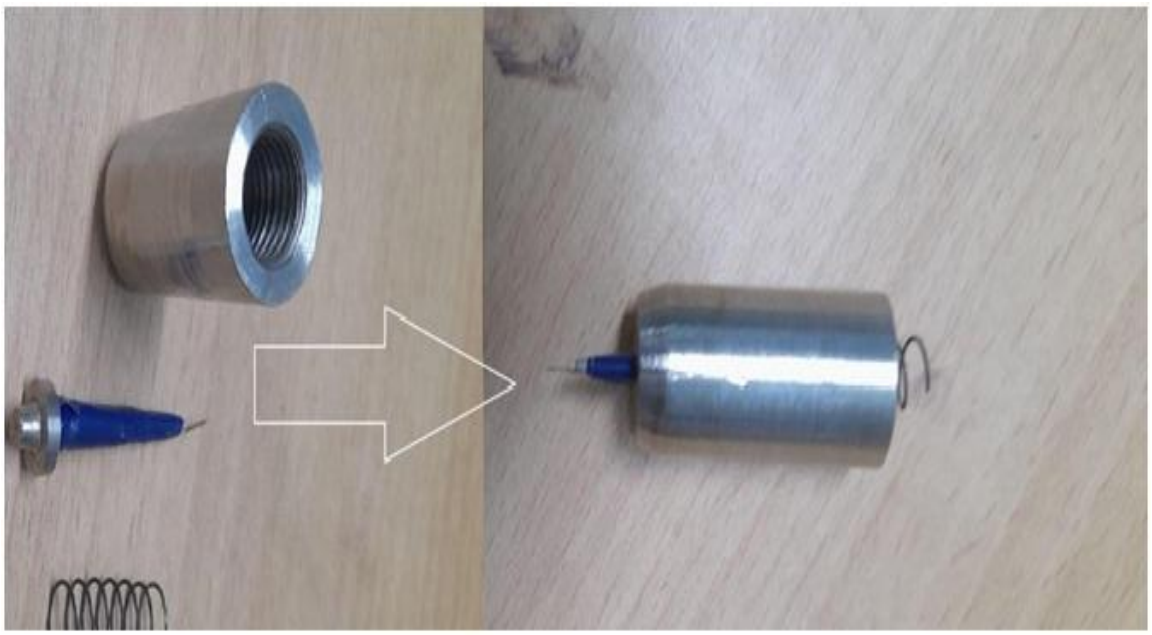

Fig. 2.10 Tool and it's assembly

2.2.5 Detailed Specifications of µ-ECDG Setup

The details specifications of newly developed µ-ECDG setup are given below:

- Size of machining chamber: 270 mm X 270 mm X 10 mm
- Maximum movement of tool in horizontal direction: 20mm
- Maximum movement of tool in horizontal direction: 14 mm
- Maximum diameter of workpiece that can be machined: 6 mm
- Spindle speed Range (RPM): 0-100 RPM
- Electrolyte tank capacity: 6 litres
- Max IEG gap: 80 mm
- Auxiliary electrode: Graphite plate (100 mm X 100 mm X 10 mm)
- Tool electrode: Coper (200-300 µm)

2.2.5.1 Details of Electrical Power Supply

- Input Voltage: 3 phase 440 V A.C.
- Power supply: Pulsed D.C.
- Voltage range: 0 to 200 V
- Range of current: 0 to 10 A.
- Pulse frequency: 50Hz
- Duty Ratio: 0.5

2.2.5.2 Details of Stepper Motor Used

- **Type:** Bipolar Stepper Motor
- **Step Angle:** 1.8°
- **Torque:** 1.2 Nm
- **Voltage:** 3.2V
- **Current:** 2.5A
- **Shaft Diameter:** 6.35mm (1/4 inch)
- **Inductance:** 4.8 mH
- **Resistance:** 1.2Ω
- **Rotational speed range:** 0-100 RPM

2.3 OUTCOME OF THE PRESENT RESEARCH

A well-designed experimental setup for μ-ECDG process is essential for achieving high performance, precision, and efficiency. Important parameters such as electrolyte concentration, applied voltage, inter-electrode gap, duty ratio, and pulse frequency must be carefully selected and controlled to enhance machining accuracy and material removal rate. Two different types of experimental setup have been developed and modified to enable the production of micro-grooves on both flat and cylindrical surfaces of glass. The multiple trial experiments are conducted utilizing the developed experimental setup and the satisfactory machining performances are observed during μ-ECDG operation on flat and cylindrical surface of glass.

CHAPTER 3: MATERIALS AND METHODS

3.1 EXPERIMENTAL SCHEME

Previous chapters have detailed the potential of the electrochemical discharge micro-grooving (μ-ECDG) process, its fundamental mechanisms, and design and development of μ-ECDG setup. While numerous techniques exist for machining conductive materials, options for electrically non-conductive hard and brittle materials are limited and have constraints. Recognizing the significant potential of this hybrid machining technique for machining of non-conductive materials, a series of pre-planned experiments were conducted. These experiments aimed to thoroughly examine and analyze process parameters, leading to definitive conclusions and determining optimal machining conditions for μ-ECDG in micromachining domain with nonconductive materials. The upcoming sections outline the essential steps for systematically planning and executing this research work.

The experimental design has been crafted to effectively meet the study's objectives. In the μ-ECDG process, both the workpiece and tool experience material loss due to thermal effects, while the machined groove's dimensions deviate from exact measurements because of sparking from the tool's side wall. Extensive study of previous research reveals that the most influential process parameters in μ-ECDG are the applied voltage, electrolyte concentration, and the rotational speed of the workpiece. This research focuses on investigating μ-ECDG characteristics, such as Material Removal Rate (MRR), Width of Groove (WG) and Depth of Groove (DG) during micro-grooving operation on glass.

3.1.1 Selection of Process Parameters

In the experiments, applied voltage, electrolyte concentration, and rotational speed of workpiece are the key process parameters under consideration. Numerous trial experiments were conducted to determine the appropriate ranges for the input process variables. The machining time was kept constant across all the experiments. All the experiments were conducted at a fixed inter-electrode gap of 50 mm.

(i) Applied Voltage: The electric potential difference between the tool electrode and workpiece is determined by the applied voltage. This applied voltage is an important parameter for micro-grooving on both flat and cylindrical surfaces and it affects different responses. Selecting the appropriate voltage, it requires balancing efficient material removal with avoiding excessive discharge energy, which could cause undesirable effects like surface damage or tool wear.

Initial tests revealed that bubble generation started when applied voltage cross 15-20V and sparking began between 27-30 V. At 30 V, only a machining surface impression was created without significant material removal but after 32V notable amount of material removal took place. The lower voltage limit was set at 35 V, as it produced a prominent profile of micro-grooves while voltages above 60 V resulted in width of grooves exceeding 500 µm. Consequently, five voltage levels i.e. 35 V, 40 V, 45 V, 50 V, and 55 V were selected for the experiments.

(ii) Type of electrolyte and its concentrations: Electrolyte composition is another important factor in electrochemical discharge process. The electrolyte and its concentration affect conductivity, chemical reactions, and dissolution characteristics during µ-ECDG process. Various electrolytes can influence material removal rate, surface finish, and tool life differently. Aqueous solutions of $NaNO_3$, NaCl, NaOH, and KOH can serve as electrolyte solutions. However, previous research [1] showed that NaCl and $NaNO_3$ resulted in low material removal due to minimal sparking and low MRR, despite reducing overcut of the machined profile. So, in this research study experiments were conducted using NaOH and KOH electrolyte solutions at 10, 15, 20, 25, and 30 wt% concentrations.

(iii) Rotational speed of workpiece: The third input process parameter considered is the rotational speed of workpiece. This parameter is selected for micro-grooves on cylindrical surface of glass. It is the speed at which the workpiece rotates during micro-grooving operations. Trials experiments showed that the rotational speed of workpiece highly affects the material removal rate and width of grooves. Initial experiments showed that at higher rotational speed (>60 rpm) very less amount of material was removed and machining depth of grooves was also reduced. To study the effect of the rotational speed on the selected machining criteria during micro-grooving operations on glass, five levels of rotational speed i.e. 10, 20, 30, 40 and 50 rpm were chosen.

(iv) Duty Ratio: In the µ-ECDG technique for creating micro-grooves on flat surfaces, duty ratio has been selected as a key input parameter. This factor significantly impacts machining performance, particularly in MRR, surface quality and the extent of the Heat Affected Zone (HAZ). A well-selected duty ratio helps in controlling the HAZ, thereby reducing thermal damage to the workpiece. An optimal duty ratio can enhance MRR in the machining area by regulating both thermal and chemical effects. For experimental purposes various duty ratio levels in percentage were chosen including 45, 50, 55, 60, and 65%.

(v) Tool Polarity: During trial experiments, it was observed that tool polarity significantly affects various output responses, including material removal rate, groove width, and tool wear. This process parameter has been selected for micro-grooving on both flat and horizontal surfaces. Positive tool polarity refers to the setup where the workpiece is connected to the positive terminal and the tool to the negative terminal and it is known as Direct Polarity (DP). In Reverse Polarity (RP) that is also known as indirect polarity which refers to the conditions when the tool electrode is connected to the positive terminal, and the workpiece is connected to the negative terminal. In this study, effects of tool polarity on different machining criteria were also examined.

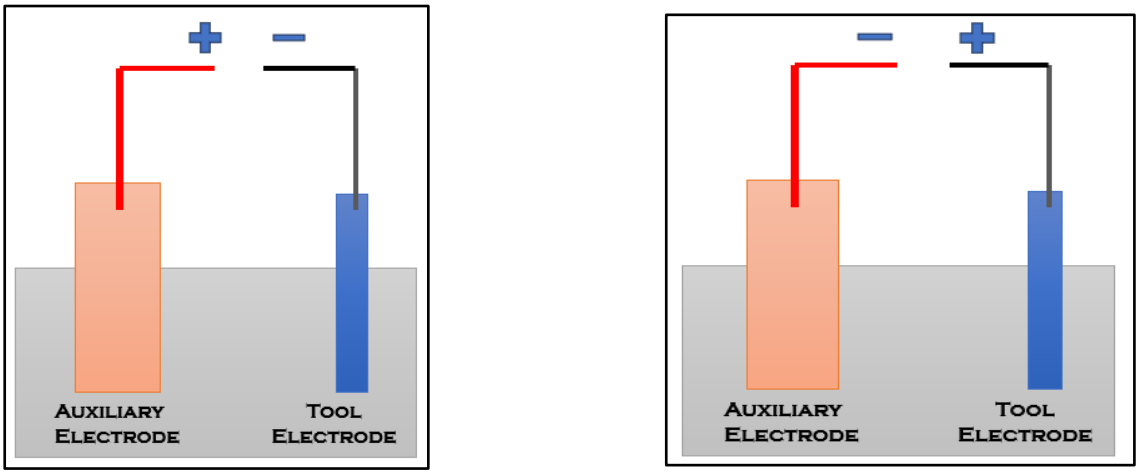

Direct Polarity Reverse Polarity

Fig. 3.1 Convention of tool polarity

3.1.2 Selection of Responses

Optimizing machining processes of any technique requires careful consideration of different response parameters like Material Removal Rate, surface quality, machining depth and width. The selection of appropriate parameters is very important for enhancing the process efficiency, output quality and cost-effectiveness. These parameters ensure consistent, high-quality production, improve predictability and reliability of the process and allow for better process understanding and control. As a result, this improves problem-solving abilities, cuts down on waste, and lowers production costs, making the entire process more efficient and dependable. This study examined the following response parameters:

(i) Material Removal Rate (MRR): MRR is a key indicator of μ-ECDG process effectiveness. It measures how efficiently extra material is being removed from the job material during micro-grooving operation on glass. So basically, MRR measures the speed of material removal. Higher MRR values indicate faster machining, thereby increasing process productivity. Optimising MRR aids in striking a balance between precision and surface finish quality and machining speed, especially when dealing with challenging materials such as ceramics or glass. It also reflects the efficiency of material removal from the workpiece, directly impacting the overall time and cost associated with machining.

(ii) Width of Groove (WG): The quality and dimensional accuracy of the machined component are determined by the groove width. Maintaining precise width is required in the fields of applications such as microfluidics or biomedical device manufacturing, to ensure that micro-features meet design specifications. The width of the groove was measured using an optical microscope at a magnifications of 5X. Fig. 3.2 shows the schematic diagram of width of groove on a cylindrical surface.

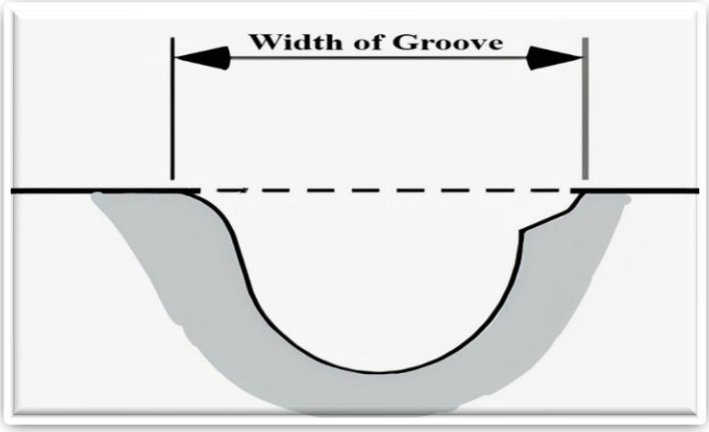

Fig. 3.2 Width of micro-groove on workpiece

(iii) Depth of Groove (DG): The proper depth of groove is required for achieving desired features or patterns on the workpiece. Accurate control of the machining depth ensures the production of micro-grooves or cavities that conform to required specifications. This is particularly important for applications demanding precise micro-features. Fig. 3.3 shows the schematic diagram of depth of groove on a cylindrical surface.

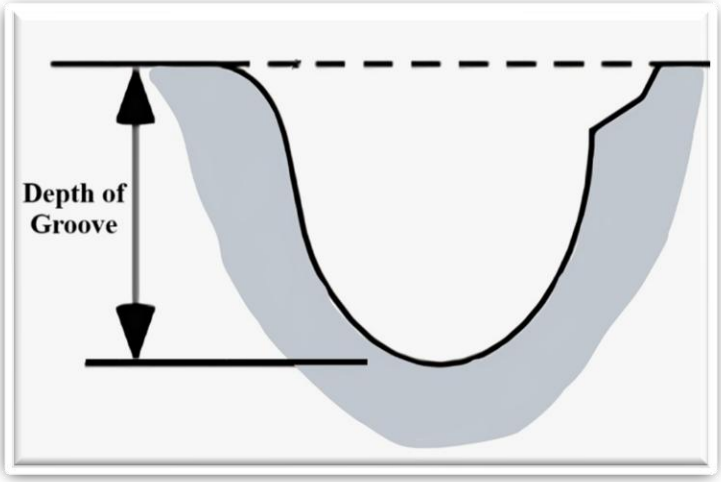

Fig. 3.3 Depth of micro-groove on workpiece

(iv) Overcut (OC): Overcut is defined as the unintended removal of material beyond the desired dimensions of the machined feature. This is an important response parameter for micro-groove on flat surface. In μ-ECDG process overcut presents a significant challenge due to the interplay of thermal, chemical and electrical discharge effects. Overcut reduces the resolution of fine features in micromachining, which compromises the geometric integrity of intricate patterns and results in detail loss. So, it is essential to measure the overcut in order to get high precision finishing.

(v) Heat Affect Zone (HAZ) area: Heat Affected Zone (HAZ) is an area adjacent to the machined surface that undergoes thermal modification due to the high temperatures produced during μ-ECDG process. This region experiences changes in its structure and mechanical properties without actually melting or being removed. HAZ plays an important role in determining the dimensional accuracy, surface quality and mechanical characteristics of the workpiece machined using this process. HAZ area is identified and measured using Leica microscope in μm^2. It is important to minimize HAZ area so that machining performance can be enhanced.

3.1.3 Selection of Workpiece Material

Choosing the appropriate workpiece material for a hybrid machining is important to ensure process compatibility. Thus, it will enhance the machining efficiency, reduce tool degradation, manage expenses and fulfill specific application needs. This selection enables manufacturers to exploit the benefits of particular machining techniques to create high-precision parts from materials that are typically challenging to machine, ultimately resulting in superior product quality and more efficient production processes. Thorough reviews of past research work have revealed that numerous conventional and unconventional machining methods exist for conductive metals such as aluminum, copper, titanium, and their alloys, as well as semiconductors like silicon and germanium. However, machining non-conductive materials presents challenges due to the lack of fully developed techniques for processing such hard and brittle substances**.**

In the present research study, glass is used as workpiece material for micro-grooving with the help of the newly developed hybrid machining method μ-ECDG. This, it will minimize the risk of damage and enabling smoother grooving, particularly on fragile or thin glass components. Glass materials are extensively used in various fields such as microfabrication, microfluidics, optics, and electronic components, where precise and delicate features are essential. This process provides the necessary level of control to achieve these dimensions with high accuracy. Fig. 3.4 shows the actual picture of workpiece before micro-machining. All the workpieces used for experimentation had a diameter of 4.5 mm and length of 3 cm each.

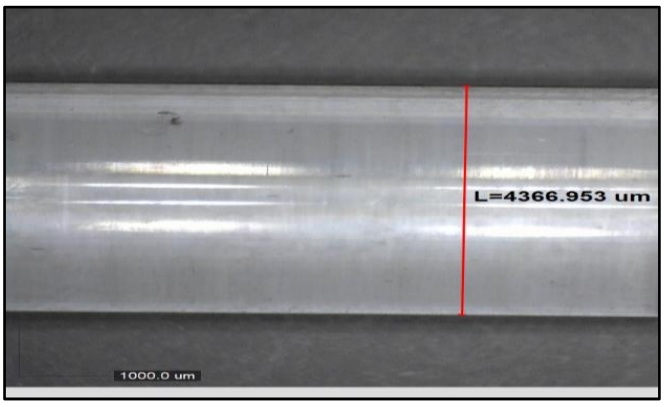

Fig. 3.4 Pictorial view of glass workpiece taken using DINO-microscope

3.1.4 Selection of Tool Electrode

To examine the effects of these process parameters on various machining criteria including MRR, width of groove and machining depth during micro-grooving using µ-ECDG technique, a tool diameter of 300 µm was initially selected. Using a tool diameter of 300 µm resulted in groove dimensions exceeding 500 µm. However, when a 280 µm tool diameter was used, the obtained dimensions were within the desired 500 µm range for the present micro-machining study. Copper rod was chosen as tool electrode because of their superior electrical and thermal conductivity, which guarantees good heat dissipation and efficient energy transmission. These materials produce consistent and accurate machining results because these are strong, resilient to wear, and retain their shape. In addition to being corrosion-resistant and simple to manufacture into complex shapes, copper is dependable and long-lasting. Fig. 3.5 illustrate the views of micro-tools before machining operation and those views are obtained using Leica Microscope.

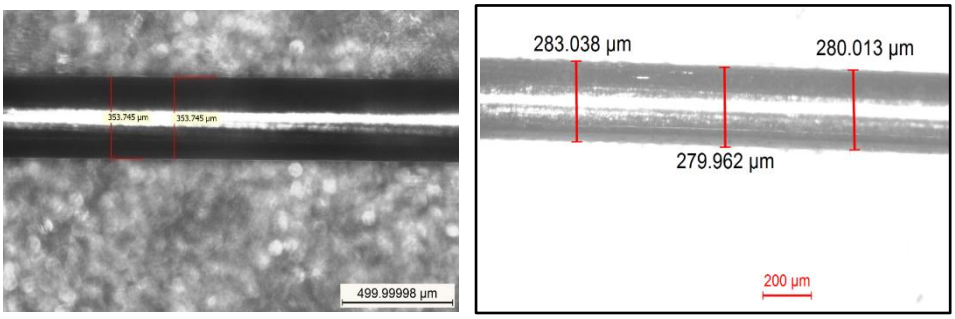

(a) (b)

(a) Stainless-steel micro-tool used for flat surface (b) copper micro-tool used for cylindrical surface

Fig. 3.5 Pictorial view of micro-tools before machining taken with Leica Microscope

3.2 PROPERTIES OF GLASS WORKPIECE

(i) Properties of Soda-Lime Glass:

In present research, Soda-lime glass is selected as workpiece material for micro-grooves on its cylindrical surface. Soda-lime glass is strong, clear, and resistant to chemicals, making it ideal for applications like microfabrication, microfluidics, optics, and electronics, where accuracy and delicate features are essential. Additionally, its resistance to water and mild acids makes it durable and well-suited for storing biomedical liquids. The most widely utilized kind of glass in a wide range of applications is soda-lime glass. Because of its unique qualities, soda-lime glass can be used in a variety of ways. Fig. 3.6 presents an in-depth review of its characteristics.

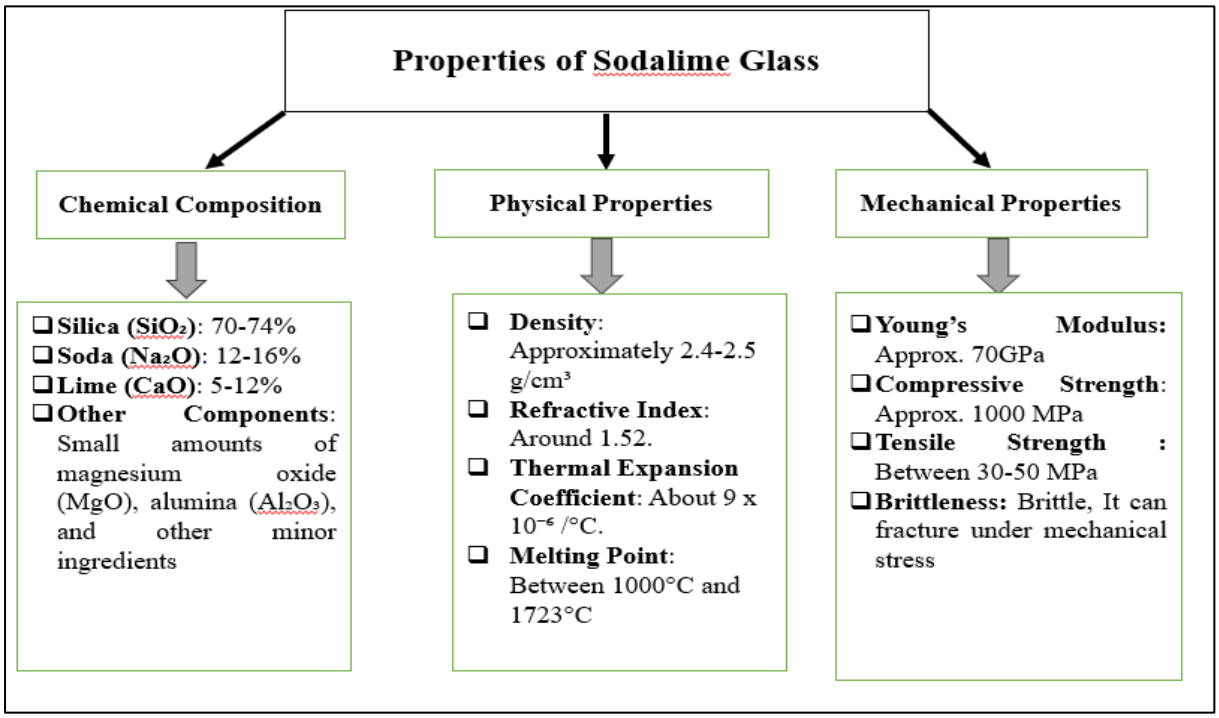

Fig. 3.6 Properties of sodalime glass

(ii) Properties of Silica Glass:

For micro-grooving on the flat surface of a workpiece, silica glass is selected due to its various applications in different industries. It has a tensile strength of 5.0×10^7 N/m², making it highly durable. Its thermal expansion coefficient is 0.54×10^{-6} K^{-1}, indicating minimal expansion with temperature change. The thermal conductivity of silica glass is 1.2 W/m-K, which contributes to heat resistance. The liquidus temperature is 1040°C, highlighting its high melting point. In terms of density, silica glass has a value of 2.52×10^3 Kg/m³, ensuring a balance between strength and weight. Its refractive index is 1.518, making it suitable for optical applications. Lastly, it possesses a Young's modulus of 7.2×10^{10} N/m², which defines its rigidity and elasticity under stress

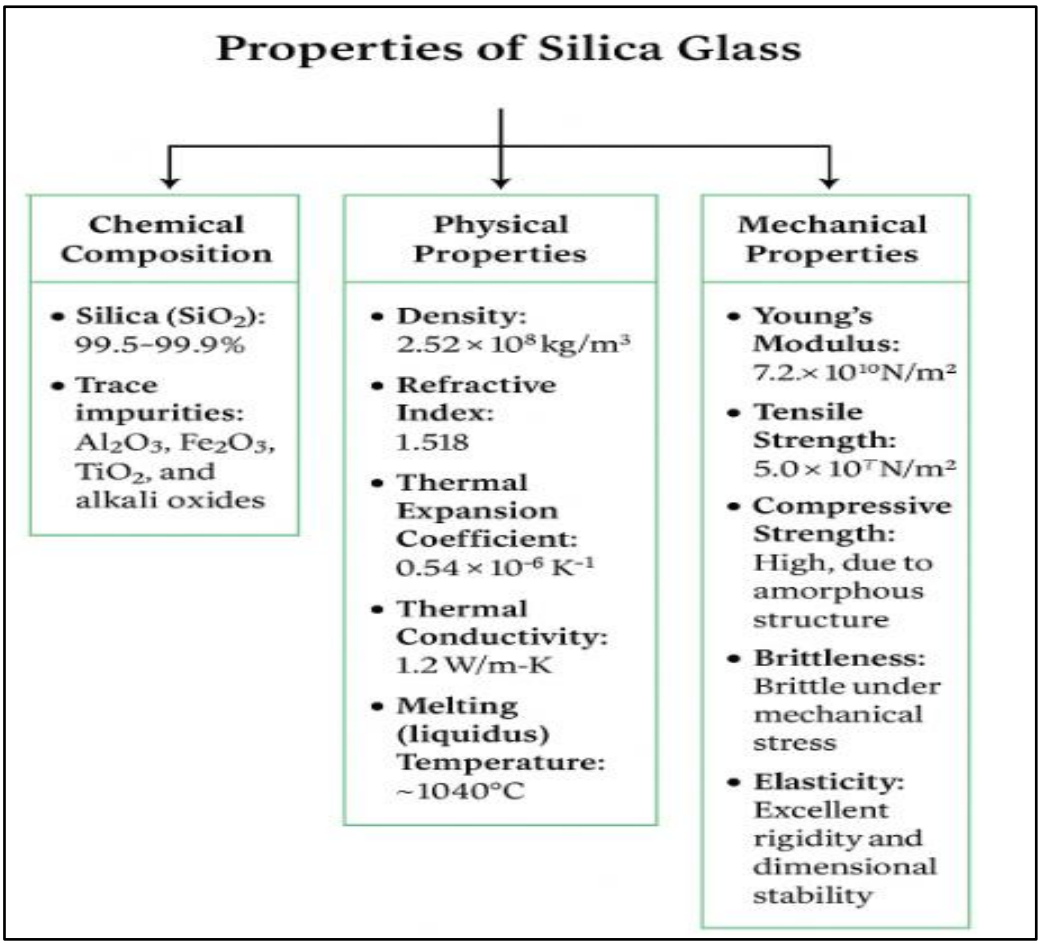

Fig. 3.7 Properties of Silica glass

3.3 DESIGN OF EXPERIMENTS

Design of Experiments (DOE) is a methodical strategy for planning, executing, and evaluating experiments to determine how different variables affect a process or result. Its primary objective is to enhance performances, boost quality, and pinpoint significant factors that affect impact outcomes. DOE enables researchers to efficiently examine multiple variables simultaneously, conserving time and resources while revealing important interactions between factors. This technique improves process quality and performance, yields reliable data for informed decision-making. In a nutshell, DOE is an effective tool for problem-solving and maximizing resource utilization. In the present research study, following DOEs were utilized to analyze the effects of different input process parameters on multiple responses and to identify the relationships between the input process variables.

3.3.1 One Factor at a Time:

One Factor at a Time (OFAT) serves as an experimental plan for initial factor exploration, helping to identify potentially significant variables before conducting more elaborate experiments. The straightforward nature of OFAT makes it easy to design and implement,

which is especially beneficial for beginners in experimental design. By altering only one factor at a time, OFAT clearly demonstrates the direct impact of individual variables on the outcome, aiding in understanding each factor's specific role. In the early stages of experimentation, OFAT can be more effective for preliminary testing. This approach makes it easier to analyze and understand the results by avoiding the complications that come with changing multiple variables at the same time. However, it's important to realize that while OFAT has its benefits, it may not be as efficient or thorough as more advanced methods like Design of Experiments (DOE), especially when dealing with multiple factors and how they interact. The following are the experimental conditions shown in Table 3.1 where the OFAT method is used to analyze the experimental results.

Table. 3.1 Experimental condition for micro-grooving on cylindrical surface on glass

Working Conditions	Description
Workpiece Material	Sodalime Glass
Tool Material	Copper (280 μm)
Applied Voltages(V)	35,40,45,50,55
Type of Electrolyte	KOH
Electrolyte Concentration (wt%)	10,15,20,25,30
Rotational speed (RPM)	10,20,30,40,50
Polarity	Direct Polarity, Reverse Polarity

3.3.2 Response Surface Methodology (RSM)

Response Surface Methodology (RSM) is a statistical approach used to optimize processes where the outcome is affected by several variables. In this technique, mathematical and statistical approaches employed to model and examine problems where multiple variables affect the outcome. RSM proves especially valuable when the connection between the outcome and variables is intricate and nonlinear. It finds widespread application in fields including manufacturing for enhancing product design, optimizing processes, and improving quality. RSM is a powerful tool for optimizing processes and analysing experiments. It helps researchers and engineers systematically explore how different factors affect a result. RSM helps analyze multiple factors and their interactions with fewer experiments, saving time and money. It gives a clear understanding of how variables affect the outcome, and using response

surface and contour plots makes it easier to visualize these relationships. Through the utilization of RSM, industries can enhance product quality, decrease expenses, and boost efficiency, it plays a vital role in current research and development activities. However, it assumes a quadratic relationship between factors and results, which may not always be accurate, and it works best with continuous factors rather than categorical ones.

The first step in RSM is to use a structured experimental design to systematically vary the factors. Common designs include Central Composite Design, Box-Behnken Design and Face-Centered Central Composite Design. In the present research work Central Composite Design (CCD) was used. Central Composite Design (CCD) is a key experimental design technique employed in RSM. It stands out as a preferred method for constructing quadratic models without the need for a complete three-level factorial experiment. The CCD framework incorporates three distinct point types: factorial, axial, and center points. This configuration enables the assessment of curvature in the response surface and is utilized to fit second-order polynomial models. CCD is very much efficient to construct quadratic model and effective for process or product optimization, helping to identify factor combinations that optimize the desired response.

The CCD structure comprises:

(a). Factorial Points: Derived from a factorial design, typically at -1 and +1 levels.

(b). Axial Points: Positioned along each axis at a specific distance (α) from the center, these points expand the factor space exploration.

(c). Center Points: Located where all factors are set to their midpoint values, these points aid in estimating model curvature and provide a measure of experimental error.

To study the effect of input process variables on different responses of the μ-ECDG process, and to construct a mathematical model establishing the relationship among various factors, the RSM method for Design of Experiments was used with 3 factors and 5 levels, using Minitab 17 software. The following Table 3.2 shows the combinations of input variables used to conduct the experiments.

Table 3.2 Experimental Conditions based on RSM for cylindrical surface

RSM_Central Composite Design_Unblock		Electrolyte: NaOH Tool Polarity: Direct Polarity	
Run	**Electrolyte Concentration(wt%)**	**Rotational speed (RPM)**	**Applied Voltage(V)**
1	15	20	40
2	25	20	40
3	15	40	40
4	25	40	40
5	15	20	50
6	25	20	50
7	15	40	50
8	25	40	50
9	10	30	45
10	30	30	45
11	20	10	45
12	20	50	45
13	20	30	35
14	20	30	55
15	20	30	45
16	20	30	45
17	20	30	45
18	20	30	45
19	20	30	45
20	20	30	45

3.4 MEASUREMENT OF RESPONSES

This study primarily focuses on three process outcomes: Material Removal Rate (MRR), Width of Groove (WG), and Depth of Groove (DG). The importance of these responses in connection with the micro-machining of glass material was discussed in the previous section under the selection of responses. This section will focus on how these responses of μ-ECDG process were measured.

(i) Material Removal Rate:

In μ-ECDG, MRR is defined as the volume of material extracted from the workpiece per unit time, typically expressed in μg/min or μg/sec. This study utilizes μg/sec as the unit of measurement. To determine the workpiece weight, a weight balance with specific characteristics was employed. The workpiece is weighed before and after the machining process using METTELER TOLLEDO weighing machine (LC of 1 x 10^{-4} gm). This device boasts a minimum measurement of 1 x 10^{-4} grams, making it an exceptionally accurate tool for tasks demanding high precision. Its sophisticated calibration capabilities ensure consistent performance over time, while its digital interface and data recording functions enhance user experience for intricate measurements and evaluations. The instrument can detect weight variations as small as 0.01 milligrams and is engineered to minimize external factors such as vibrations and air movements, thereby ensuring steady and precise measurements. The difference between these measurements represents the total amount of material removed. Dividing this amount by the total processing time yields the MRR for the machining operation. A stopwatch is used to record the machining duration. The MRR is calculated using the following formula shown in Eqn no 3.1.

$$MRR = \frac{W_1 - W_2}{t} \ \mu g/s. \qquad Eqn\ 3.1$$

Where,

W_1 = Weight of the workpiece before machining, in μg ;

W_2 = Weight of the workpiece after machining, in μg ;

t = Total time taken for the machining, in second

(ii) Width of Groove (WG)

In domains that need extreme precision, such as the production of biomedical devices or microfluidics, maintaining exact width of groove is essential to guarantee that micro-features as per requirements. A high-resolution microscope LEICA at magnifications of 5X was used

to capture detailed images of the micro-grooves on glass. This microscope is renowned for their exceptional optical performance, delivering sharp and comprehensive images with high magnification for scientific examination and meticulous work. These microscopes are distinguished by their high-resolution optics, adaptable design, and cutting-edge fluorescence imaging abilities, making them well-suited for both research and industrial uses. They incorporate built-in digital imaging systems for instantaneous visualization and analysis the micro-grooves generated using μ-ECDG process.

iii) Depth of Groove (DG)

In order to get desired features or patterns on glass, the depth of the micro-groove is crucial. Precise management of the cutting depth guarantees the creation of micro-grooves or cavities that meet the necessary requirements. Depth of micro-grooves were measured with the help of a Dino-Lite microscope. This microscope is compact digital microscope extensively utilized in industries and scientific research purposes. It interfaces with a computer or mobile device to provide magnified, high-resolution images and videos of minute objects or surfaces. The captured images are digitally displayed on a computer, enabling real-time observation, examination, and documentation.Fig. 3.7 shows the schematic diagram of depth of micro-grooves and Depth of micro-groove was measured with the help of following formula present in Eqn no. 3.2 using the image captured in Dino-Lite microscope.

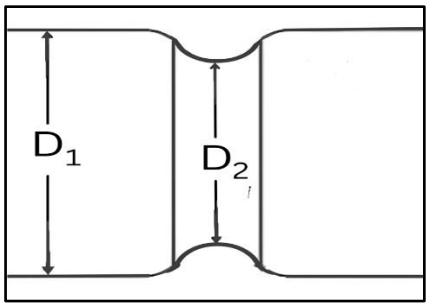

Fig. 3.8 schematic diagram showing depth of micro-grooves

$$Depth\ of\ Groove = \frac{D_1 - D_2}{2} \qquad Eqn\ 3.2$$

Where D_1= Diameter of workpiece before machining;

D_2 = diameter of grooved portion of workpiece.

3.5 PROCESS SEQUENCES:

The experimental procedure is outlined as follows:

i). Initially, the machining chamber is thoroughly cleaned using pure distilled water.

ii). Prior to machining, workpieces and micro-tool are weighed using a METTELER TOLLEDO weighing machine.

iii). A LEICA microscope at 5X magnification is utilized to measure the diameter of each micro-tool before machining.

iv). Micro-tools, supported by a spring, are properly attached to the tool holder, which is fitted to the XZ table.

v). The workpiece is secured with the workpiece holding unit which is coupled with the stepper motor for rotational motion. The speed of stepper motor is controlled by a speed controller.

vi). The workpiece is placed just beneath the tool tip, which is submerged 2 to 3 mm below the electrolyte's surface.

vii). A digital oscilloscope may be employed to set and record voltage and other parameters such as pulse frequency and duty ratio.

viii). For direct polarity, the tool connects to the negative terminal and the auxiliary electrode to the positive terminal of the power supply system. This configuration is reversed for reverse polarity, as shown in Fig. 3.1.

ix). Electrolyte level fluctuations due to boiling and evaporation are adjusted using a control valve unit in the machining chamber.

x). Each job has a constant machining time. Each machining operation is conducted for 10 minutes, timed by a stopwatch, according to the design of experiments.

xi). After machining, the main power is turned off, and the workpiece is removed and dried. Its weight is measured using the METTELER TOLLEDO weighing machine.

xii). Width of micro-groove is measured at 5X magnification using the LEICA microscope.

xiii). The Material Removal Rate (MRR) of the micro- is determined using the following formula shown in Eqn no 3.1.

xiv). The depth of micro-groove is measured with the help of a Dino-Lite Microscope using the the formula presents in Eqn no 3. 2.

3.6 OUTCOMES OF THE PRESENT RESEARCH

A well-defined experimental scheme ensures that the research is systematic, repeatable, and provides useful information. It involves careful planning of process parameters, responses, materials, and tools. In this study, various input parameters such as electrolyte concentration (EC), voltage, rotational speed of the workpiece and tool polarity are selected, as these directly influence the performance and quality of the process. Selecting appropriate responses is also very much important since it evaluates the machining performance of the experimental setup. The present research focuses on different responses, including material removal rate (MRR), width of groove and depth of groove during the micro-grooving operation on glass. A systematic experimental design helps to minimize the number of trials while providing deeper understanding of the process. In this study, both One Factor at Time (OFAT) and Response Surface Methodology (RSM) based experimental plans are used to conduct experiments, ensuring a in-depth analysis of the process.

CHAPTER 4: EXPERIMENTAL INVESTIGATION INTO ELECTROCHEMICAL DISCHARGE MICRO-GROOVING (μ-ECDG) ON FLAT SURFACE OF GLASS

4.1 EXPERIMENTAL SCHEME

The experimental scheme is designed in such a way that it can fulfil the purposes of present project and research work with a great satisfaction. In μ-ECDG process, removal of materials occurs from job as well as from tool due to thermal effect and the exact dimensional accuracy of machined channel is not obtained due to the sparking phenomenon from the tool's sidewall. Also, micro-cracks are developed because of thermal effect of electrostatic discharge. Therefore, three response parameters e.g. (i) Material Removal Rate (MRR), (ii) Heat Affected Zone (HAZ) area and (iii) Overcut (OC) have been identified as performance criteria. All experiments were conducted to study the effects of different process factors on various machining criteria.

In this study, the focus was on achieving a given micro-grooves width but there was no specific requirement on the micro-groove's depth. Though a dimension less than 1mm is literally considered in the range of micron, the target width of the micro-grooves was chosen to be 500 μm, which coincided with the upper limit of the micron range as referred in the documents published by the CIRP ((**C**ollege **I**nternational pour la **R**echerche en **P**roductique), The International Academy for Production Engineering) [63-65]. The tool holding unit of the newly developed experimental set up of μ-ECDG process is made suitable to hold a micro-tool in the range of 300 - 400 μm in order to observe the effects of various input process variables, namely Applied Voltage (V), Pulse Frequency (PF), Electrolyte Concentration (EC) and Duty Ratio (DR) on above-mentioned machining criteria. During trial experiments it was noticed that tool diameter of 300 μm was found more appropriate for experimentation since the width of grooves was found within 500 μm. Ni coated Stainless steel was selected as tool material for its high stiffness, cheap rate and availability in the market. Exhaustive experiments were performed to find the range of applied voltage (V) required for spark generation and range of other process variables like Pulse Frequency (PF), Electrolyte Concentration (EC) and Duty Ratio (DR). The higher levels of different parameters were fixed based on the values of width of micro-grooves i.e. 500 micron and the lower levels of all process variables were fixed on the basis of prominent formation of micro-grooves (as shown in the Figure 4.1). Machining time was considered to be constant for all experiments. A pulsed D.C. power supply was provided for experimentation

and it was decided to conduct the experiments at five different voltage levels, *i.e.* at 35 V, 40 V, 45 V, 50 V and 55 V. The duty ratio was defined as the ratio of pulse on-time and pulse off-time of a cycle of DC voltage. Here, both pulse on-time and pulse off-time were variable quantities. The frequency of applied voltage was varied from 60 Hz to 1.2 kHz and the duty ratio varies from 35% to 70%. Five different levels of pulse frequency *i.e.* 200, 400, 600, 800, 1000 Hz and five different levels of duty ratio *i.e.* 45%, 50%, 55%, 60% and 65% were chosen to conduct the experiments. To study the effect of polarity on different machining criteria the tool-electrode was connected to positive as well as negative terminal of the DC power supply and these were referred as reverse polarity and direct polarity of tool-electrode respectively

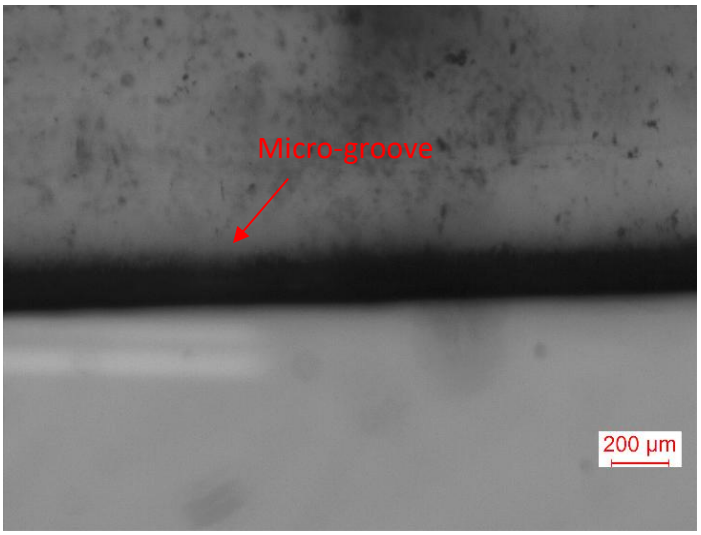

Fig. 4.1: Optical image of a micro-groove on glass at 30V/10wt% NaOH/200Hz/45%

The selection of electrolyte type and concentration is a pivotal process variable in µ-ECDG process because of the electro-chemical reactions, which have significant role on various machining criteria. Different types of electrolytes such as NaOH, KOH, $NaNO_3$, NaCl, H_2SO_4, HCl etc can be used in µ-ECDG process. But the acidic solution is harmful to skin. Also, workpiece material is removed only at high applied voltage when neutral salt solution is used as an electrolyte in ECDM process [1] and it is not desirable in µ-ECDG process. So, NaOH, KOH and mixed of these two were selected as electrolyte in the study. The experiments were performed with aqueous NaOH, KOH and mixture of KOH & NaOH (mixed in equal wt. percentage) as electrolytes at 10, 15, 20, 25 and 30 wt% concentrations.

In μ-ECDG process, normally an electrically non-conducting material is used to machine and there is always a gap gilled with hydrogen gas bubble layer between the micro-tool and the workpiece due to surface irregularities, which are responsible for development of spark. The experimentation was conducted at the fixed inter- electrode gap of 50 mm between the tool and auxiliary electrode. It was prearranged to machine a micro-groove of 500 micron width and 10 mm long. The depth of grooves was not prime concern of this investigation so it was not intended to attain a fixed level of depth. The machining operation was performed at the parametric settings as listed in the Table 4.1 for 15 minutes, which was recorded by a stopwatch. The main power supply unit was disconnected after completing the machining operation successfully and the workpiece is removed. Then the workpiece was dried and measured with the METTELER TOLLEDO weighing machine (Least Count of 1 x 10^{-4}g) for calculating MRR. The workpiece was cleaned properly in an ultrasonic bath of distilled water in order to remove sludge/ precipitate and the micro-grooves were observed under a microscope by adjusting its focus and magnification. The measurement of two response parameters i.e. Overcut and HAZ (in the subsequent optical images of micro-grooves in this paper) area were done with LEICA microscope (least measurement = 0.1 μm) at 5X magnification. HAZ were measured for the entire length of micro-grooves.

Overcut of the micro-grooves was calculated as follow:

Overcut= (Width of Cut (WOC) of the groove – Diameter of the tool used to cut the groove) *Eqn 4.1*

Table 4.1: Experimental condition for machining micro-groove on glass

	Working Condition	***Summary***
Set 1	Workpiece Material	Silica Glass
	Tool Material	Stainless steel
	Applied Voltages(V)	35, 40, 45, 50, 55
	Type of Electrolyte	NaOH
	Elect Conc. (wt%)	10, 15, 20, 25, 30
	Pulse Frequency(Hz)	200, 400, 600, 800, 1000
	Duty ratio (%)	45, 50, 55, 60, 65
	Polarity	Direct Polarity
Set 2	Workpiece Material	Silica Glass
	Tool Material	Stainless steel
	Applied Voltages(V)	35
	Electrolyte	NaOH, KOH, KOH + NaOH
	Elect Conc. (wt%)	10
	Pulse Frequency (Hz)	200
	Duty ratio (%)	45
	Polarity	Direct Polarity (DP)
Set 3	Workpiece Material	Silica Glass
	Tool Material	Stainless steel
	Applied Voltages(V)	35
	Type of Electrolyte	NaOH, KOH, NaOH+KOH
	Elect Conc. (wt%)	10
	Pulse Frequency (Hz)	200
	Duty ratio (%)	45
	Polarity	Direct Polarity (DP) and Reverse Polarity (RP)

4.2 EXPERIMENTAL RESULTS

Based on the experimental plan, three sets of experiments *i.e.* set 1, set 2, and set 3 were conducted and each set was conducted three times to achieve good repeatability *i.e.* all total of 90 experiments were conducted. For performing the experiments, one factor varied at a time (OFAT) was employed to study its effect on response characteristics and the remaining parameters were fixed at their lowest level. In this way, the effects of these process parameters were analysed. The dimension of micro-grooves achieved during experiments was within 10 mm long and 500-micron width. Table 4.2 includes the experimental results obtained at different parametric combinations based on Set 1.

Table 4.2: Experimental results at different parametric combinations based on Set 1

SL No	Experimental condition				Experimental Results		
	Voltage (V)	Elect Conc. (wt %)	Pulse Freq. (Hz)	Duty Ratio (%)	MRR (mg/hr)	OC (µm)	HAZ Area (μm^2)x10^3
1	35	10	200	45	12.13	198.826	327.323
2	35	10	200	50	14.53	45.842	438.461
3	35	10	200	55	18.53	86.356	232.298
4	35	10	200	60	19.06	84.878	264.316
5	35	10	200	65	23.87	133.443	352.374
6	35	10	400	45	11.06	112.780	525.679
7	35	10	600	45	11.87	92.241	554.657
8	35	10	800	45	11.6	132.299	318.508
9	35	10	1000	45	8.53	116.617	294.514
10	40	10	200	45	24.13	165.009	392.858
11	45	10	200	45	31.6	259.524	452.955
12	50	10	200	45	30.27	264.494	714.806
13	55	10	200	45	51.33	457.347	1048.131
14	35	15	200	45	36.8	119.431	760.221
15	35	20	200	45	70.93	309.583	706.739
16	35	25	200	45	74.27	342.867	908.92
17	35	30	200	45	105.47	273.210	894.771

In Set 2, the experiments were conducted at 35 V applied voltage, 200 Hz pulse frequency and 45% duty ratio to study the effects of different electrolytes with respect to the changes of their concentrations. All experimental results are given in the Table 4.3.

Table 4.3: Experimental results for different electrolytes based on Set 2

SL No	Parametric combination					Experimental results		
	Voltage (V)	Elect. Conc. (wt %)	Pulse Freq. (Hz)	Duty Ratio (%)	Electrolyte	MRR (mg/hr)	OC (μm)	HAZ Area (μm^2)x10^3
1	35	10	200	45	NaOH	12.13	198.826	327.323
2	35	15	200	45	NaOH	36.8	119.431	760.221
3	35	20	200	45	NaOH	70.93	309.583	706.739
4	35	25	200	45	NaOH	74.27	342.867	908.92
5	35	30	200	45	NaOH	105.47	273.210	894.771
6	35	10	200	45	KOH	27.25	64.681	288.734
7	35	15	200	45	KOH	52.25	206.243	390.6813
8	35	20	200	45	KOH	72.17	219.38	460.8199
9	35	25	200	45	KOH	63.5	198.536	411.7924
10	35	30	200	45	KOH	89	241.515	742.5197
11	35	10	200	45	NaOH+KOH	22	121.437	331.356
12	35	15	200	45	NaOH+KOH	29.75	200.507	382.524
13	35	20	200	45	NaOH+KOH	59	271.090	426.861
14	35	25	200	45	NaOH+KOH	90.75	199.660	681.099
15	35	30	200	45	NaOH+KOH	69	292.462	512.489

Various machining criteria *e.g.* MRR, overcut and HAZ were measured in order to compare the effect of reversed polarity with the effect of direct polarity of μ-ECDG process for micro-grooving on flat surface of glass. Other input process variables *i.e.* applied voltage, pulse frequency, electrolyte concentration and duty ratio were fixed at their low level as given in the Table 4.1 in order to have their least effects on responses. The experimental results are mentioned in the Table 4.4 as below.

Table 4.4: Experimental results at different polarities based on Set 3

SL No	Parametric combination						Experimental results		
	Voltage (V)	Elect. Conc. (wt %)	Pulse Freq. (Hz)	Duty Ratio (%)	Electrolyte	Polarity	MRR (mg/hr)	OC (μm)	HAZ area ((μm^2)x10^3)
1	35	10	200	45	NaOH	DP	12.13	198.826	327.323
2	35	10	200	45	KOH	DP	27.25	64.681	288.734
3	35	10	200	45	NaOH+KOH	DP	22	121.437	331.356
4	35	10	200	45	NaOH	RP	5.8	78.475	136.356
5	35	10	200	45	KOH	RP	3.2	42.266	123.780
6	35	10	200	45	NaOH+KOH	RP	10	96.135	162.386

4.3 PARAMETRIC INFLUENCES ON VARIOUS MACHINING RESPONSES

The Set 1 *i.e.* first Set of experiments were conducted using aqueous NaOH to examine the influences of selected input process variables on machining responses e.g. MRR, overcut and HAZ area (as given in Table 4.2) as below.

4.3.1 Influence of Process Parameters on Material Removal Rate (MRR)

Figures 4.2(a) to 4.2(d) show the effects of applied voltage, Electrolyte Concentration (EC), Pulse Frequency (PF) and Duty Ratio (DR) on average MRR. These figures show that MRR was improved with the increase of applied voltage, EC and DR for fixed levels of other process variables but in case of pulse frequency it was decreased. The intensity of sparking as shown in Figures 4.3 (a) and (b) was increased when both applied voltage and EC were increased [1, 3]. The spark generation was intensified for the rise of both current density and electrochemical reactions since increasing applied voltage boosted up the current density and electrolyte concentration accelerated the electrochemical reactions. In μ-ECDG process, the development and growth of vapour bubble and gas bubble depend completely on the Joule heating of electrolyte and electrochemical reactions respectively. The accumulated gas and vapour bubbles are responsible for rapid evolution of isolating gas layer at the surroundings of tool-electrode, which as a result causes the spark discharges. With increase in spark discharge, more thermal energy is developed and it causes more MRR. Figures 4.2(a) and (b) reveal that MRR was high at 55V applied voltage and 30 wt% EC. By increasing pulse on-time duration, which is increased with the duty ratio, MRR is also enhanced. When the duration of discharge inside the micro-grooves on glass is increased, the temperature of that region also rises and results higher material removal rate. But the effect of pulse frequency on MRR had an opposite trend. This is because of the fact that the discharge duration increases with the decrease of pulse frequency. Thermal energy is dissipated more at the machining zone for low frequency and it helps to melt or vapourised more material from the workpiece. Figure 4.2(c) shows that MRR would be almost same for the pulse frequencies of 400, 600 and 800 Hz. MRR was high at 200 Hz pulse frequency and 65% duty ratio as shown in Figures 4.2(c) and (d) respectively.

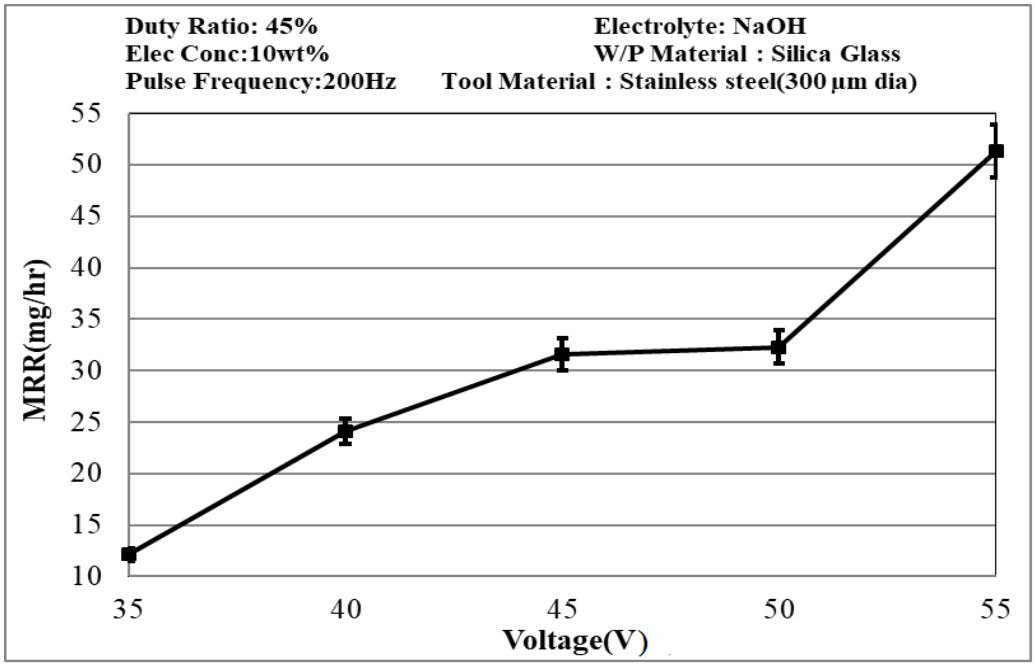

(a) Effect of applied voltage

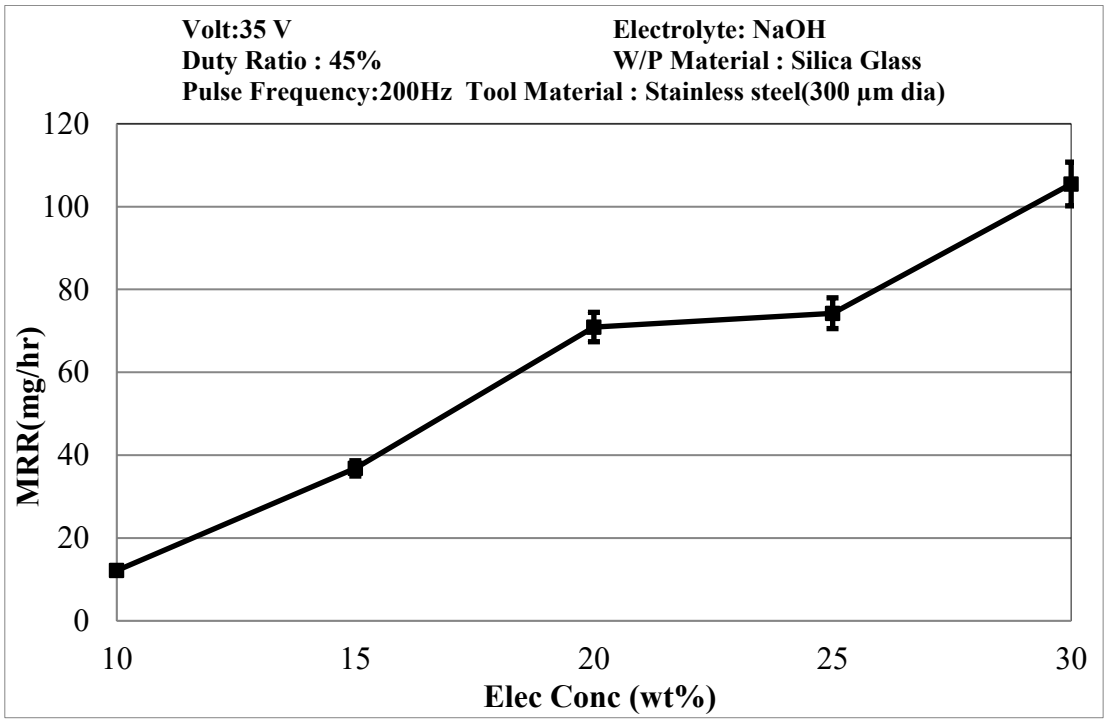

(b) Effect of electrolyte concentration

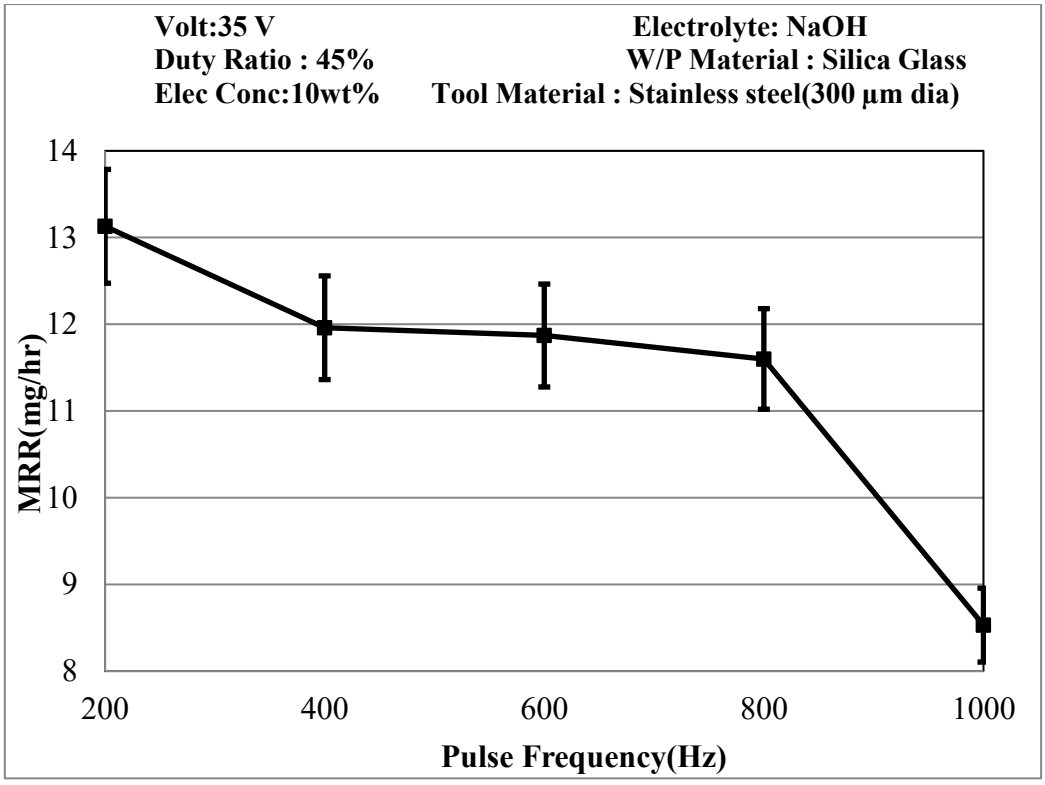

(c) Effect of pulse frequency

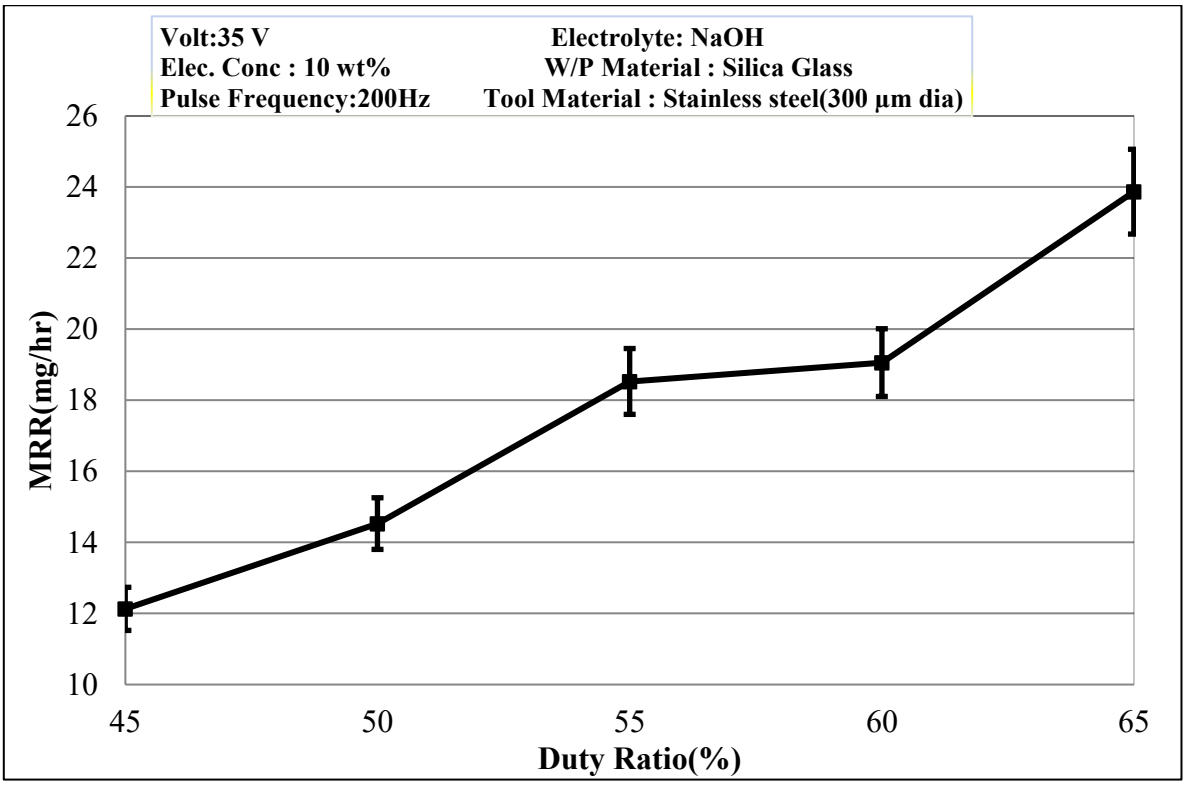

(d) Effect of duty ratio

Fig. 4.2: Effects of input process parameters on MRR

(a) at 35V/10wt%/200Hz/45% **(b) at 55V/10wt%/200Hz/45%**

Fig. 4.3: Sparks discharges at tool tip

4.3.2 Influence of Process Parameters on Overcut (OC)

Overcut is an undesirable characteristic in case of machining operations. In the present work, overcut has also been observed with varying the input process parameters. Figures 4.4(a) & (b) reveal that the values of overcut went up with these variables within their selected ranges. Usually, the spark discharging rate boosts up with the increase of applied voltage and EC due to the reason explained previously. As a consequence, Width of Cut (WOC) along with MRR also increased due to the discharge from the side-wall of cathode cum tool-electrode [67]. Also, the rate of electrochemical etching is enhanced with increase in electrolyte concentration as well as with the current density. This causes the increase in WOC. Micro-grooves were observed under an optical microscope and the images of micro-grooves machined on glass at different concentrations of NaOH electrolyte were shown in the Figures 4.5(a) & (b). Figures 4.4 (c) and (d) exhibit that overcut went down with rise of PF and enlarged with the rise of DR. One possible reason for decreasing overcut with PF and increasing with DR is that the discharges from the tool's side surface become stronger due to high current density. A high DR increases the pulse on time and consequently raises the current density leading to more intense lateral discharges and greater overcut.

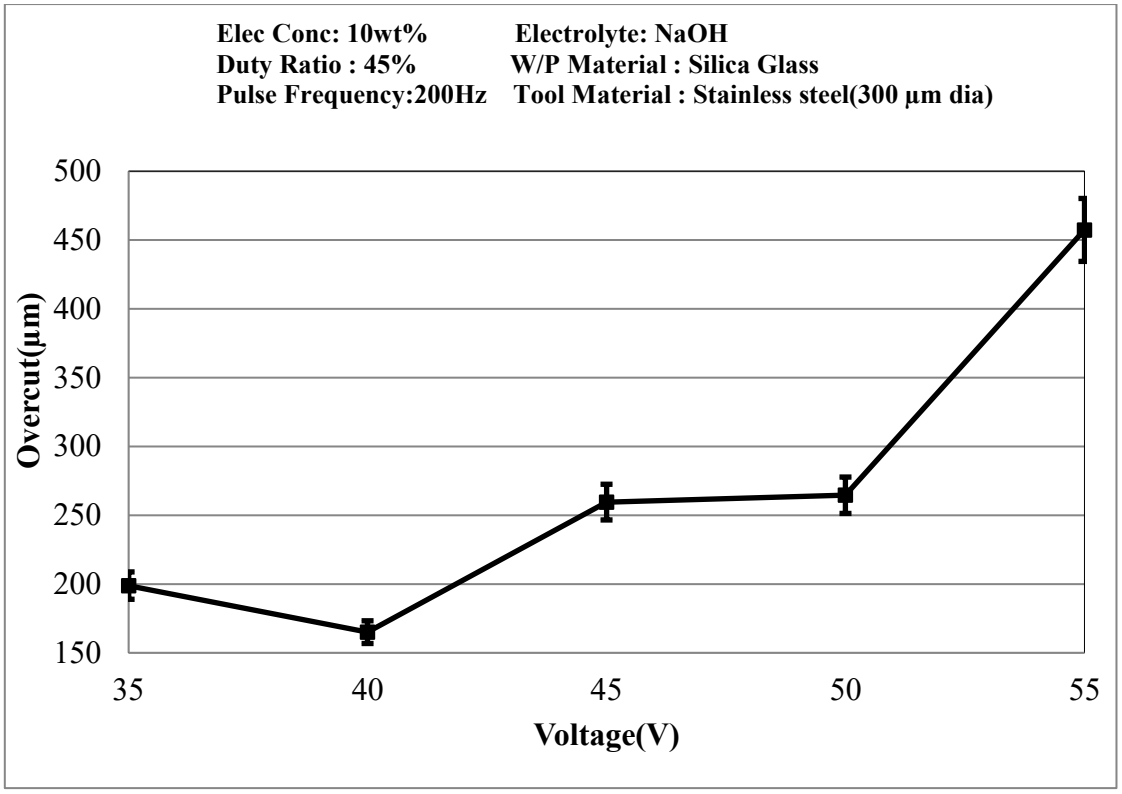

(a) Effect of applied voltage

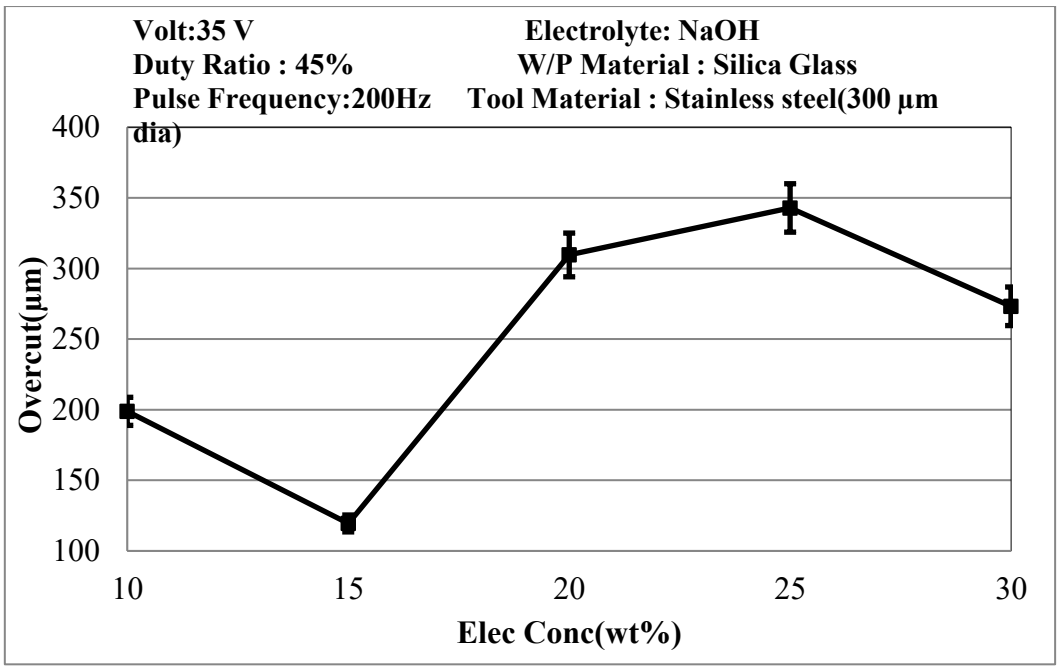

(b) Effect of Electrolyte concentration

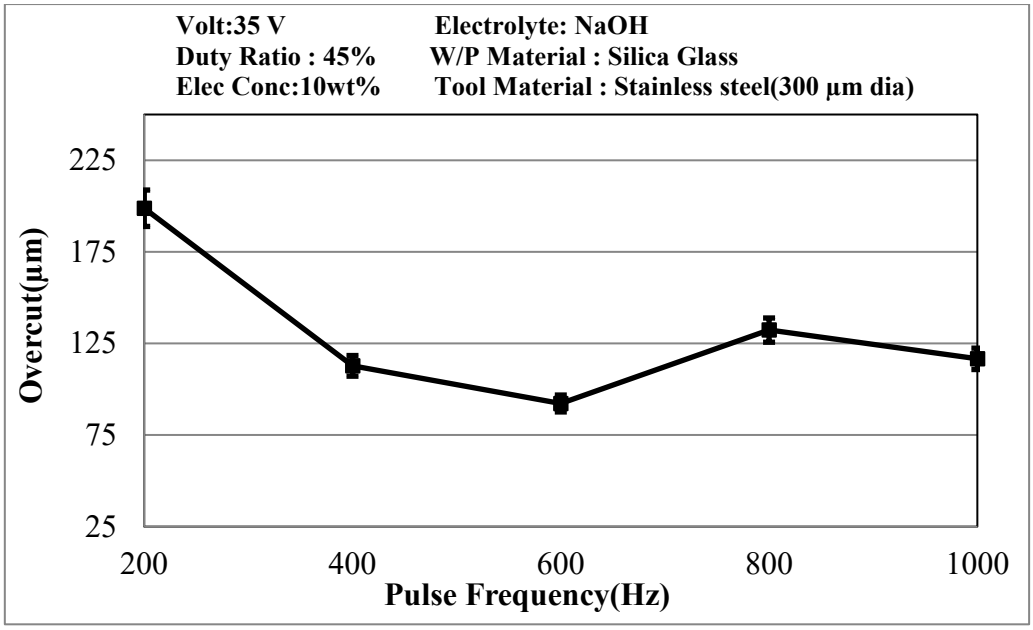

(c) Effect of Pulse frequency

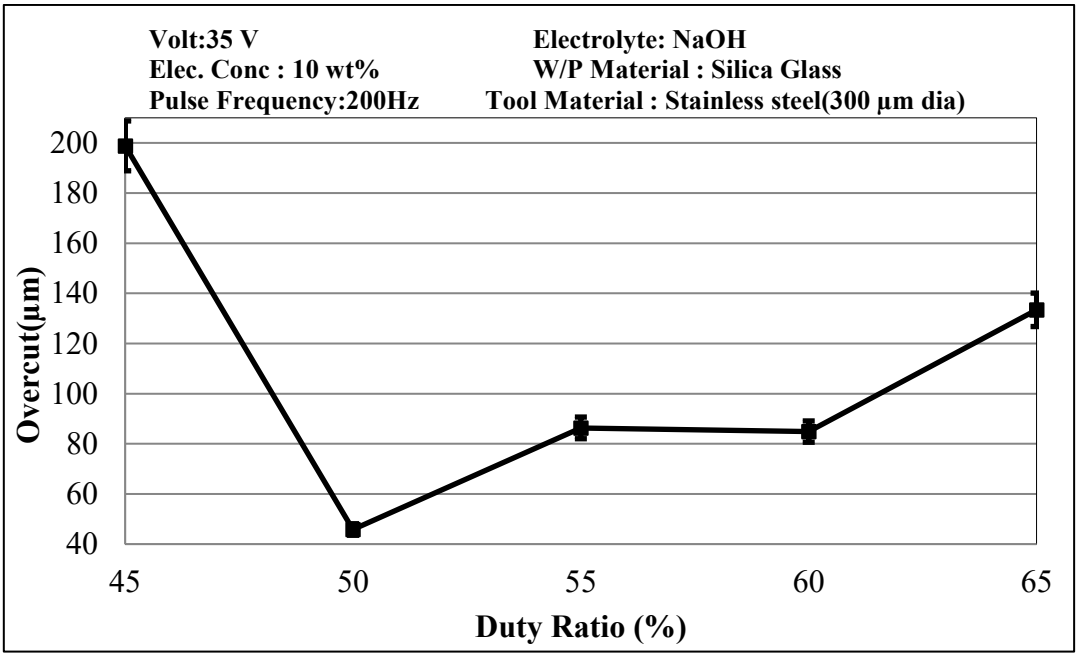

(d) Effect of Duty Ratio

Fig. 4.4: Effects of process parameters on Overcut

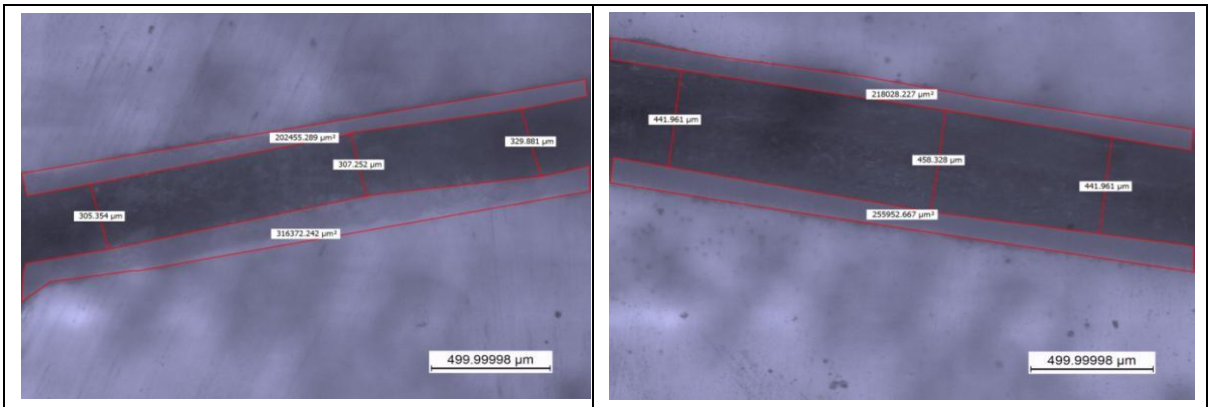

(a) at 35V/10wt% NaOH/200Hz/45% **(b) at 35V/25wt% NaOH/200Hz/45%**

Fig. 4.5: Optical images of µ-grooves on glass

4.3.3 Influence of Process Parameters on Heat Affected Zone (HAZ) area

Material removal mechanism of µ-ECDG is associated with melting and vapourisation, which are the results of thermal effect of spark discharges. A fraction of thermal energy during spark discharge is transferred to the workpiece by conduction mode. A small amount of heat is transferred to electrolyte by means of convection mode. Remaining heat is lost through radiation. The heat, which is transferred to the workpiece, causes HAZ area on the machined groove surface. Figures 4.6(a) and (b) clearly show that HAZ area was expanded with the rise of voltage applied and EC as the thermal energy increase with voltage and EC [12]. With rise of voltage and EC the spark density at the front as well as at the side-wall of the tool-electrode is increased and thereby thermal energy is dissipated more, resulting bigger HAZ. Photographs of micro-grooves with HAZ area obtained at different applied voltages are exhibited in the Figures 4.7 (a) and (b). HAZ area was obtained as comparatively larger at 55 V applied voltage and 25 wt% EC. Again Figures 4.6(c) and (d) show that initially HAZ area grew more with the pulse frequency and then it decreased but in case of duty ratio it increased after 55 %. Higher duty ratio means longer duration of discharge. So, more heat is generated for longer pulse duration i.e. pulse on-time. From the experimental results, it may be noted that HAZ area produced during micro-grooves generation is controlled by increasing PF and decreasing DR for same applied voltage.

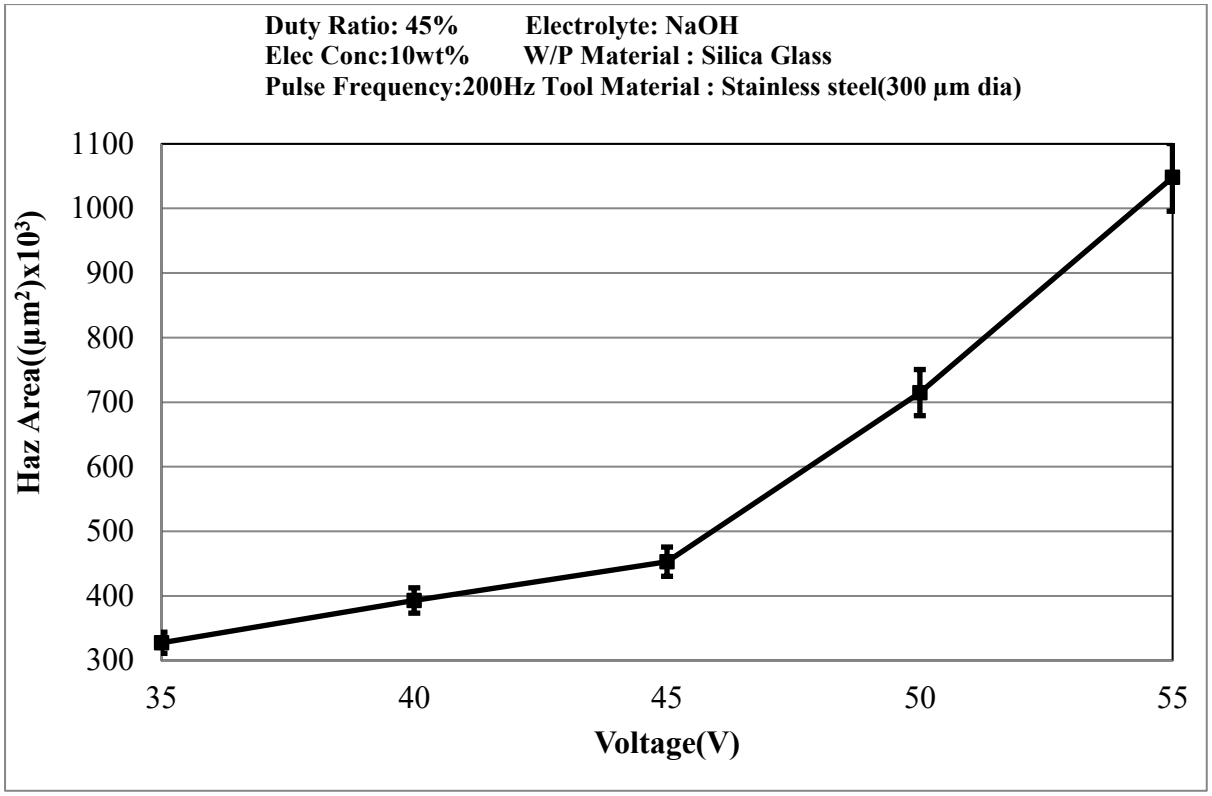

(a) Effect of applied voltage

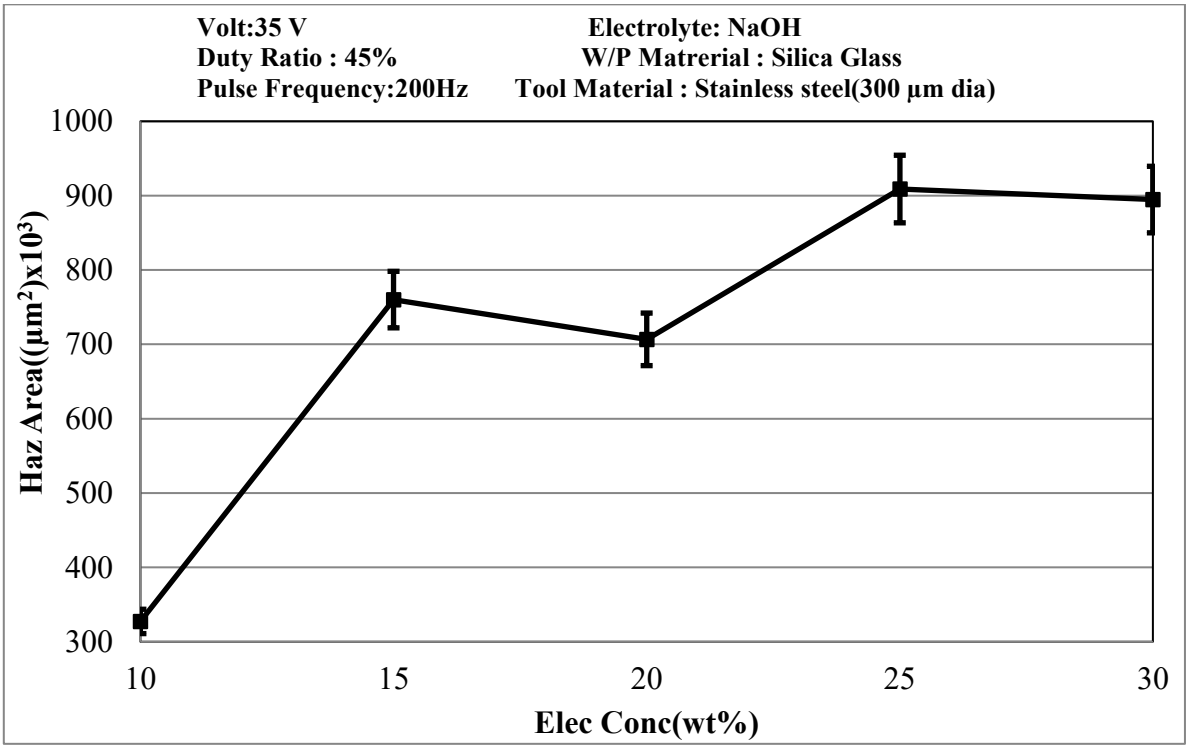

(b) Effect of Electrolyte Concentration

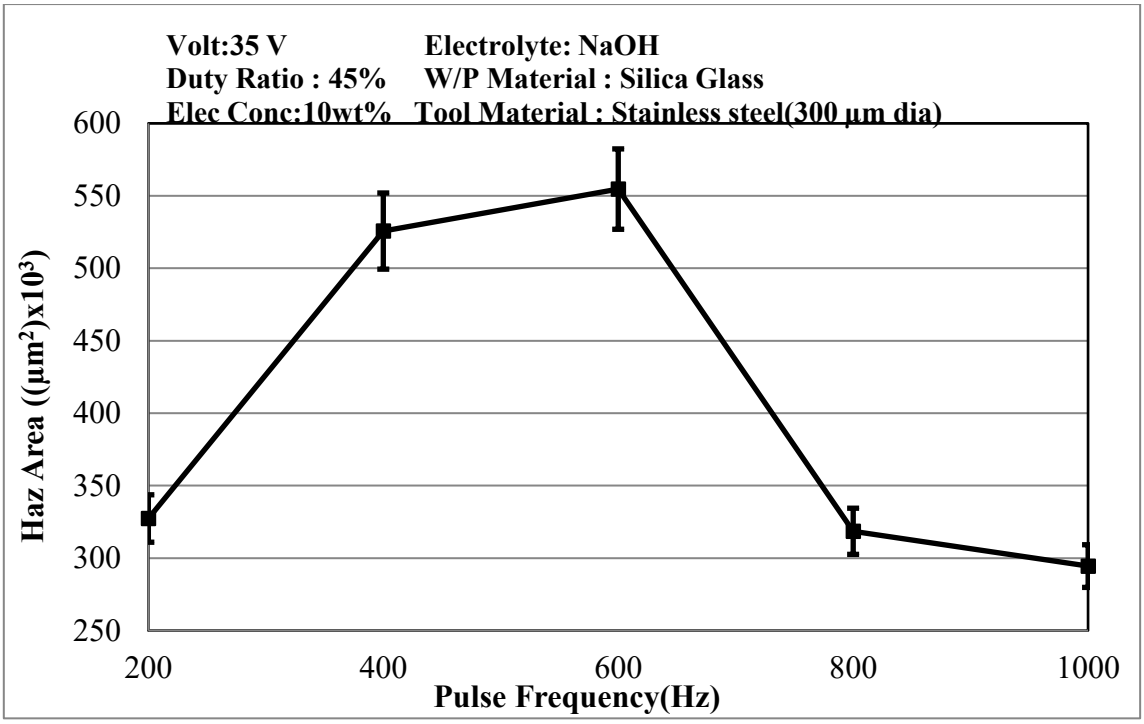

(c)Effect of Pulse frequency

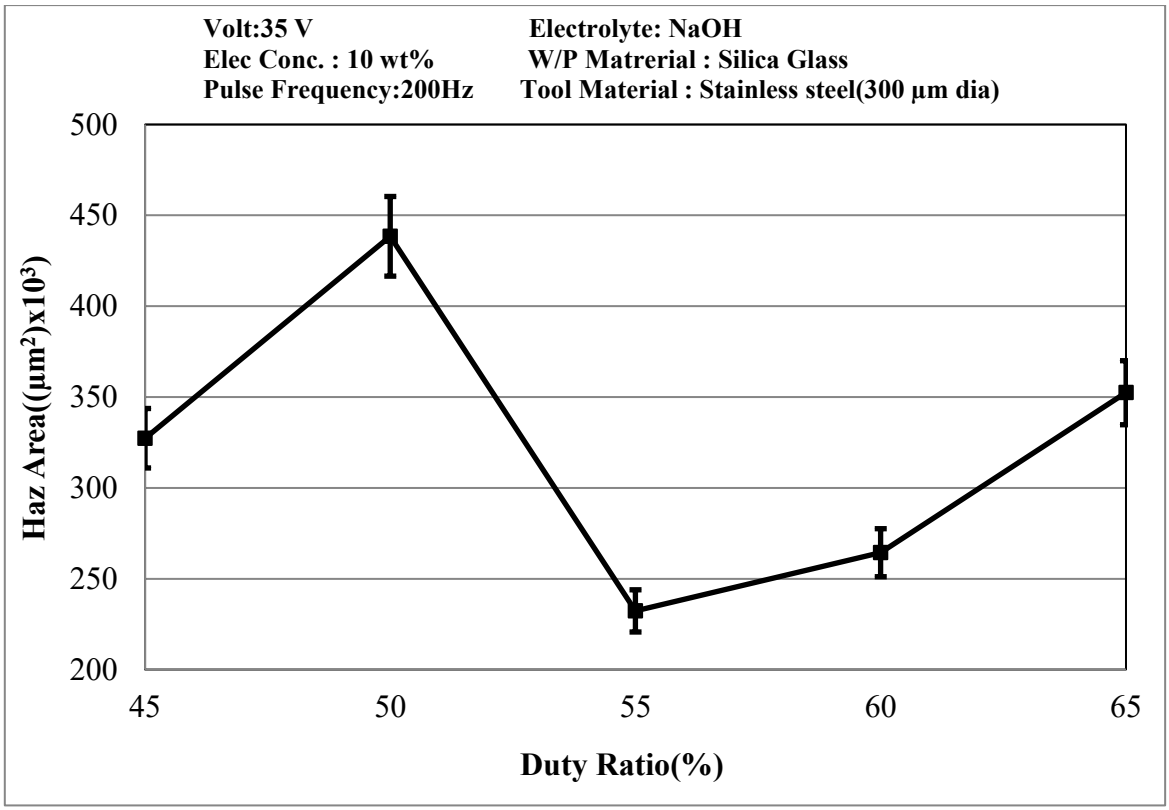

(d) Effect of Duty Ratio

Fig. 4.6 Effects of process parameters on HAZ area

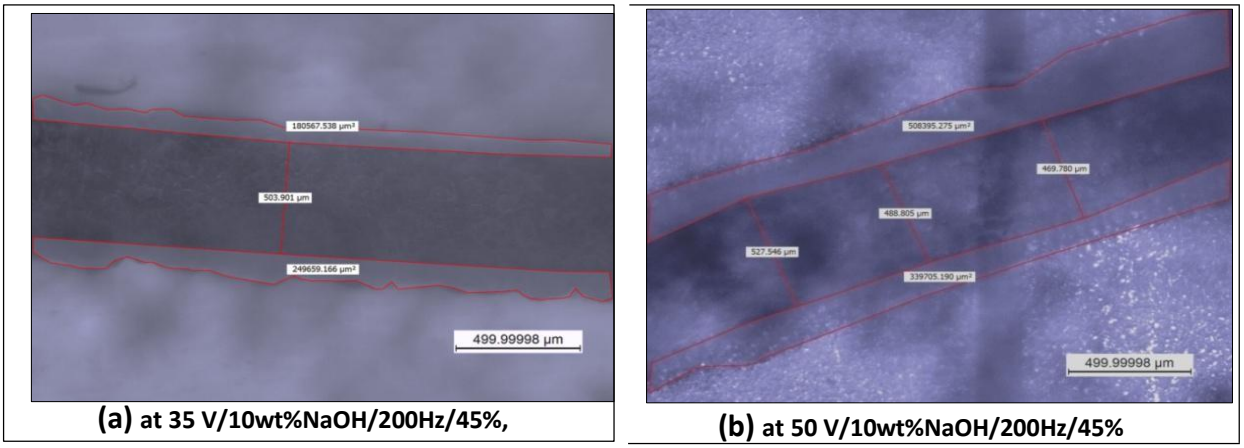

(a) at 35 V/10wt%NaOH/200Hz/45%, **(b)** at 50 V/10wt%NaOH/200Hz/45%

Fig. 4.7: Optical images of µ-grooves on glass

4.4 EFFECTS OF DIFFERENT ELECTROLYTES ON VARIOUS MACHINING PERFORMANCES

A detailed comparative study of various machining criteria has been conducted for three different electrolytes *i.e.* aqueous NaOH, KOH and mixture of NaOH & KOH electrolytes during micro-machining on glass material. The comparison has been presented and analysed with the help of variations of performance characteristics as given in the Table 4.3.

4.4.1 Effects of Different Electrolytes on MRR

The comparison of MRR using three different electrolytes (aqueous NaOH, KOH & NaOH+KOH) with their varying concentrations has been shown in the Figure 4.8. It is clear from the graph that initially MRR was greater for KOH electrolyte than that for both NaOH and mixture of these two electrolytes owing to higher sparking as shown in the Figures 4.9(i) & (ii). The reason behind this phenomenon is the ionic mobility factor and conductivity rate of K^+ ion. The ionic mobility factor and conductivity of K^+ ion are 7.620×10^{-8} m^2/sV and 73.5 S-cm^2/mol respectively whereas the values of these factors of Na^+ ion are 5.190×10^{-8} m^2/sV and 50.1 S-cm^2/mol respectively. The higher mobility factor and conductivity rate lead to the faster chemical reactions, which cause more bubbles' generation and ultimately more sparking density. So, MRR was found more for KOH as compared to that of other two electrolytes. Though the chemical reactions increase with increase of electrolyte concentration of all electrolytes, the workpiece material removed by using either NaOH or KOH electrolyte reached its higher value at 30 wt% EC and also found higher at 25 wt% in case of NaOH+KOH electrolyte for 35 V applied voltage, 200 Hz PF and 45% DR. A highly energised sparking is triggered for higher rate of chemical reactions. Further the effect of

chemical etching is enhanced with the increase of electrolyte concentration. But there might be a chance of being deposited of the melting material for re-solidification on the machining zone at the concentration of 25 wt% of NaOH and KOH electrolytes. This was also observed by using NaOH+KOH electrolyte at 30wt% and it indicated low MRR. From the Figure 4.10, it is clear that no such phenomenon of solidification was occurred at lower concentrations of electrolytes. Material removal in both cases of using NaOH and KOH solutions attained the higher value (i.e. 105.47 mg/hr for NaOH and 89 mg/hr for KOH) at 30 wt% electrolyte concentration but in case of NaOH+KOH electrolyte it was comparatively lower (i.e. 90.75 mg/hr) at 25 wt%.

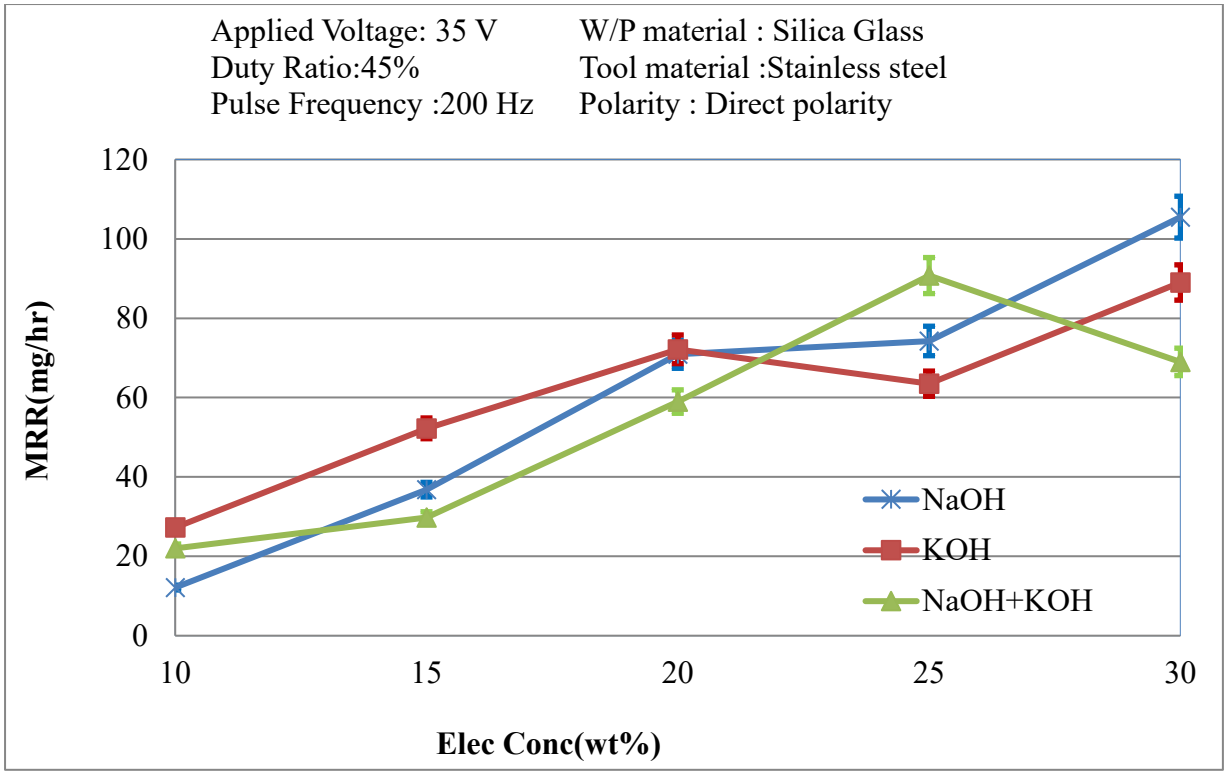

Fig. 4.8: Influences of different electrolytes on MRR with varying electrolyte concentration

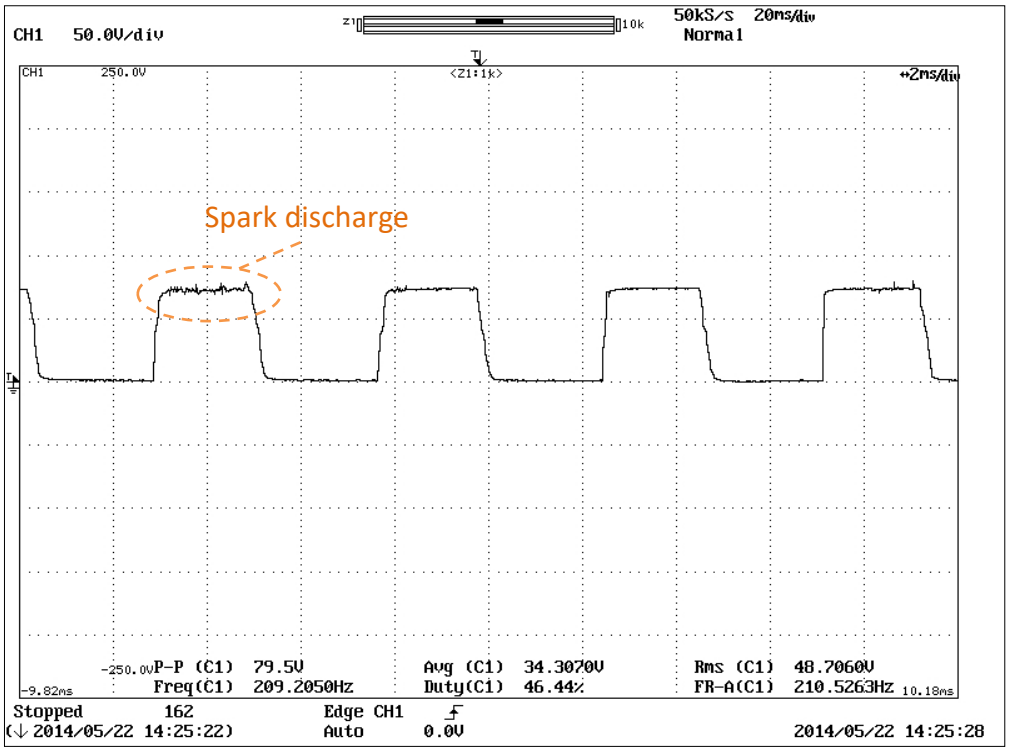

(i) at 20wt% NaOH

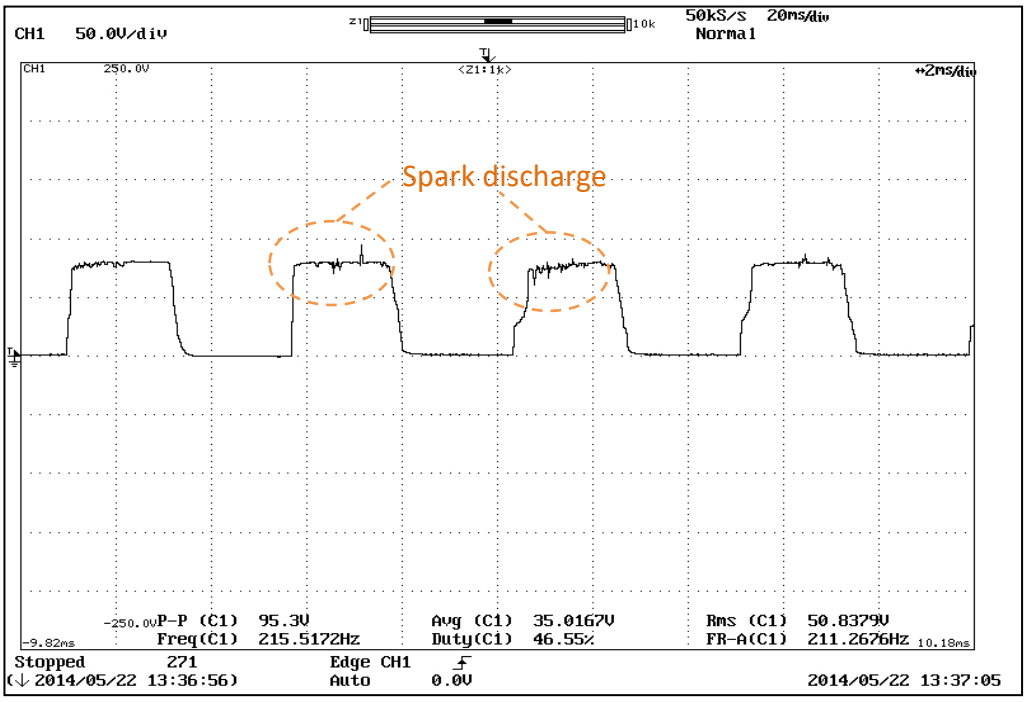

(ii) at 20 wt% KOH

Fig. 4.9: Voltage-time characteristic graphs

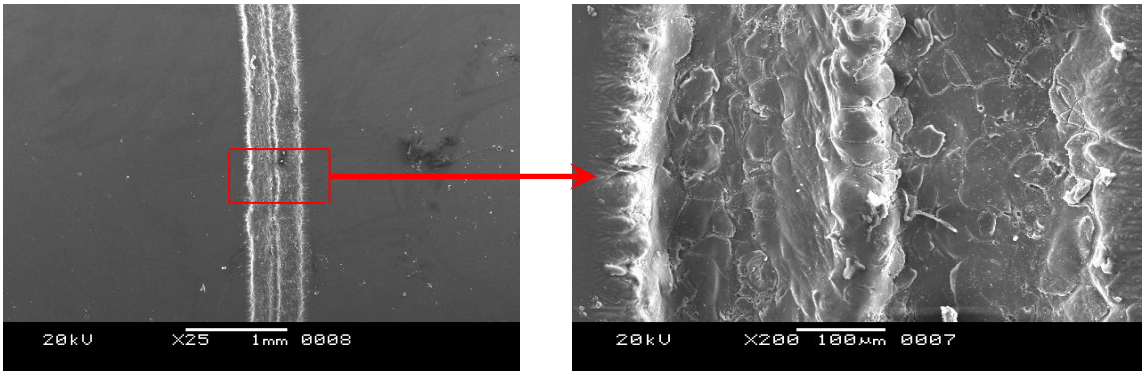

(i) at 35V/25wt%KOH/200Hz/45%

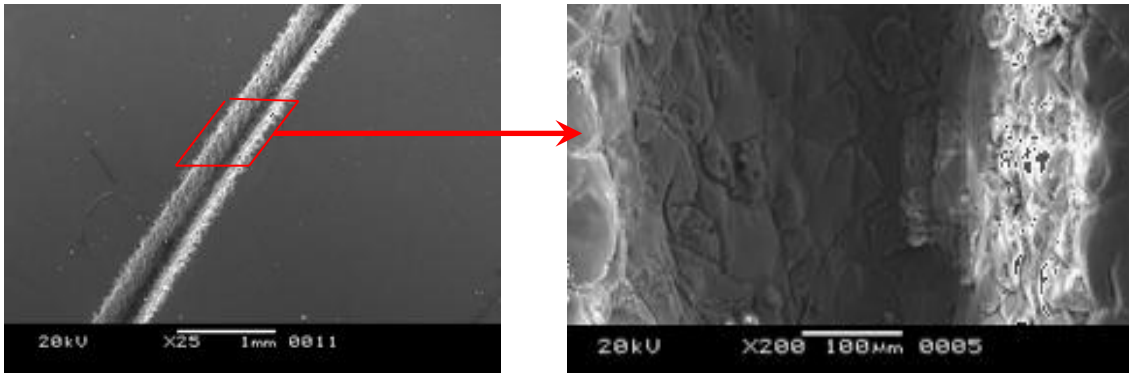

(ii) at 35V/10wt%NaOH/200Hz/45%

Fig. 4.10: SEM images of µ-grooves on glass

4.4.2. Effects of Different Electrolytes on Overcut (OC)

The comparison of Overcut (OC) with their varying electrolyte concentration at 35 V, 200 Hz and 45% DR is exhibited in the Figure 4.11. From the Figure 4.11, it is clear that overcut was larger when NaOH electrolyte was used and smaller for KOH electrolyte. Overcut was found moderate by using the mixture of these two electrolytes. Micro-grooves cutting above 20 wt% NaOH electrolyte is not desirable since the width of cut became bigger in size and entered dimensionally to the meso range instead of micro range. This may take place for the intensification of side sparking from the tool wall. The micro-grooves' SEM images for aqueous NaOH, KOH and NaOH+KOH electrolytes are exhibited in the Figures 4.12 (a), (b) and (c) respectively.

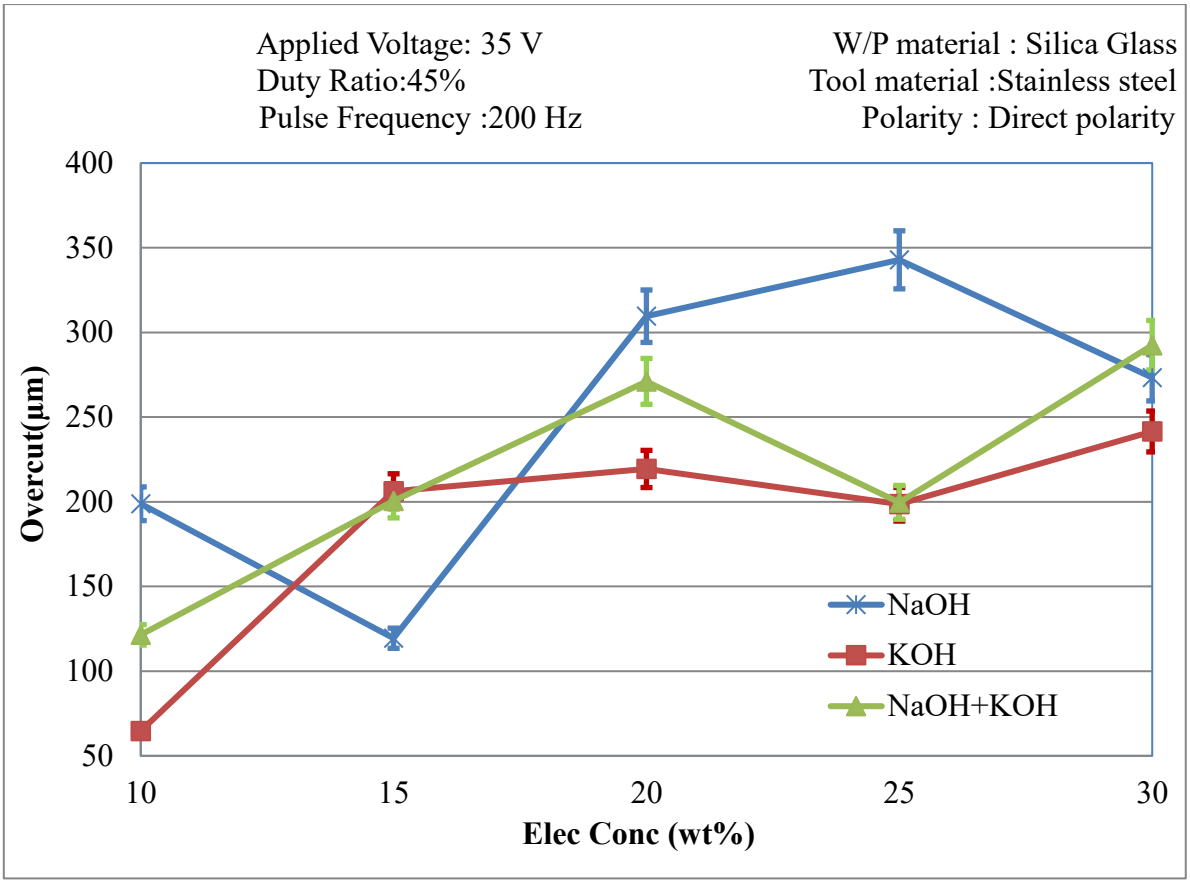

Fig. 4.11: Influences of different electrolytes on Overcut with varying electrolyte concentration

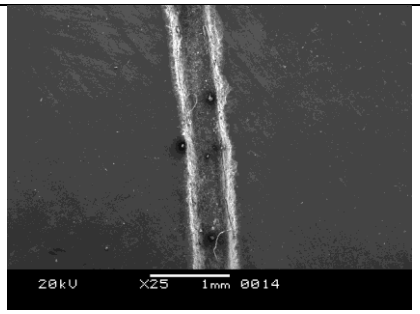

(a) at 10wt% NaOH electrolyte

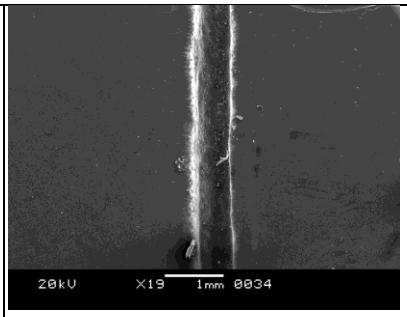

(b) at 10wt%KOH electrolyte

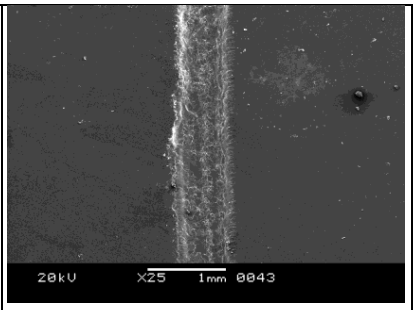

(c) at 10wt% NaOH+KOH electrolyte

Fig. 4.12: SEM images of µ-grooves

4.4.3 Effects of Different Electrolytes on Heat Affected Zone (HAZ) area

The effects of three electrolytes on HAZ area have been illustrated with the aid of Figure 4.13. It is found that HAZ area was increased more with the rise of concentration of all electrolytes. The machined grooved surface became rougher because of thermal disruption on HAZ area. HAZ area was found very large for NaOH solution in comparison to KOH & NaOH+KOH at 35 V, 45 % DR and 200 Hz. Heat-affected zone area was slightly varied for KOH and NaOH+KOH solutions at 10, 25 & 20 wt% concentrations. Figure 4.12 shows that HAZ area

was found as the lower at 10 wt% KOH EC, 35 V applied voltage, 200 Hz PF and 45% DR. Figures 4.14 (a), (b) and (c) exhibit the surface conditions of micro-grooves due to formation of HAZ on the machining zone using three different electrolytes *i.e.* aqueous NaOH, KOH & NaOH+KOH respectively. From this investigation, it can be said that the parametric condition 35V/25wt%KOH/200Hz/45% is suitable for high MRR whereas the parametric condition 35V/10wt%KOH/200Hz/45% is good for low overcut and HAZ area.

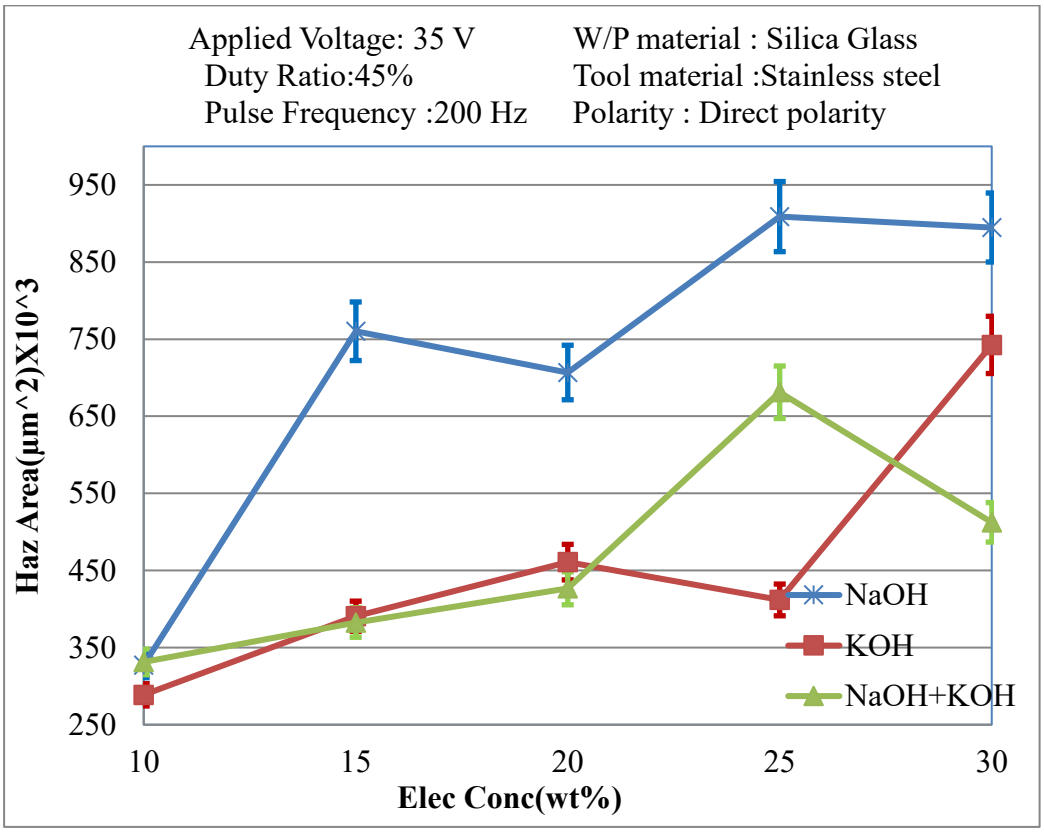

Fig. 4.13: Influences of different electrolytes on HAZ area with varying electrolyte concentration

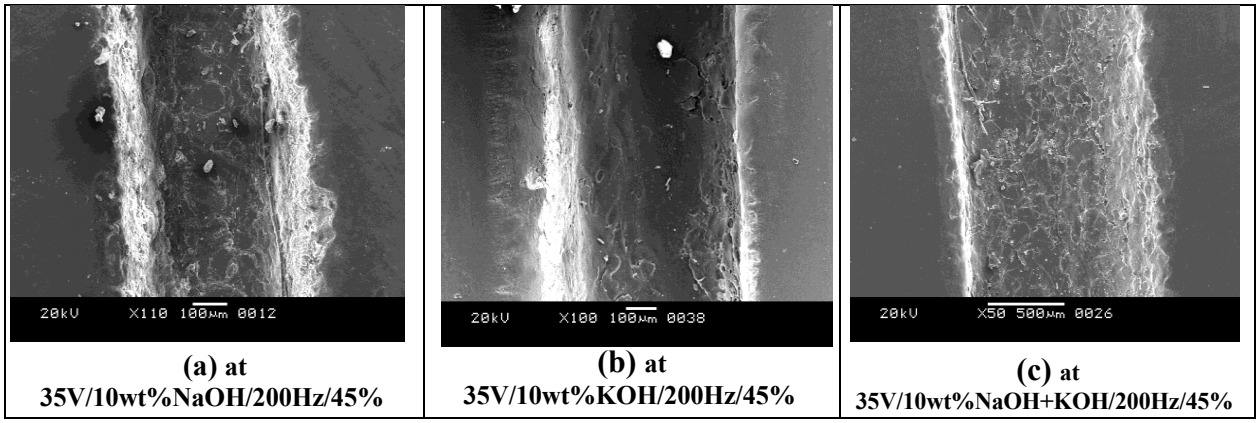

(a) at 35V/10wt%NaOH/200Hz/45% **(b) at 35V/10wt%KOH/200Hz/45%** **(c) at 35V/10wt%NaOH+KOH/200Hz/45%**

Fig. 4.14: SEM images of µ-grooves

4.5 EFFECTS OF TOOL POLARITIES ON VARIOUS MACHINING PERFORMANCES

In the third set, experiments have been conducted with the reversed polarity (*i.e.* tool +ve) for three electrolytes *viz* NaOH, KOH and NaOH+KOH by fixing their concentrations at 10 wt%.

4.5.1 Effects of Tool Polarities on MRR

A comparative study for material removal rate was carried out between the direct polarity and the reverse polarity using three electrolytes *i.e.* NaOH, KOH & NaOH+KOH at fixed concentration of 10 wt%, applied voltage of 35 V, PF of 200 Hz and DR of 45 %. It is clear from Figure 4.15 that MRR was much higher in the direct polarity than the reverse polarity since the intensity of spark discharges at the tool was very low for the reverse polarity. In direct polarity (*i.e.* tool "-ve'), the hydrogen bubbles are evolved at the tool since here tool acts as cathode but the oxygen gas bubbles are formed at the tool in reverse polarity due to electro-chemical reactions. Quantity of the hydrogen bubble by volume is evolved more than the oxygen bubbles [3, 68]. So, the electro- chemical spark is discharged more in the direct polarity than the reverse polarity. Figure 4.15 also indicates that MRR was found high at the direct polarity only for the separate use of KOH as electrolyte but MRR was obtained more at the reverses polarity by using NaOH+KOH than the separate use of NaOH and KOH. It can be noticed from the Figures 4.16 (a) and (b) that more number of micro-cracks was observed for the reverse polarity and smoother surface could be obtained by using the direct polarity. Therefore, it is learnt that the surface texture of machined zone improves where the direct polarities applied.

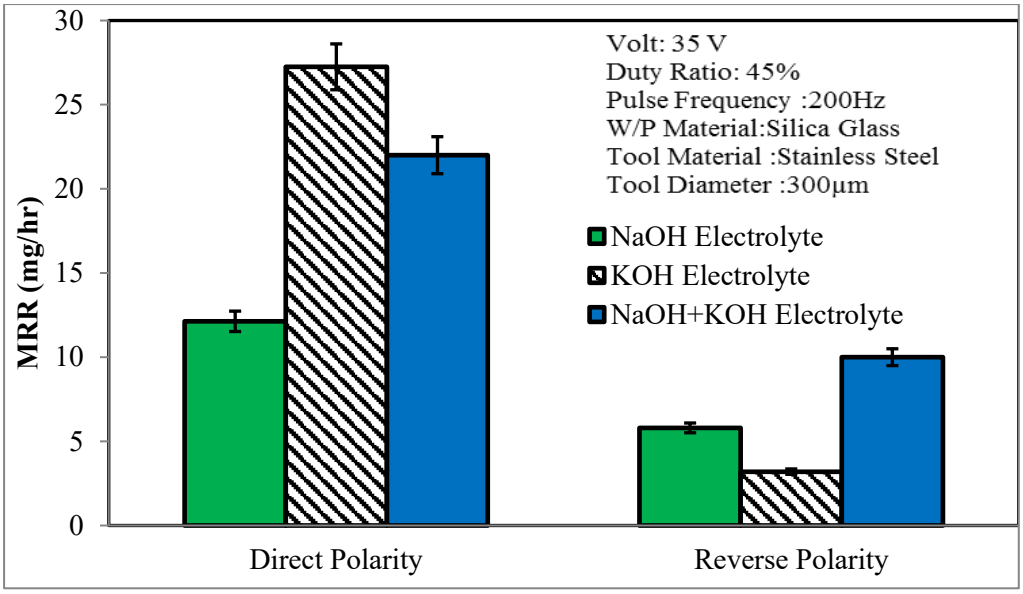

Fig. 4.15: Effects of direct polarity and reverse polarity on MRR

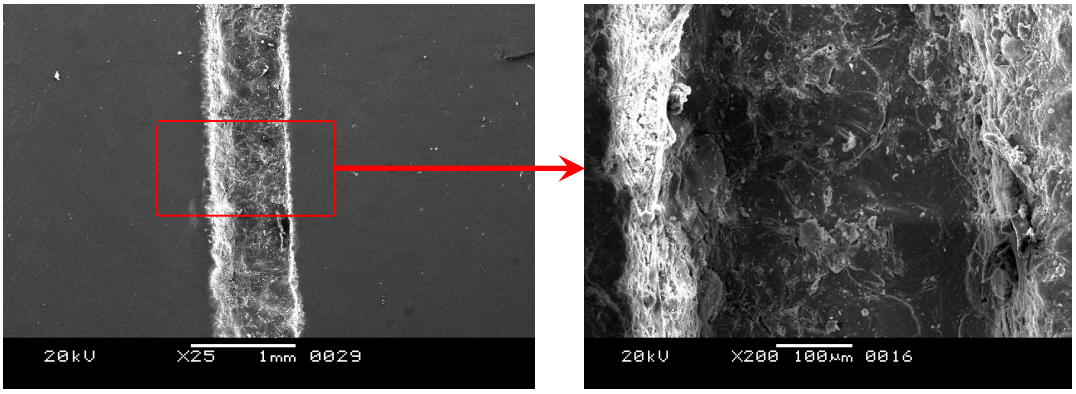

(a) Direct Polarity at 35V/10wt%NaOH/200Hz/45%

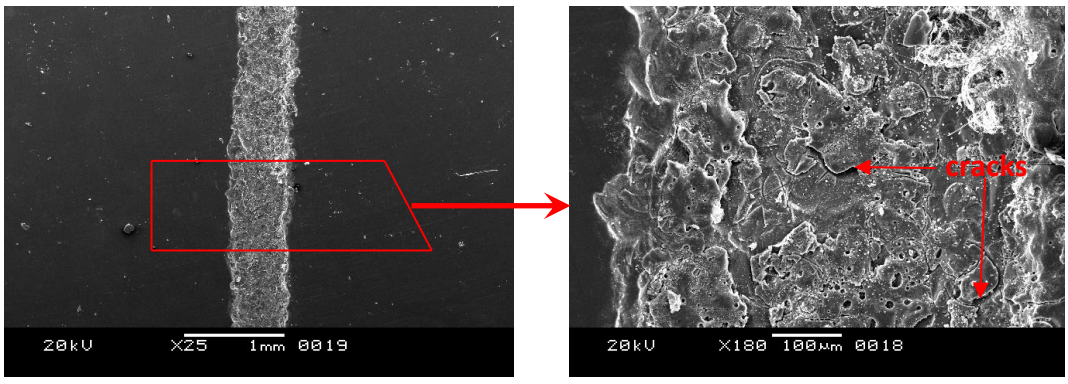

(b) Reverse Polarity at 35V/10wt%NaOH/200Hz/45%

Fig. 4.16: SEM images of µ-grooves

4.5.2 Effects of Tool Polarities on Overcut (OC)

Figure 4.17 shows the comparison of overcut between the direct polarity and the reverse polarity for three electrolytes. NaOH electrolyte solution produced high overcut at direct polarity but medium overcut in reverse polarity. From the figure, it can be observed that OC was the lower for KOH electrolyte at both direct and reverse polarities. Gas bubbles evolve more in aqueous KOH and grow rapidly due to faster electrochemical reactions. The spark discharges are also found to be concentrated more at the tool tip than the tool surroundings [3, 69]. NaOH+KOH solution produced medium overcut at direct polarity and while at reverse polarity it produced large overcut. Figures 4.18 (a) and (b) exhibit the photographs of micro-grooves cut on glass using the direct polarity and the reverse polarity respectively.

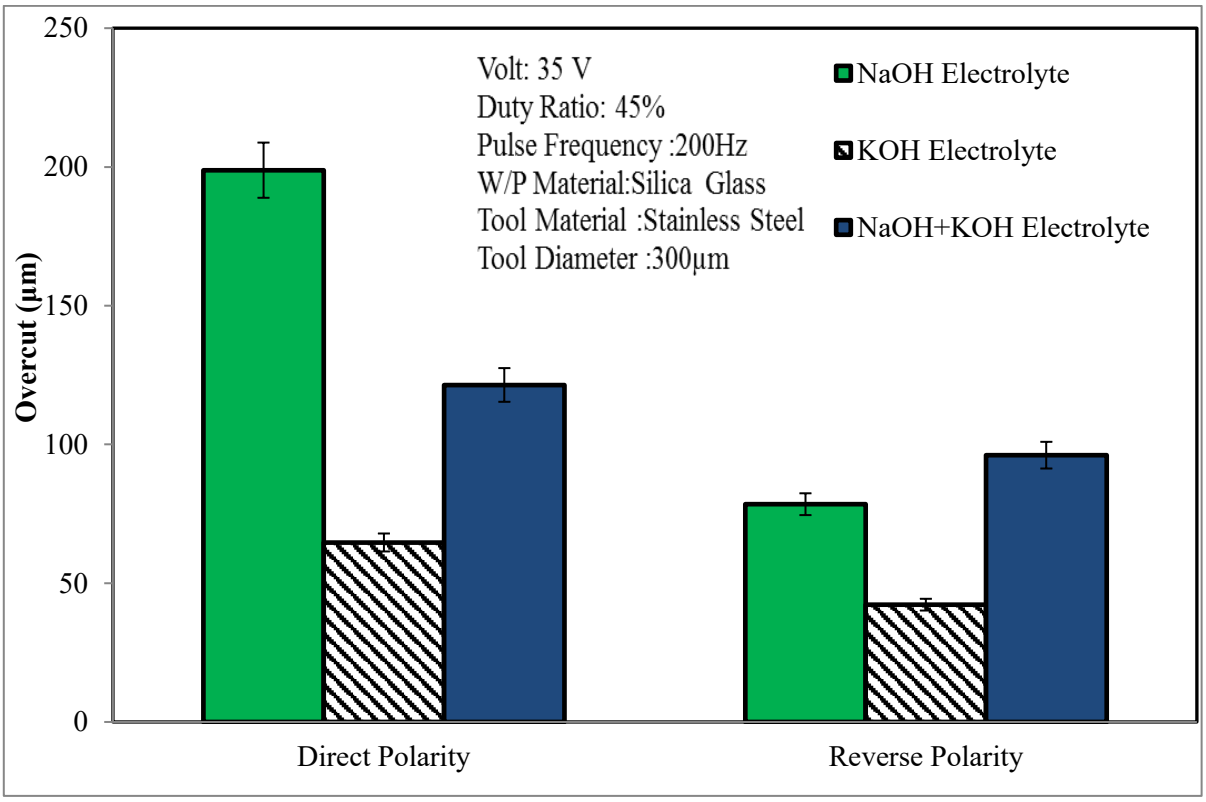

Fig. 4.17: Effects of direct polarity and reverse polarity on Overcut

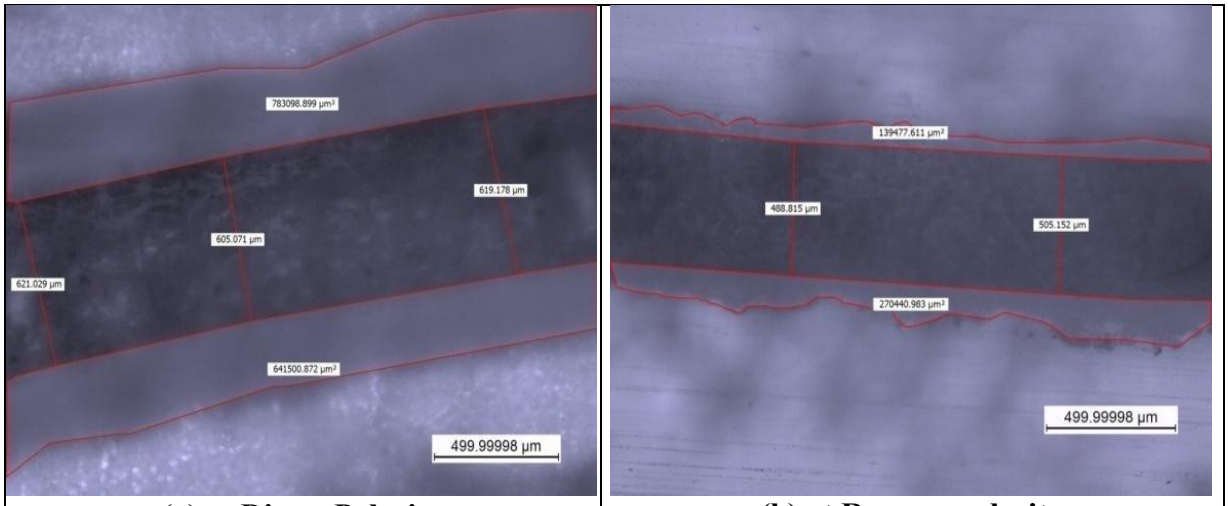

(a) at Direct Polarity | **(b) at Reverse polarity**

Fig. 4.18: Photograph of µ-grooves at 35V/30wt%KOH/200Hz/45%

4.5.3 Effects of Tool Polarities on Heat Affected Zone (HAZ) area

As it is known that excessive heat affects the micro structural properties of material one should try to reduce HAZ for the sake of material's dimensions, physical properties and micro-structural properties. In the comparative study on HAZ area, HAZ area was found medium for NaOH; lower for KOH electrolyte solutions and larger for mixed electrolyte (*i.e.* NaOH+KOH) solution at both direct and reverse polarities. Figures 4.18 (a) and (b) depict the photographs of micro-grooves obtained with direct polarity and reverse polarity respectively. Figure 4.19 shows that the smallest HAZ area was noticed by using reverse polarity in KOH electrolyte solution.

In µ-ECDG process tool material is also worn out due to the thermal effects of electrochemical spark discharges. Moreover, heat generated during the process depends on the tool polarity. A worn-out tool causes dimensional inaccuracy and the tool cannot be reused. Every time a new fresh tool is used. It is expensive and consumes time as well. So, a comprehensive study was made to understand the effect of tool polarity on the tool itself. The photographs of micro-tool after machining with the direct and reverse polarities are shown in the Figures 4.20(a), (b) and (c). From these photographs, it is clear that more tool wear took place for the direct polarity than the reverse polarity. The surface condition of tool after machining with the reverse polarity appeared similar to that of tool before machining.

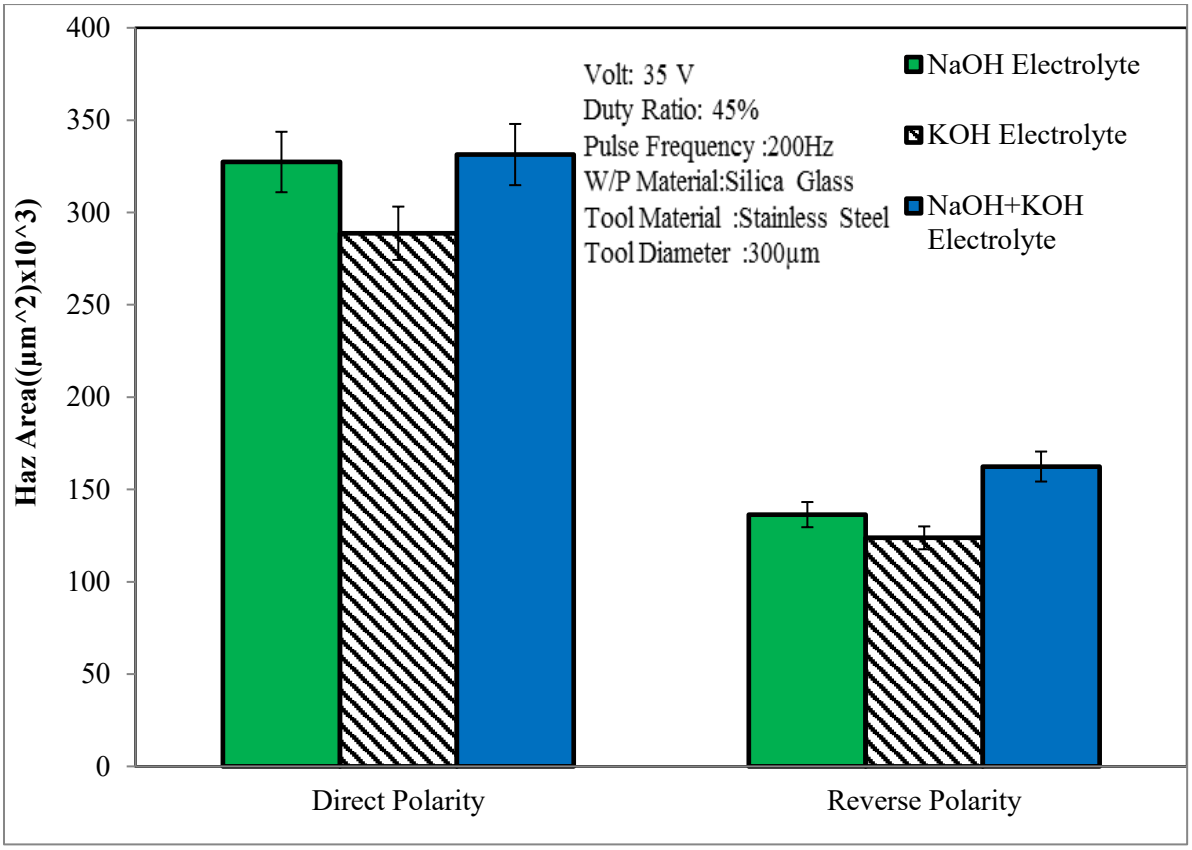

Fig. 4.19: Effects of direct polarity and reverse polarity on HAZ area

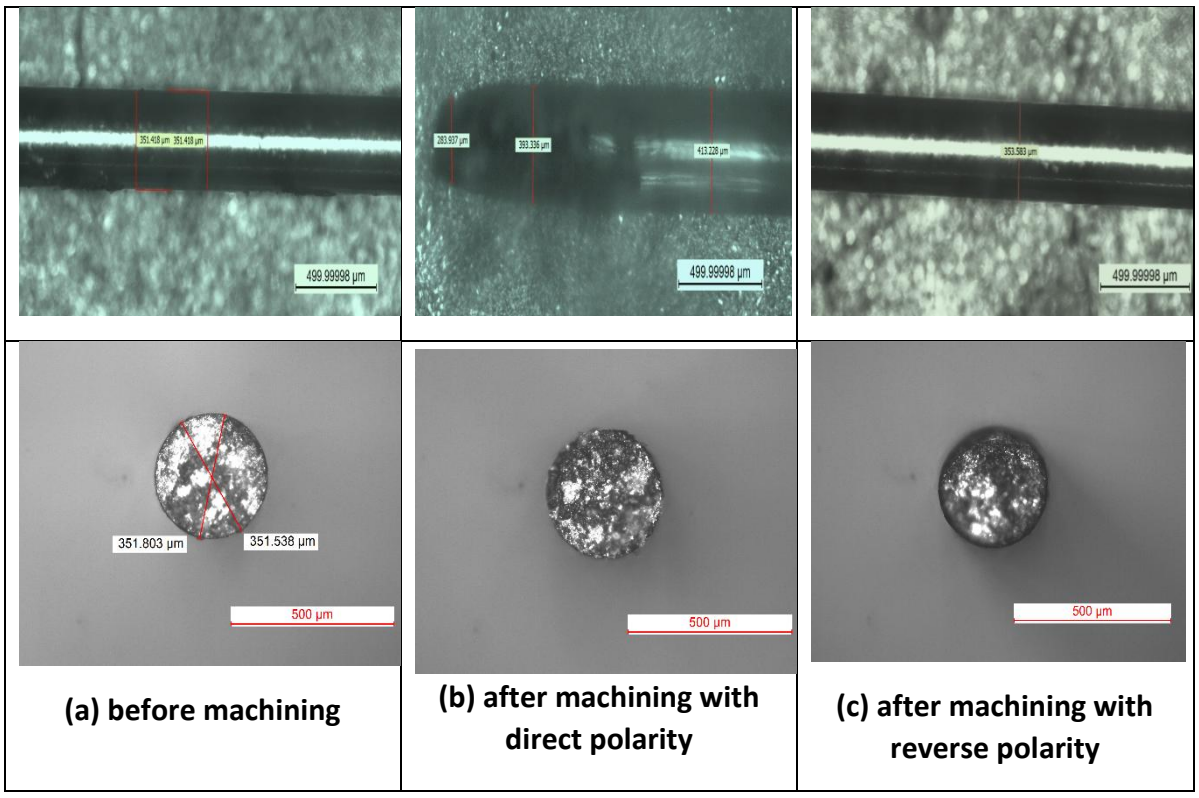

Fig. 4.20: Photographic views of micro-tool

4.6 OUTCOMES OF THE PRESENT RESEARCH

In this study, three different approaches have been used to make grooves on flat surface of glass workpiece materials. Within the constraints of the investigation, the following inferences are drawn:

(i) If NaOH solution is used as electrolyte during micro-grooves cutting on glass, MRR improves with rise of applied voltage, EC, DR but drops with PF. Overcut and HAZ area always increase with the boost of applied voltage when NaOH electrolyte is used.

(ii) MRR enhances with the increase of concentration of all electrolytes i.e. NaOH, KOH and NaOH+KOH at direct polarity. MRR is greater for KOH solution than NaOH and mixture of these electrolytes. MRR is very low at the reverse polarity (3.2 mg/hr) as compared to the direct polarity (27.25 mg/hr) for separate use of KOH as electrolyte.

(iii) Overcut has tendency to increase with concentration of NaOH, KOH and NaOH+KOH electrolytes. KOH electrolyte solution yields lower overcut (64.68 μm) whereas NaOH solution produces larger overcut (198.826 μm). Medium overcut is found by using NaOH+KOH as electrolyte. KOH electrolyte offers low overcut at both direct and reverse polarities.

(iv) HAZ area increases with increase of concentration of electrolytes and is very large (908.92 x 10^3 μm^2) for NaOH electrolyte as compared to KOH & NaOH+KOH. HAZ area is observed as the smaller by using KOH electrolyte (288.734 x 10^3 μm^2 & 123.78 x 10^3 μm^2) while HAZ becomes larger for mixed electrolyte solutions at both direct and reverse polarities *i.e.* 313.356 x 10^3 μm^2 and 162.387 x 10^3 μm^2 respectively.

(v) KOH electrolyte used at direct polarity is suitable for achieving high MRR whereas KOH electrolyte with reverse polarity is good for low overcut, HAZ area and tool wear.

After successfully producing micro-grooves on a flat surface of glass material, it is also essential to generate micro-grooves on a cylindrical surface, as this has many applications in various industries. The next chapter focuses on a detailed analysis of micro-grooving on the cylindrical surface of glass using the μ-ECDG process.

CHAPTER 5: EXPERIMENTAL INVESTIGATION INTO ELECTROCHEMICAL DISCHARGE MICRO-GROOVING (µ-ECDG) ON CYLINDRICAL SURFACE OF GLASS

5.1 EXPERIMENTATION

To achieve the objectives of the current research project and effectively control input process variables such as voltage, electrolyte concentration, and workpiece rotational speed, a specialized µ-ECDG experimental setup was developed. All experiments were conducted based on a well-planned experimental design.

A cylindrical glass rod was utilized as the workpiece, and a copper micro-tool with a 260 µm diameter served as the tool-electrode in each experiment to examine the effects of various input process variables on machining responses for micro-grooving on glass. These variables included electrolyte concentration (EC), rotational speed of workpiece and voltage, while the responses measured were Material Removal Rate (MRR), Width of Groove (WG) and Depth of Groove (DG). All experiments were conducted using NaOH and KOH electrolyte with a fixed Inter-Electrode Gap (40mm). During the experiments, both the One Factor at a Time (OFAT) and Response Surface Methodology (RSM) approaches were used for experimental design. The parametric settings for both approaches are provided in Set 4 and Set 5 of Table 5.1, respectively. The levels for each process parameter were determined through trial experiments, which revealed that spark discharge occurred at 35 volts but resulted in less amount of material removal due to low intensity. Significant material removal was observed at 40 V of applied voltage. It was noted that the increase in applied voltage and electrolyte concentration beyond 55 V and 30 wt%, respectively, resulted in such strong spark discharge that the glass rod's surface was thermally damaged. To achieve micro-grooving (<500 µm) on the workpiece, a tool diameter of 260 µm was chosen. The rotational speed of workpiece was another important process variable. The machining above 50 RPM deemed unsuitable due to bubble formation interference.

Table 5.1 Parametric settings for micro-grooving on glass

Parameters	Set 4	Set 5
	Values	Values
Applied Voltage (V)	40, 45, 50,55	35, 40, 45, 50,55
Electrolyte Conc. (wt%)	10, 15, 20,25	10, 15, 20,25,30
Rotational Speed (RPM)	10, 20, 30,40	10, 20, 30, 40, 50
Electrolyte	KOH Solution	NaOH Solution
Tool Electrode	Copper (260µm diameter)	Copper (250µm diameter)
Workpiece	Glass	Glass
Polarity	Direct, Reverse	Direct

5.2 RESULTS AND DISCUSSION

In µ-ECDG, cylindrical shape of glass rod was chosen as workpiece material due to its non-conducting, hard and brittle nature. Electrolyte concentration, rotational speed of workpiece and applied voltage were selected as input process parameters to investigate the machining characteristics such as Material Removal Rate (MRR) and Width of Groove (WG) during micro-grooving operation. The experimental conditions and results presented in Table 5.2 are based on the parameter settings from Set 1 in Table 5.1. MRR and WG were measured using both direct poarity (DP) and reverse polarity (RP) and the responses were compared to determine the optimal parametric conditions for achieving the best results. Width of micro-groove was measured at 5X magnification using the LEICA microscope. MRR of the µ-groove was determined using the following formula is given in equation no 3.1

Table 5.2. Experimental conditions and responses

Sl no.	EC (wt%)	Rotational Speed (RPM)	Voltage(V)	Direct Polarity		Reverse Polarity	
				Avg. MRR(µg/s)	Avg WG (µm)	Avg MRR(µg/s)	Avg WG(µm)
1	10	10	40	1.67	305.29	1.39	277.30
2	10	10	45	4.86	424.411	2.22	337.21
3	10	10	50	8.33	440.54	6.81	484.85
4	10	10	55	9.72	477.47	5.42	486.49
5	10	20	40	1.56	364.47	0.97	268.65
6	10	30	40	1.33	259.36	1.27	253.47
7	10	40	40	1.11	249.65	1.08	245.47
8	15	10	40	2.08	367.57	3.12	458.65
9	20	10	40	7.36	321.58	4.24	366.3
10	25	10	40	4.31	538.46	3.75	467.66

5.2.1 Effect of Electrolyte Concentration (EC) on MRR and WG at Different Tool Polarities

Fig. 5.1 (a) & (b) illustrate the effect of EC on average MRR and WG during micro-grooving on glass using both direct and reverse polarity. From the graph, it is obvious that both MRR and WG are increased with the rise in electrolyte concentration for both the polarities. It is revealed that maximum MRR and WG are obtained at 20 wt% and 25 wt% EC respectively using direct polarity. The increase of EC results in the rise of number of ions, particularly hydroxyl ions, which play a key role in high-temperature chemical etching during the micro-grooving process. This also enhances electrochemical etching and current density. Consequently, electrical conductivity improves, leading to the generation of high-intensity sparks and more MRR. However, higher electrolyte concentration levels may generate enough heat to damage the micro-groove structure. Fig 5.2 (a) and (b) show the micro-groove on glass at different EC for both polarities. It is found that more MRR and WG are obtained with direct polarity compared to reverse polarity.

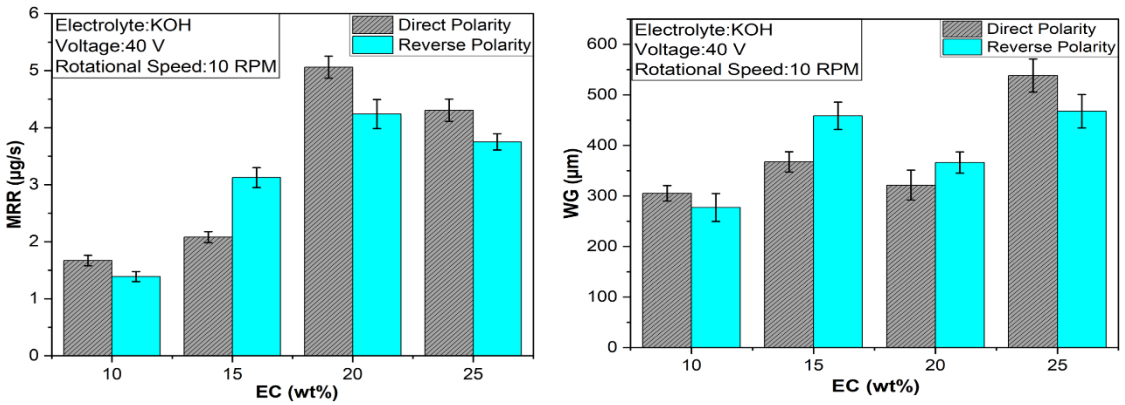

Fig.5.1 a) Effect of EC on MRR b) Effect of EC on WG

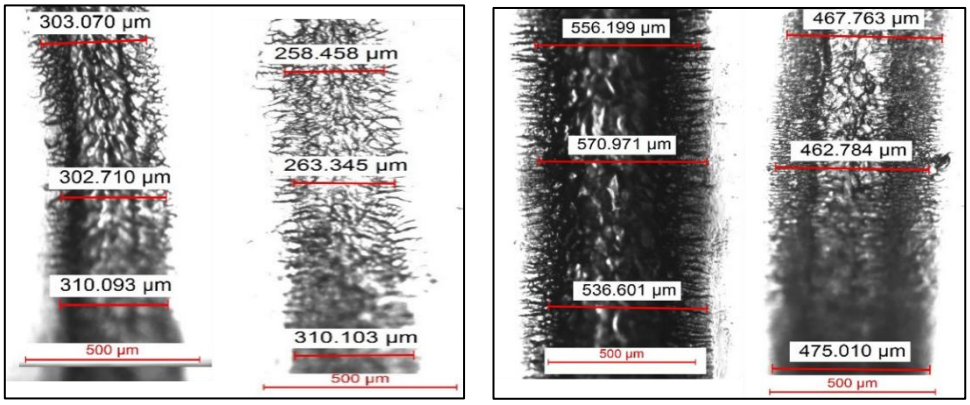

Fig.5.2 Optical image of µ-groove (a) DP vs RP at EC 10 wt% (b) DP vs RP at EC 25 wt%

5.2.2 Effect of Applied Voltage on MRR and WG at Different Tool Polarities

The enhancement of spark generation improved both current density and electrochemical reactions. This is achieved through increased applied voltage, which elevates current density and enhances electrochemical conductivity. As a result, electrochemical reactions accelerate, leading to the production of more materials. Fig. 5.3 (a) & (b) illustrate the effect of applied voltage on MRR and WG with both direct and indirect polarity. It is obvious from the chart that both MRR and WG increase with applied voltage, and MRR is higher with direct polarity compared to reverse polarity. This is because, in reverse polarity the tool (anode) absorbs most of the spark energy, while the discharge energy near workpiece is, resulting in lower MRR. From Fig 5.4 (a), it is clear that spark intensity is greater at higher EC as a result greater width of groove is achieved which has been shown in Fig.5.4 (b).

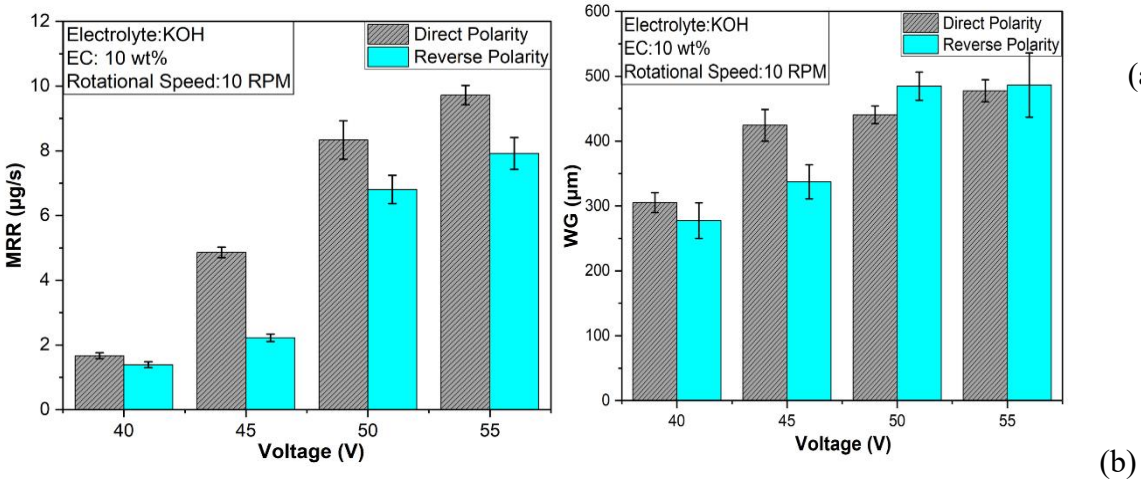

(a)

(b)

Fig.5.3 (a) Effect of Voltage on MRR (b) Effect of Voltage on WG

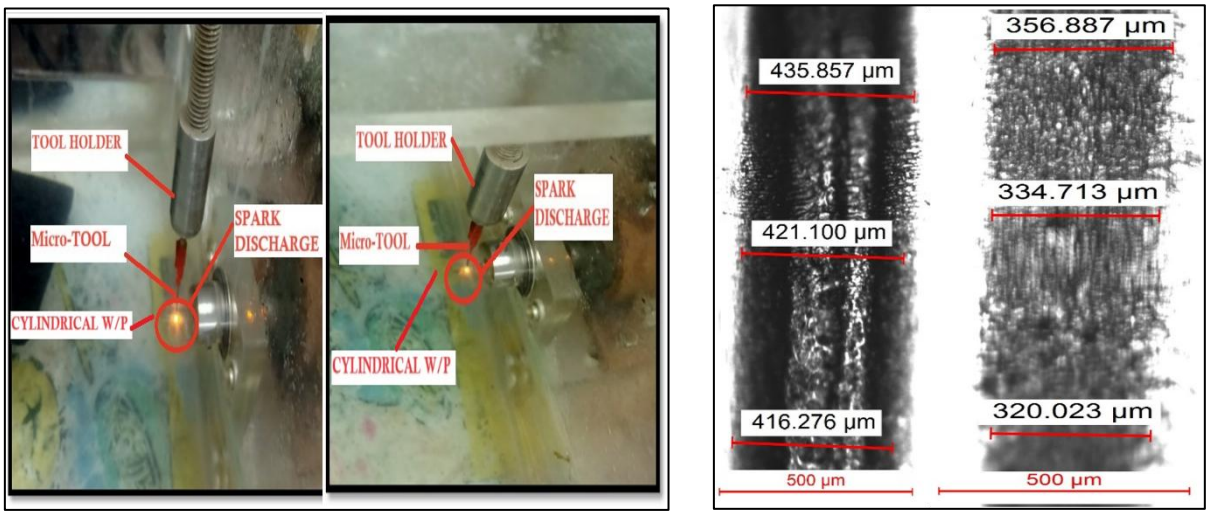

(a) (b)

Fig. 5.4 (a) Spark Discharge at 25 wt% EC/ 50 V/10 RPM vs 10 wt% EC/ 40 V/10 RPM (b) Optical image of µ-groove on DP vs RP at 45V voltage

5.2.3 Effect of Rotational Speed on MRR and WG at Different Tool Polarities

Fig.5.5 (a) & (b) indicate the influence of the rotational speed of workpiece on MRR and WG with both polarities. It is observed from the graph, both MRR and WG are decreased as the rotational speed of workpiece increases for both the polarity. At a lower rotational speed of the workpiece, it becomes easier to inject the electrolyte into the gap between the tool and workpiece. As a result, more access of the electrolyte to the machining zone and more efficient removal of materials. Another reason may be due to more surface contact between the tool and workpiece at lower rotational speed, resulting in more localised heating and faster material

removal. Fig. 5.6 depicts the pictorial view along with micro-grooves obtained at 20 rpm using reverse polarity.

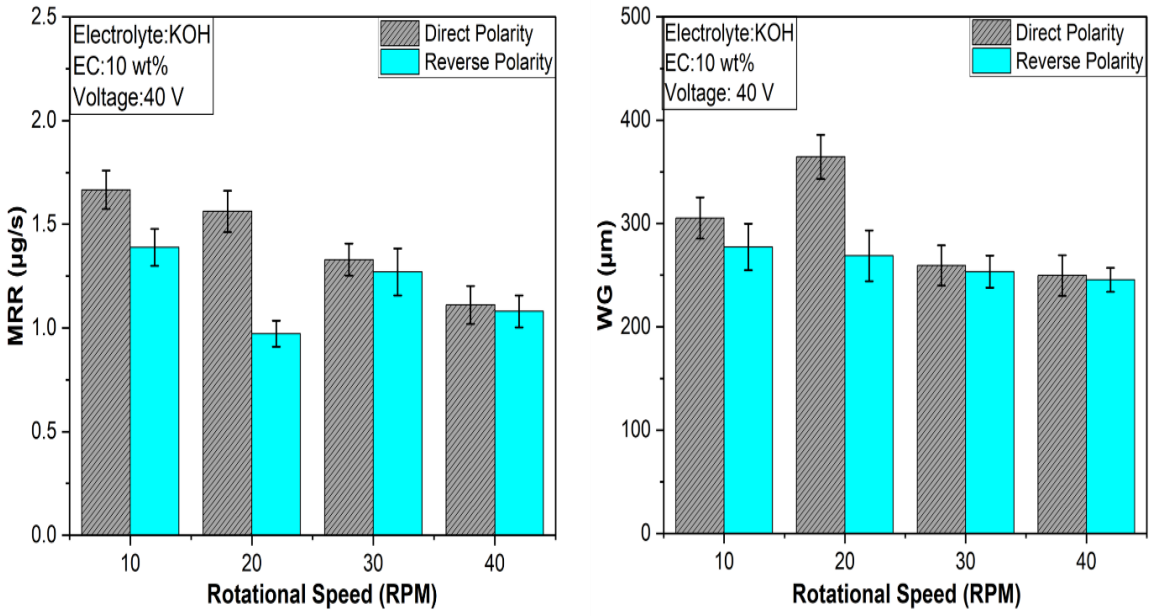

(a) (b)

Fig.5.5 (a) Effect of rotational speed on MRR (b) Effect of rotational speed on WG

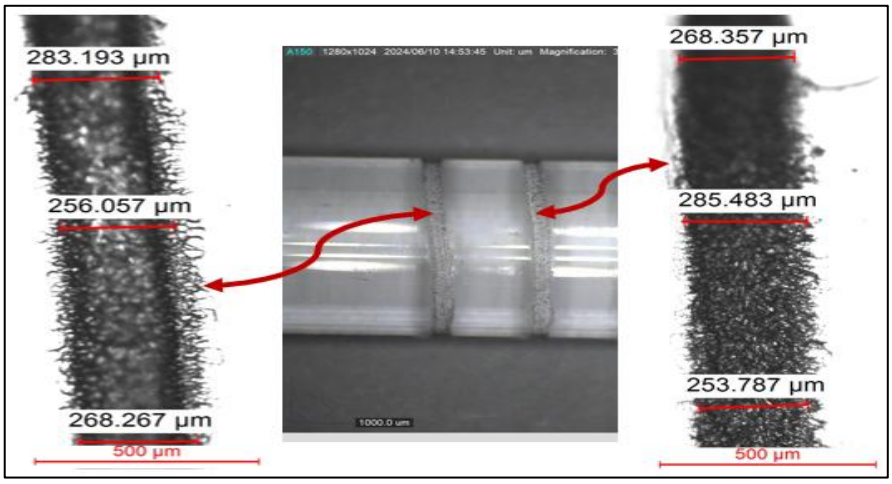

Fig. 5.6 Enlarged µ-groove image using RP at 10 wt% EC/20RPM/40V

5.3 ANALYSIS BASED ON RESPONSE SURFACE METHODOLOGY (RSM)

In the current section, the results of experiments conducted based on response surface methodology are presented in Table 5.3. Depth of Groove (DG) is measured with the help of a Dino-Lite Microscope using the followig formula presented in equation no 3.2

Fig. 5.7 shows the depth of micro-groove on cylindrical glass measured using Dino-Lite Microscope.

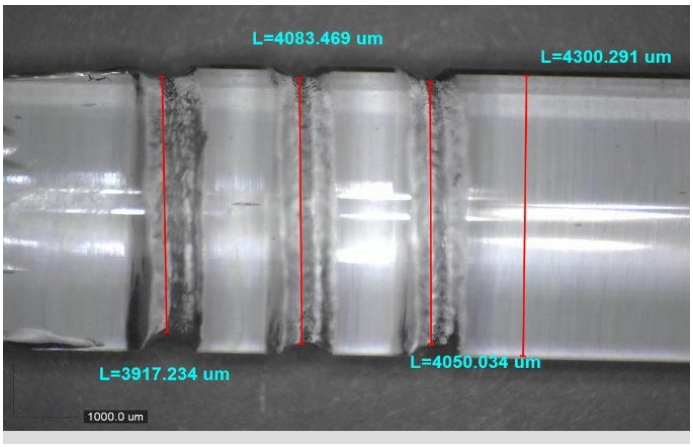

Fig. 5.7 Depth of µ-groove at EC 20wt%/30 RPM/35V

Table 5.3 Experimental conditions and responses based on RSM

Sl No.	EC (wt%)	Rotational Speed (RPM)	Voltage(V)	MRR (µg/s)	Width of Groove (µm)	Depth of Groove (µm)
1	15	20	40	9.04	388.08	127.58
2	25	20	40	13.58	456.13	230.54
3	15	40	40	5.00	315.03	63.83
4	25	40	40	13.59	410.19	163.69
5	15	20	50	17.08	422.55	147.11
6	25	20	50	47.54	439.76	429.22
7	15	40	50	9.86	383.96	87.34
8	25	40	50	38.89	484.09	335.47
9	10	30	45	3.61	298.89	52.82
10	30	30	45	32.16	483.24	335.67
11	20	10	45	17.36	433.27	177.54
12	20	50	45	5.67	299.55	76.43

13	20	30	35	11.49	390.50	130.72
14	20	30	55	52.50	505.42	366.57
15	20	30	45	21.39	474.86	213.69
16	20	30	45	16.39	425.87	172.26
17	20	30	45	19.58	456.13	201.26
18	20	30	45	13.24	397.93	160.58
19	20	30	45	14.72	415.13	141.69
20	20	30	45	18.06	443.01	199.92

The mathematical relationship between the response and the process parameters for MRR, Width of Groove and Depth of Groove on cylindrical surface of glass are given as follows:

MRR(µg/s) = $364.2 - 9.22 X_1 + 1.806 X_2 - 15.00 X_3 + 0.0054 X_1^2 - 0.01459 X_2^2 + 0.1464 X_3^3 + 0.0066 X_1X_2 + 0.2318 X_1X_3 - 0.0296 X_2X_3$ (5.3)

Width of Groove(µm) = $446 + 27.6 X_1 - 11.68 X_2 - 11.8 X_3 - 0.436 X_1^2 - 0.1707 X_2^2 + 0.133 X_3^3 + 0.275 X_1X_2 - 0.229 X_1X_3 + 0.312 X_2X_3$ (5.4)

Depth of Groove (µm) = $2177 - 61.2 X_1 + 9.02 X_2 - 83.7 X_3 + 0.164 X_1^2 - 0.1272 X_2^2 + 0.708 X_3^3 - 0.093 X_1X_2 + 1.637 X_1X_3 - 0.057 X_2X_3$ (5.5)

In the above equation, X_1 is the electrolyte concentration in wt%, X_2 is the rotational speed of workpiece in RPM and X_3 is the applied voltage in Volt. The AVOVA for MRR, Width of Groove and Depth of Groove have been shown in Table 5.4, 5.5 and 5.6 respectively. Regression equation for MRR, WG and DG are expressed in equation 5.3, 5.4 and 5.5 respectively.

Table 5.4. Results of ANOVA for MRR:

Source	DF	Adj SS	Adj MS	F-Value	P-Value
Model	9	3412.85	379.21	52.25	0.000
Linear	3	2654.45	884.82	121.92	0.000
EC(wt%)-X_1	1	1051.58	1051.58	144.89	0.000
Rotational Speed(RPM)-X_2	1	117.09	117.09	16.13	0.002
Voltage(V)-X_3	1	1485.78	1485.78	204.72	0.000
Square	3	471.41	157.14	21.65	0.000
X_1*X_1	1	0.45	0.45	0.06	0.808
X_2*X_2	1	53.51	53.51	7.37	0.022
X_3*X_3	1	337.02	337.02	46.44	0.000
2-Way Interaction	3	286.98	95.66	13.18	0.001
X_1*X_2	1	0.86	0.86	0.12	0.738
X_1*X_3	1	268.59	268.59	37.01	0.000
X_2*X_3	1	17.53	17.53	2.42	0.151
Error	10	72.58	7.26		
Lack-of-Fit	5	26.11	5.22	0.56	0.729
Pure Error	5	46.46	9.29		
Total	19	3485.42			

All linear terms EC (wt%), Rotational Speed of Workpiece (RPM) and Voltage (V)) are significant with p-values of 0.000, 0.002, and 0.000, respectively, as shown in Table 5.4. Voltage (V) has the highest F-value (204.72), indicating it has the most substantial impact on MRR among the linear terms. The overall model is highly significant, as indicated by F-value of 52.25 and p-value of 0.000. This suggests that the model effectively explains the variation in MRR. The lack-of-fit test is not significant (p-value = 0.729), indicating that the model adequately fits the data. The model fits the data well, making it a useful tool for process optimization.

Table 5.5 Results of ANOVA for Width of Groove

Source	DF	Adj SS	Adj MS	F-Value	P-Value
Model	9	59227.2	6580.8	9.93	0.001
Linear	3	44945.4	14981.8	22.60	0.000
EC(wt%)-X_1	1	26343.4	26343.4	39.74	0.000
Rotational Speed(RPM)-X_2	1	9057.9	9057.9	13.66	0.004
Voltage(V)-X_3	1	9544.1	9544.1	14.40	0.004
Square	3	10560.1	3520.0	5.31	0.019
X_1*X_1	1	2988.2	2988.2	4.51	0.060
X_2*X_2	1	7322.6	7322.6	11.05	0.008
X_3*X_3	1	277.3	277.3	0.42	0.532
2-Way Interaction	3	3721.7	1240.6	1.87	0.198
X_1*X_2	1	1513.4	1513.4	2.28	0.162
X_1*X_3	1	263.2	263.2	0.40	0.543
X_2*X_3	1	1945.1	1945.1	2.93	0.117
Error	10	6629.0			
Lack-of-Fit	5	2679.0	535.8	0.68	0.660
Pure Error	5	3950.0	790.0		
Total	19	65856.2			

All linear terms (EC (wt%), Rotational Speed of Workpiece (RPM) and Voltage (V)) are highly significant, with p-values of 0.000, 0.004, and 0.004, respectively, as shown in Table 5.5. EC (wt%) has the highest F-value (39.74), indicating it has the most substantial impact on Width of Groove (WG) among the linear terms. The lack-of-fit test is not significant (p-value = 0.660), indicating that the model adequately fits the data. The overall model is significant, as indicated by the F-value of 9.93 and a p-value of 0.001. This suggests that the model explains a significant portion of the variation in WG.

Table 5.6. Results of ANOVA for Depth of Groove

Source	DF	Adj SS	Adj MS	F-Value	P-Value
Model	9	198160	22018	32.23	0.000
Linear	3	169180	56393	82.55	0.000
EC(wt%)-X_1	1	105424	105424	154.32	0.000
Rotational Speed(RPM)-X_2	1	14782	14782	21.64	0.001
Voltage(V)-X_3	1	48974	48974	71.69	0.000
Square	3	15342	5114	7.49	0.006
X_1*X_1	1	423	423	0.62	0.450
X_2*X_2	1	4065	4065	5.95	0.035
X_3*X_3	1	7878	7878	11.53	0.007
2-Way Interaction	3	13638	4546	6.65	0.010
X_1*X_2	1	172	172	0.25	0.627
X_1*X_3	1	13400	13400	19.62	0.001
X_2*X_3	1	66	66	0.10	0.763
Error	10	6832	683		
Lack-of-Fit	5	2958	592	0.76	0.613
Pure Error	5	3874	775		
Total	19	204991			

From Table 5.6, it is clear that the linear terms EC (wt%), Rotational Speed of workpiece (RPM) and Voltage(V) are all statistically significant (p-values < 0.05), indicating they have a strong influence on Depth of Groove (DG). EC (wt%) has the most substantial effect, with an F-value of 154.32 and a p-value of 0.000. This suggests that the EC is the most critical factor. The lack-of-fit test is not significant (p-value = 0.613), which means the model adequately fits the data. The overall model is highly significant, as indicated by the F-value of 32.23 and a p-value of 0.000. This means the model explains a significant portion of the variability in DG.

5.3.1 Influence of Voltage and EC on Responses

Fig. 5.8 illustrate a contour plot that presents the relationship between EC, Voltage and MRR while keeping the rotational speed of workpiece constant at 30 rpm. The X-axis represents voltage (V), the Y-axis represents electrolyte concentration (EC) in wt% and the color gradient represents MRR (µg/s). The blue areas indicate a low MRR, while the red areas represent a high MRR. From the graph, it is evident that MRR increases as both voltage and EC increase. The higher MRR is observed in the top-right region of the plot, where both Voltage and EC are high (55V & 30 wt%), whereas the lower MRR occurs in the bottom-left region, where both parameters are at their lowest(35V & 10 wt%). Fig. 5.9 shows a surface plot which provides a more visual representation of MRR changes with variations in voltage and EC. The color gradient follows a similar pattern to the contour plot. The surface of the graph shows a non-linear relationship where MRR increases exponentially as voltage and EC increase beyond 50V and 20 wt%. The lower MRR is observed at the minimum voltage and EC values while the higher MRR occurs when both parameters are set to their maximum levels.

Fig. 5.10 and Fig. 5.11 present a contour plot and a surface plot respectively, depicting the variation in width of groove with respect to Voltage and EC while keeping the rotational speed of the workpiece constant at 30 rpm. The trend suggests that as both voltage and EC increase, WG also increases with the highest values occurring in the top-right region where both parameters are at their maximum level (55V & 30 wt%). From the surface plot it was observed that a non-linear increase in WG, meaning that at lower values of voltage and EC (below 45V & 15wt%), WG increases gradually, but as the values rise further WG increases more significantly.

Fig. 5.12 shows a contour plot of depth of groove with respect to voltage and EC. The minimal groove depth (DG) was obtained at lower voltage and EC (35V & 10 wt%) while the higher DG was observed in the top-right corner, where the voltage and EC were set at 55V and 35 wt%, respectively.Fig. 5.13 presents a surface plot for more detailed view of DG variation. The steep rise at higher Voltage and EC values(beyond 50V & 25 wt%) confirms a nonlinear increase in DG implying a more pronounced effect at higher parameter's values.

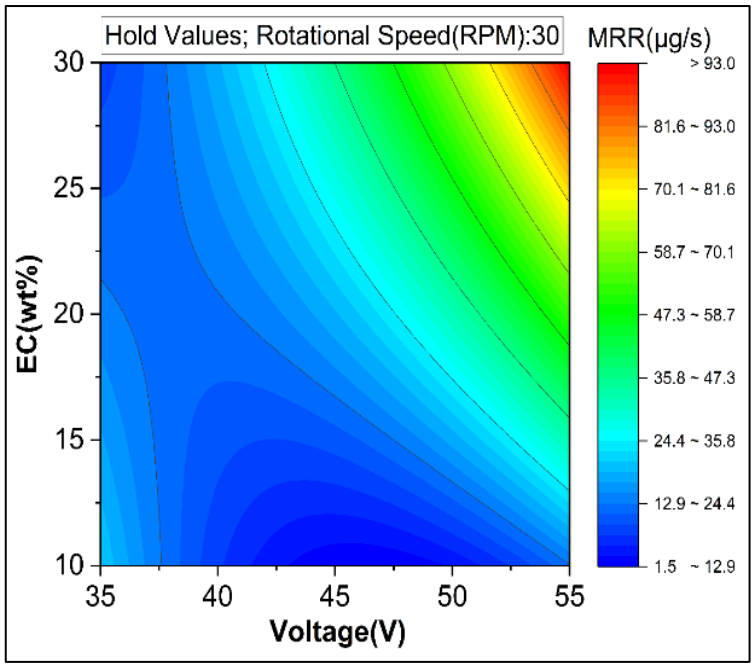

Fig. 5.8 Contour plot of MRR w.r.t Voltage and EC

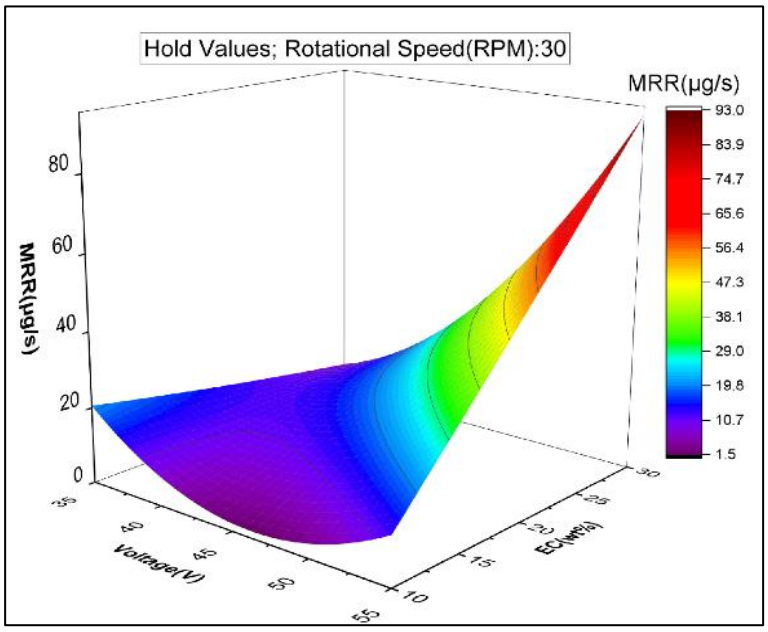

Fig. 5.9 Surface plot of MRR w.r.t Voltage and EC

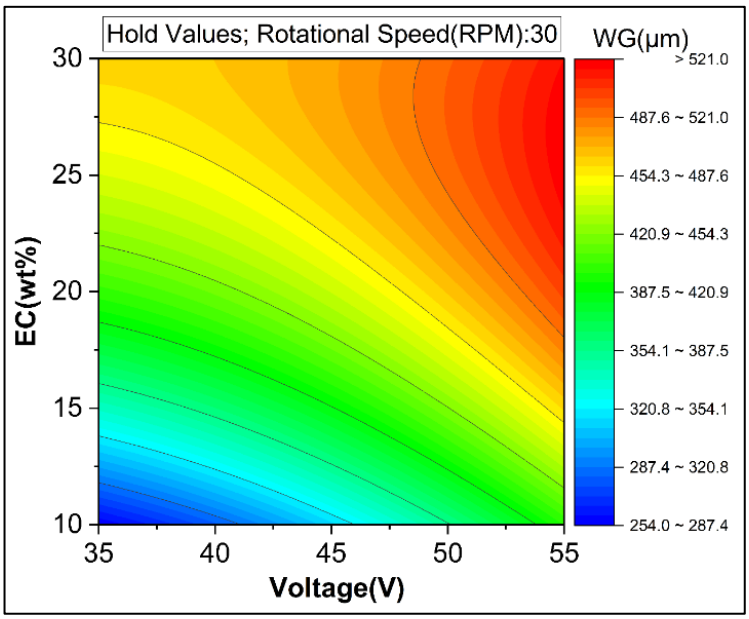

Fig. 5.10 Contour plot of WG w.r.t Voltage and EC

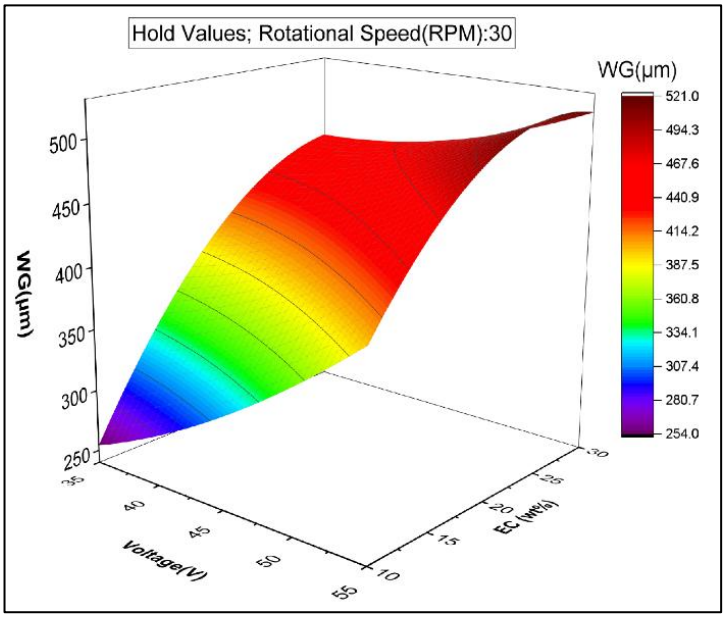

Fig. 5.11 Surface plot of WG w.r.t Voltage and EC

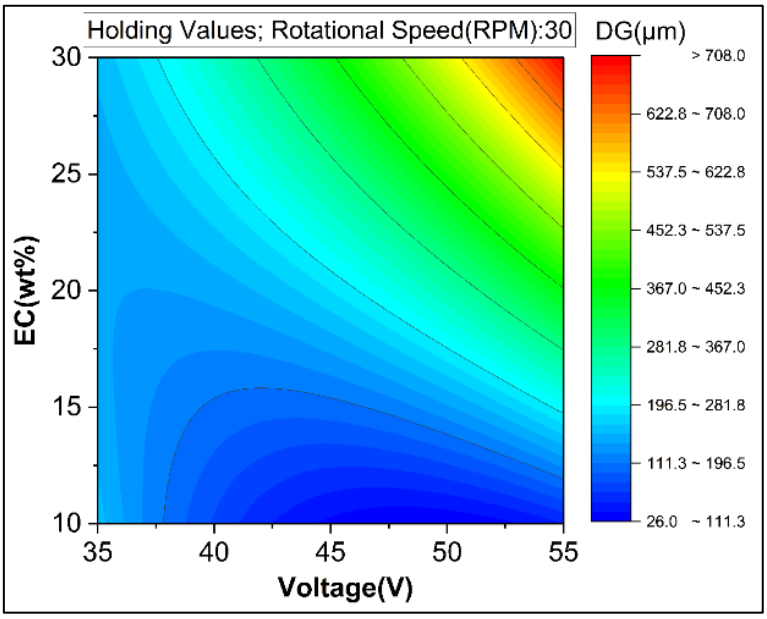

Fig. 5.12 Contour plot of DG w.r.t Voltage and EC

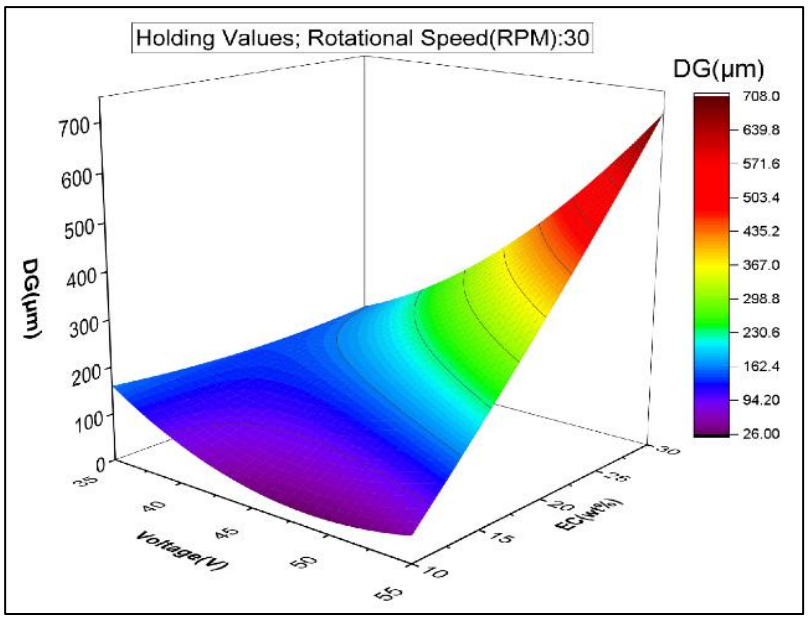

Fig. 5.13 Surface plot of DG w.r.t Voltage and EC

5.3.2 Influence of Voltage and Rotational Speed of Workpiece on Responses

Fig. 5.14 illustrate a contour plot of MRR with respect to voltage and rotational speed of workpiece by keeping constant EC at 20wt%. From the graph, it was observed that as the voltage increases, the MRR also increases significantly, especially in the higher voltage range(50V). The effect of rotational speed appears less prominent and at higher rotational speed of workpiece (above 40 rpm) MRR values decreased drastically. Fig. 5.15 depicts surface plot illustrating the same relationship between voltage, rotational speed of workpiece and MRR. It is clear from the graph that voltage has a stronger influence on MRR with a steep increase in MRR at higher voltage. The surface curvature also suggests that an optimal combination of 0voltage and rotational speed maximizes MRR, with the highest value appearing in the red region of the plot.

Fig. 5.16 and Fig. 5.17 present contour plot and surface plot that visually represents the effect of voltage and rotational speed of workpiece on WG. The color gradient from blue (lower WG) to red (higher WG) indicates that WG increases as voltage rises and lower WG was achieved at higher rotataional speed(beyond 40rpm). From the graph, it was observed that at lower voltage, WG remains relatively uniform, while at higher voltage, a significant increase. Fig.5.17 provides a more detailed visualization of the WG variation. It shows that WG exhibits a steep increase at higher voltages and moderate value of rotational speed of workpiece(55V & 30 rpm) and highlighted the dominant role of voltage in influencing WG.

Fig. 5.18 shows contour plot of depth of groove with respect to voltage and rotational speed of workpiece. It is clear from the graph that significantly increases of DG at higher voltage particularly beyond 50V. The effect of rotational speed is comparatively less dominant but contributes to the overall trend. The contour lines suggest a gradual increase in DG with increasing voltage with the highest values observed in the red regions. Fig. 5.19 illustrates surface plot of the same variables such as voltage and rotational speed. The curved surface indicates that DG increases sharply at higher voltage and lower rotational speed while at lower voltage, the change is relatively moderate. The higher DG values are observed in the red regions, confirming that voltage plays the most significant role in increasing DG.

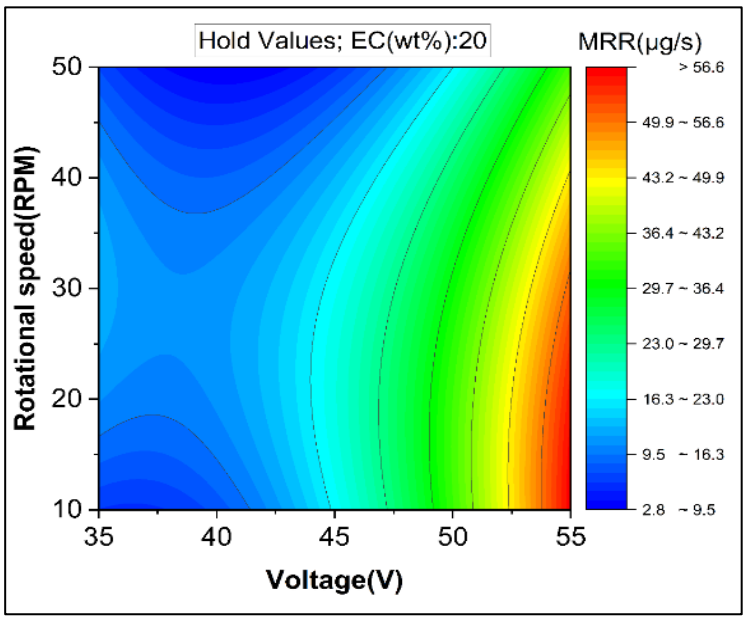

Fig. 5.14 Contour plot of MRR w.r.t Voltage and Rotational speed of workpiece

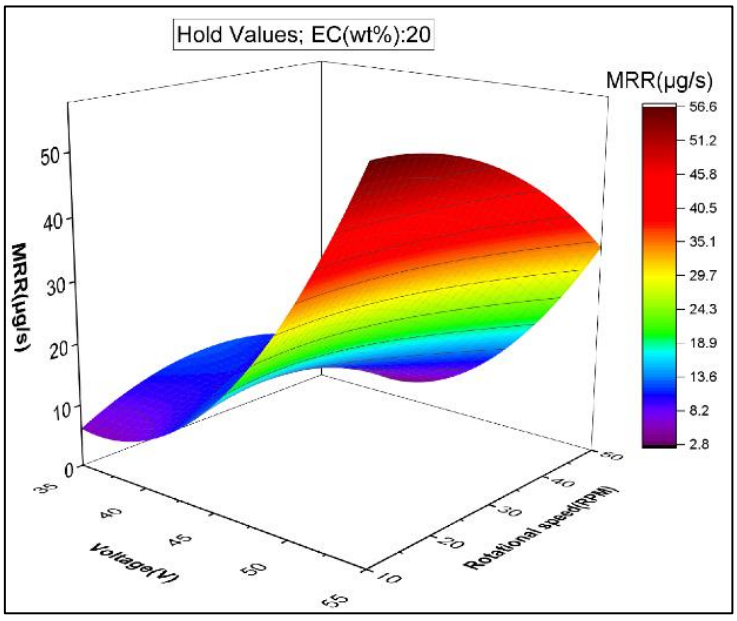

Fig.5.15 Surface plot of MRR w.r.t Voltage and Rotational speed of workpiece

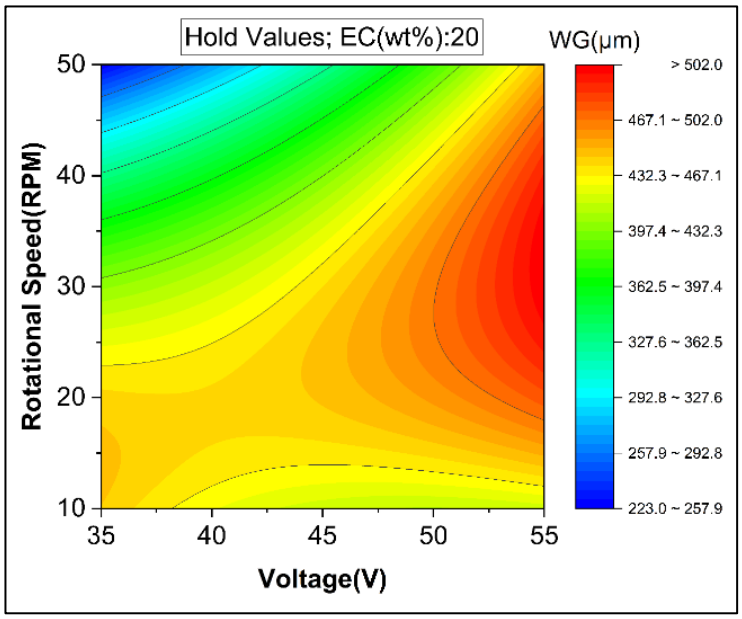

Fig. 5.16 Contour plot of WG w.r.t Voltage and Rotational speed of workpiece

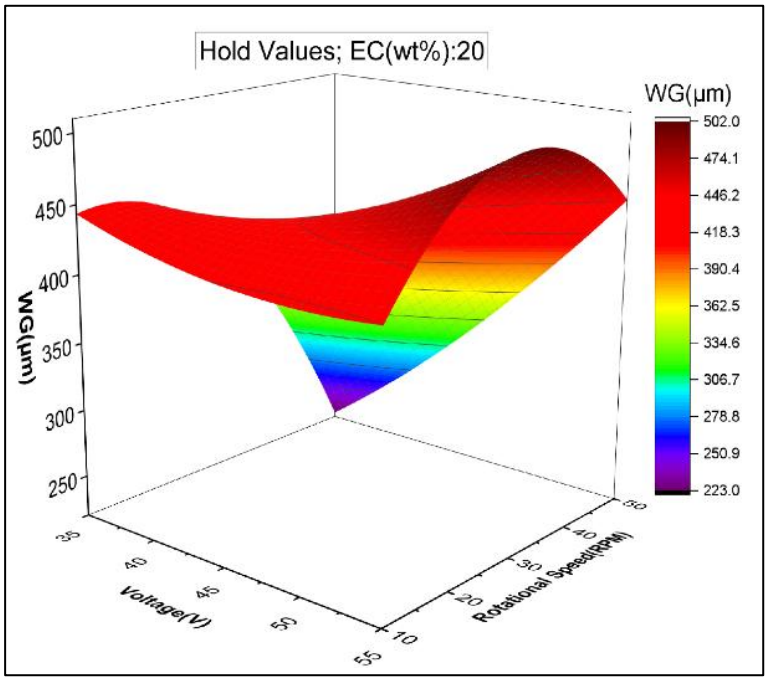

Fig. 5.17 Surface plot of WG w.r.t Voltage and Rotational speed of workpiece

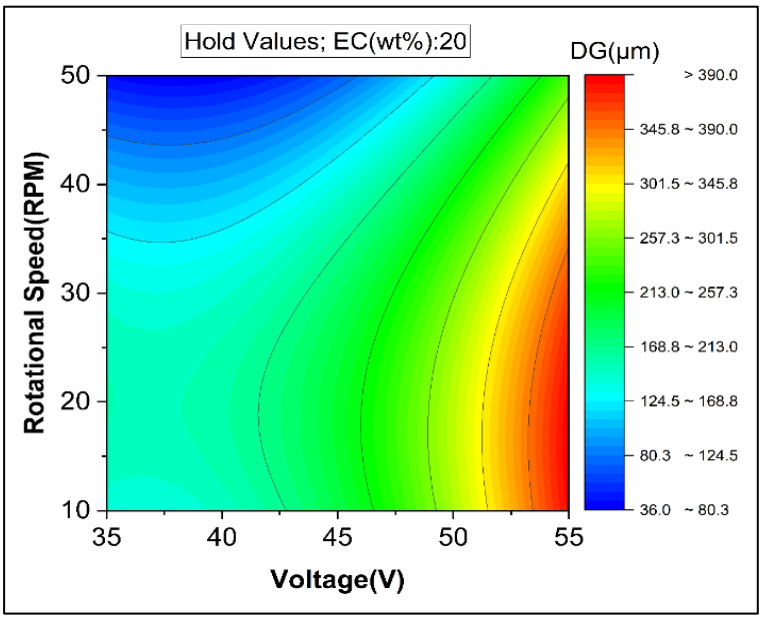

Fig. 5.18 Surface plot of DG w.r.t Voltage and Rotational speed of workpiece

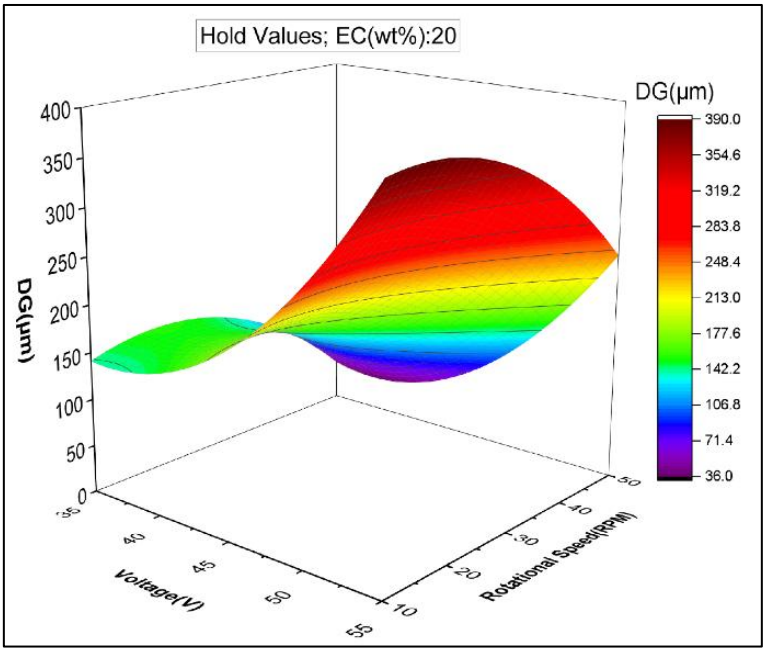

Fig. 5.19 Surface plot of DG w.r.t Voltage and Rotational speed of workpiece

5.3.3 Influence of EC and Rotational Speed of Workpiece on Responses

Fig. 5.20 illustrates a contour plot of MRR with respect to EC and rotational speed of workpiece by voltage held constant at 45V. The colour gradient from the contour plot suggests that there is a gradual increase in MRR with the increase of EC and decrease of rotational speed. The higher value of MRR is obtained beyond 20wt% EC. Fig. 5.21 presents surface plot of the same relationship between EC, rotational speed and MRR. The plot demonstrates that MRR increases with the increase of EC up to 25wt% and moderate value of rotational speed (30rpm) confirming a direct correlation between these process parameters and MRR.

Fig. 5.22 and 5.23 show a contour plot and a surface plot of the width of groove (WG) by varying EC and rotational speed of workpiece. From the color gradient of the contour plot, it is evident that a higher WG is achieved at higher value of EC(beyond 20wt%) and moderate rotational speeds(30 rpm). However, at higher rotational speeds (>40 RPM), the WG value decreases. The surface plot clearly shows that EC has a stronger influence on WG, with a steep increase in WG at higher EC (30 wt%). In contrast, lower WG is obtained at high rotational speed (50 RPM). The surface curvature also suggests that an optimal combination of EC and rotational speed maximizes WG, with the highest values appearing in the red region of the plot.

Fig.5.24 and 5.25 illustrate contour plot and surafce plot of depth of groove with respect to EC and rotational speed of workpiece by fixing voltage at 45V. From the graph, it is evident that as EC increases, DG also increases. However, with an increase in rotational speed, DG decreases. The lowest DG values (blue and green regions) are observed at lower EC and RPM, whereas the high values of DG in red region appear at high EC and moderate rotational speed. Fig.5.25 shows the surface plot for better understanding the relationship between the variables. The curved surface demonstrates a clear increasing trend of DG with rising EC and decrease in rotational speed. The graph also suggests a nonlinear dependency of DG on EC and rotational speed of workpiece.

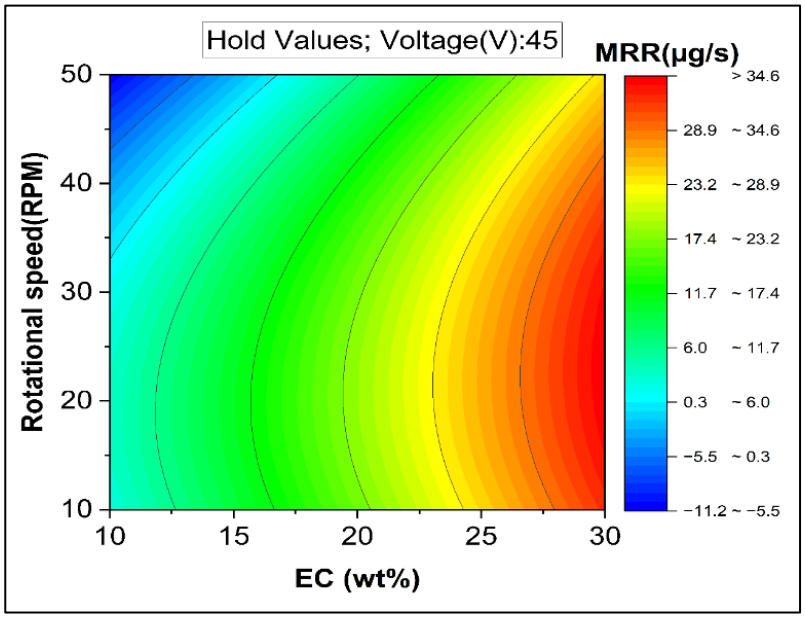

Fig. 5.20 Contour plot of MRR w.r.t EC and Rotational speed of workpiece

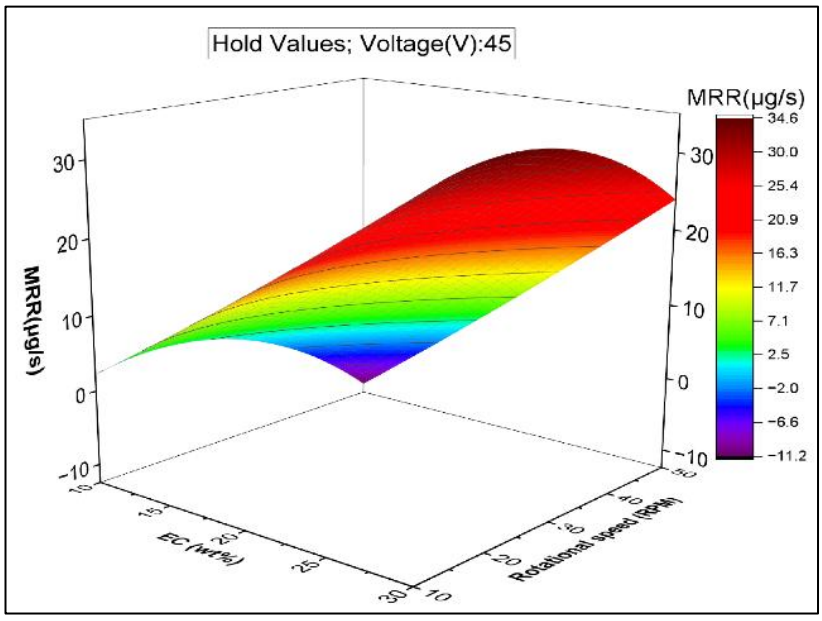

Fig. 5.21 Surface plot of MRR w.r.t EC and Rotational speed of workpiece

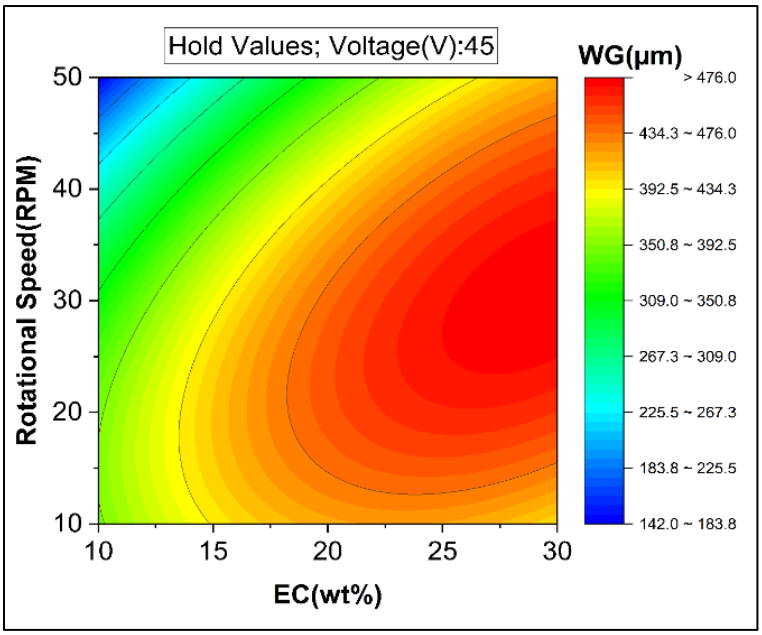

Fig. 5.22 Contour plot of WG w.r.t EC and Rotational speed of workpiece

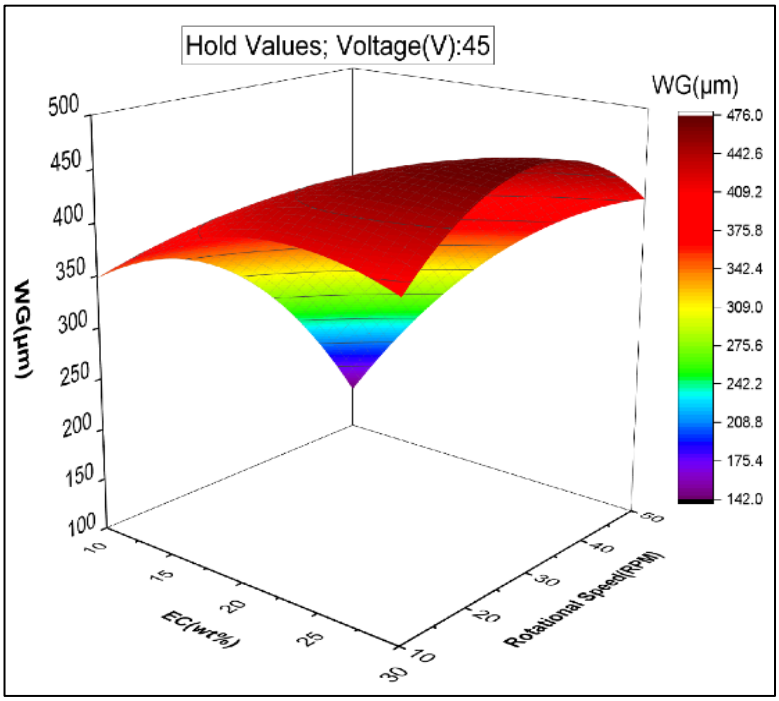

Fig. 5.23 Surface plot of WG w.r.t EC and Rotational speed of workpiece

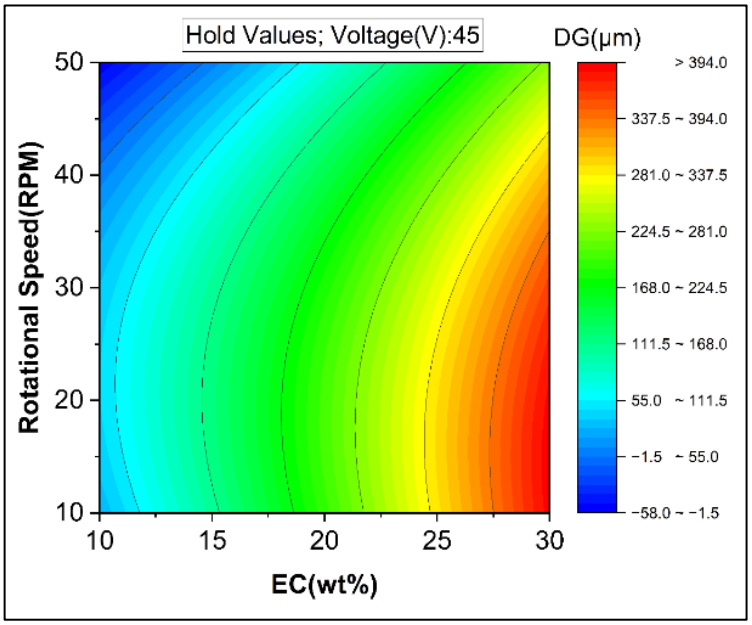

Fig. 5.24 Contour plot of DG w.r.t EC and Rotational speed of workpiece

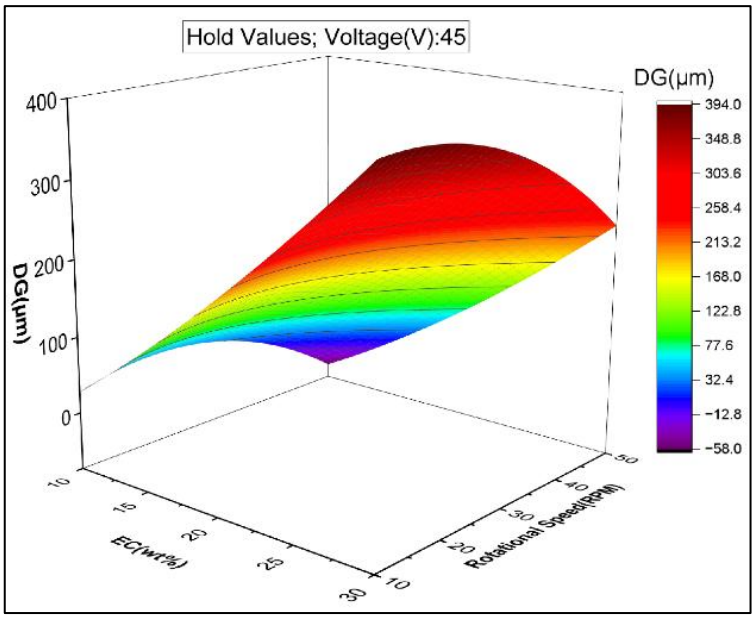

Fig. 5.25 Surface plot of DG w.r.t EC and Rotational speed of workpiece

5.4 PARAMETRIC OPTIMIZATION OF RESPONSES

This section focuses on optimizing the responses using the desirability function approach in MINITAB software. It determines the optimal process variable settings for achieving the best response output.

5.4.1 Single Objective Optimization

The analysis of individual responses was conducted using the proposed mathematical models to achieve the maximum MRR and target values of 500 μm for Width of Groove (WG) and Depth of Groove in micromachining operations. The desirability function (D) was assigned a weight value of 1 for optimal response values. For micro-grooving on sodalime glass, MINITAB 17 software was used to optimize responses through desirability function analysis. In optimization graph, columns represent factors, while rows correspond to responses. Each cell illustrates the relationship between a response and a process variable, with other variables held constant. The graph displays high and low settings of the experimental design at the column tops, and the red row indicates the current process variable values for achieving objectives. Information on response goals, desired values, current y factors, and desirability values is provided to the left of each row.

Fig. 5.26 to Fig. 5.28 present the results of single-objective optimization for the responses. Figure 5.26 reveals that the optimal process variable settings for achieving a maximum MRR of 95.31 μg/s are 30 wt% EC, 12.83 RPM rotational speed of workpiece and voltage of 55V. To attain the target value width of groove, Fig. 5.27 indicates optimal input variable settings of 29.82 wt% EC, 50 RPM rotational speed of workpiece and 53.79 V voltage. Additionally, Fig. 5.28 shows that the optimal settings for achieving the target value of Depth of Groove are 27.42 wt% EC, 10 RPM rotational speed of workpiece and 50.74 V voltage.

SINGLE OBJECTIVE OPTIMIZATION:

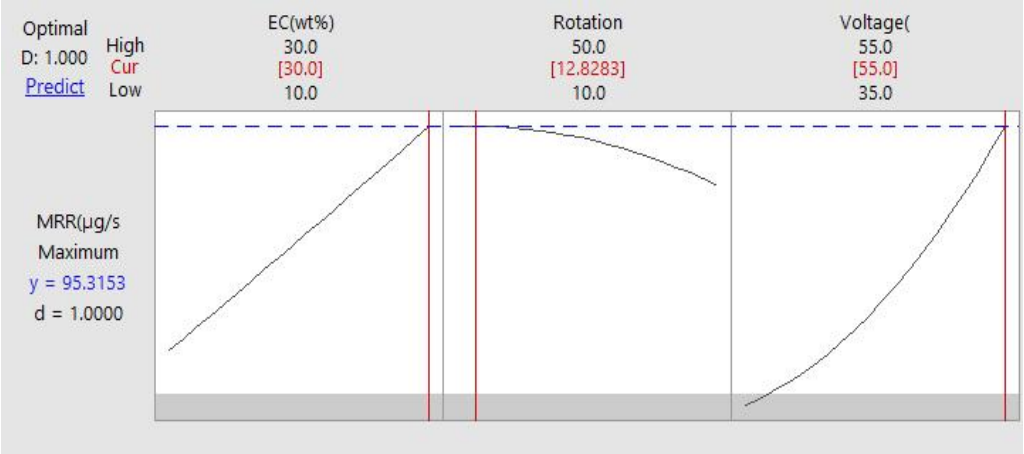

Fig. 5.26 Optimization plot for MRR

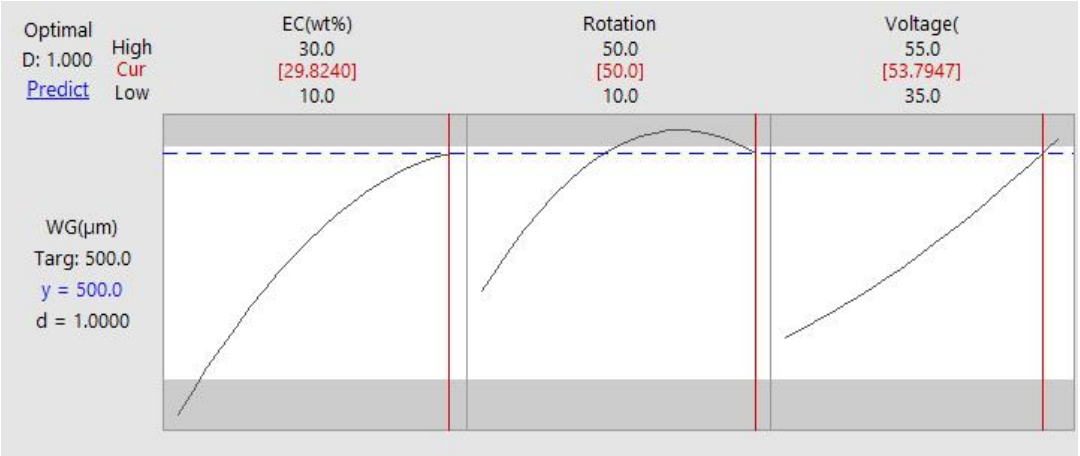

Fig. 5.27 Optimization plot for Width of Groove

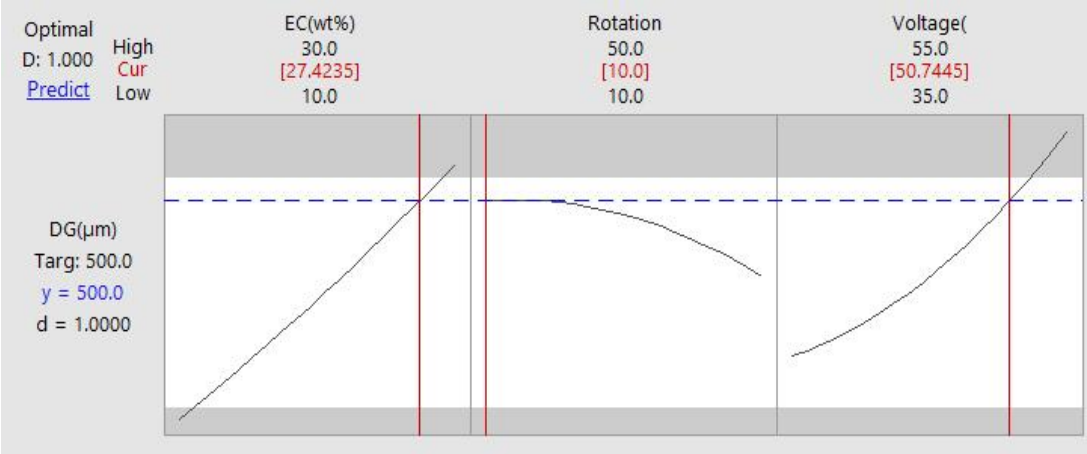

Fig 5.28 Optimization plot for Depth of Groove

5.4.2 Multi Objective Optimization

Multi objective optimization of responses have been performed using Minitab 17 software to find the optimal solution for achieving optimum values of responses and results are shown in Fig.5.29. It was observed that the overall composite desirability (D) is 0.9890 which is very close to 1, indicating that the selected parameter settings provide an almost optimal solution for the given objectives. The response variables include Depth of Groove (DG), Width of Groove (WG), and Material Removal Rate (MRR). The target for DG is 500 µm and the optimized value is 498.74 µm, with a desirability score of 0.9972, which is very close to 1. Similarly, the target for WG is 500 µm, and the optimized value is 493.99 µm, with a desirability score of 0.9701. The MRR, which is maximized in this optimization, reaches 58.04 µg/s with a perfect desirability score of 1.0000. The optimal settings for this multi objective optimization plot of input parameters are 28.70% for EC, 30.20 RPM for rotational speed of workpiece and 50.56V for voltage.

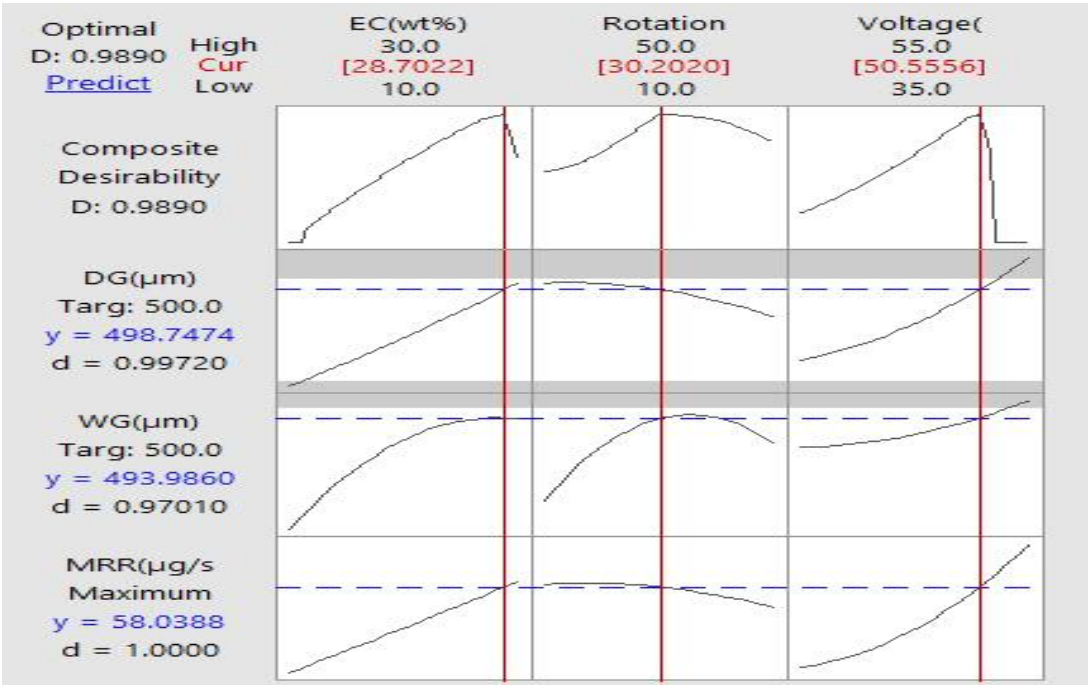

Fig. 5.29 Optimization plot for multi objective optimization

The input parameters derived from the multi-objective optimization plot are used to conduct experiments to determine the error between theoretical and predicted results. using the formula given in equation 5.6 and results are shown in Table5.7

$$\text{Error (\%)} = \left|\frac{Predicted\ Value - Actual\ Value}{Actual\ Value}\right| * 100 \qquad (5.6)$$

Table 5.7 Confirmation Test

	Responses		
	Avg MRR (µg/s)	Avg Width of Groove (µm)	Avg Depth of Groove (µm)
Actual (29wt%, 30 rpm, 50V)	55.124	514.419	479.294
Predicted (28.7022 wt%, 30.2020 rpm, 50.5556 V)	58.0388	493.986	498.7474
Error (%)	5.3	4.0	4.1

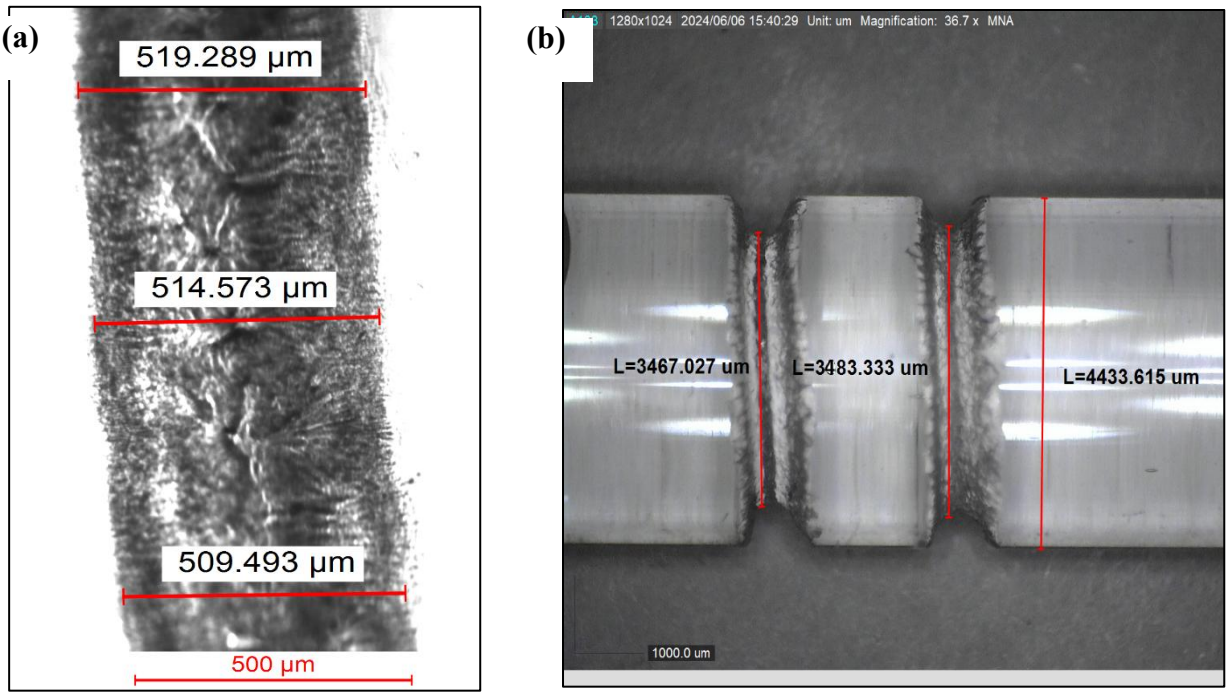

Fig. 5.30 (a) Pictorial view of width of groove and (b) depth of groove at 29 wt% EC/30 RPM/50V

The percentage of error obtained are 5.3% for MRR, 4% for width of groove and 4.1% for depth of groove. Fig. 5.30 depicts the WG and DG obtained by setting the parametric combination of 29wt% EC, 30 rpm of rotational speed of workpiece and 50V voltage which are closest values to the predicted parametric settings. Thus, a notable enhancement in machining responses during micro-grooving on glass using μ-ECDG was achieved through the application of RSM methods.

5.5 OUTCOME OF THE PRESENT RESEARCH

Upon completion and analysis of all the experiments, it is noted that both Material Removal Rate (MRR) and Width of Groove (WG) increase with higher electrolyte concentration (EC) for direct and reverse polarity. The higher MRR is observed at 20 wt% EC, while WG reaches its higher value at 25 wt% EC under direct polarity conditions. Direct polarity gives higher MRR and WG compared to reverse polarity, suggesting enhanced efficiency in the micro-grooving process. The higher MRR in direct polarity is attributed to the tool absorbing most of the spark energy in reverse polarity, thus reducing discharge energy near the workpiece. As workpiece rotational speed increases, both MRR and WG decrease for both polarities. Lower rotational speed enhances surface contact between the tool and workpiece, resulting in more localized heating and faster material removal. Further investigation has been made based on RSM method on different responses like MRR, WG and Depth of Groove (DG). ANOVA results for all the responses are presented and both single objective and multi objective optimization are performed based on desirable function approach. Contour plot and surface plot of different parametric combination on various responses have presented to visualize their effect. Single objective optimization and multi objective optimization have also been performed using desirability function approach.

CHAPTER 6: GENERAL CONCLUSIONS AND FUTURE SCOPE OF RESEARCH

6.1 GENERAL CONCLUSIONS

In this study, micro-grooves are produced on two different shapes of workpieces made up of glass i.e. a flat surface and a cylindrical surface. For micro-grooving on the flat surface, the workpiece is made of silica glass and the tool material is stainless steel. In contrast, for micro-grooving on the cylindrical surface, the workpiece is made of soda-lime glass, and the tool electrode is made up of copper. For micro-grooving on the flat surface, experiments were conducted using three different parametric combinations, varying the type of electrolyte and tool polarity. To perform micro-grooving on the cylindrical surface, two different experimental design approaches one is One Factor at a Time (OFAT) and Response Surface Methodology (RSM) were used with different parametric settings.

After successfully conducting all the experiments and analyzing detailed observations on the machining performance of the Electrochemical Discharge micro-grooving (μ-ECDG) setup during micro-grooving operations, the following general conclusions can be drawn:

(i) Electrochemical discharge micro-grooving (μ-ECDG) setup is indigenously developed to produce micro-grooves on both flat as well as cylindrical surfaces of glass materials.

(ii) μ-ECDG process can be applied successfully for μ-grooving on both flat and cylindrical surface on any electrically non-conducting material like glass regardless of its chemical composition and mechanical properties.

(iii) In μ-ECDG process while NaOH solution is used as electrolyte during micro-grooving on silica glass, MRR enhances with the increase of applied voltage, Electrolyte concentrations (EC), Duty Ratio (DR) but reduces with the increase of Pulse frequency (PF). Overcut and HAZ area always increase with the increase of applied voltage when NaOH electrolyte is used.

(iv) MRR enhances with the increase of concentration of all types of electrolytes i.e. NaOH, KOH and mixture of NaOH & KOH at direct polarity. MRR is greater for KOH solution than that of NaOH and mixture of these electrolytes. MRR is

very low at the reverse polarity as compared to the direct polarity for the use of KOH as electrolyte.

(v) Overcut has tendency to increase with concentration of NaOH, KOH and mixture of NaOH & KOH electrolytes. KOH electrolyte solution yields lower overcut of 64.68 µm whereas NaOH solution produces larger overcut of 198.826 µm. Medium value of overcut is found by using mixture of NaOH & KOH. KOH electrolyte offers low overcut at both direct and reverse polarities.

(vi) HAZ area increases with the increase of concentration of electrolytes and is large i.e. 908.92 x 10^3 μm^2 for NaOH electrolyte as compared to KOH & mixture of NaOH & KOH. HAZ area is observed as the smaller by using KOH electrolyte and comparatively larger HAZ area is observed while mixed electrolyte solutions at both direct and reverse polarities are used.

(vii) KOH electrolyte used at direct polarity is suitable for high MRR whereas KOH electrolyte with reverse polarity is good for low overcut, HAZ area and tool wear.

(viii) For micro-grooving on a cylindrical glass surface using KOH electrolyte, both MRR and Width of Groove (WG) increase with the rise in EC. The MRR of 5.06 µg/s and WG of 538.46 µm are achieved at 20 wt% and 25 wt% EC, respectively, using direct polarity. More MRR and WG are obtained with direct polarity compared to reverse polarity.

(ix) Both MRR and WG increase with the increase in applied voltage and MRR is higher with direct polarity compared to reverse polarity. The higher MRR of 9.72 µg/s is achieved at 55V using direct polarity, while the highest WG of 486.49 µm is observed at 55V using reverse polarity.

(x) As the rotational speed of the workpiece increases, both MRR and WG decrease for both polarities. Higher MRR of 1.67 µg/s is achieved at 10 RPM using direct polarity while WG of 364.47 µm is observed at 20 RPM using reverse polarity. At high speed (>40 RPM) less electrolyte stays in the machining area and there is less localized heating that lead to much lower MRR and WG.

(xi) From ANOVA table of MRR, Voltage (V) is the most influential factor on MRR, followed by EC (wt%) and rotational speed of workpiece (RPM). The

interaction between EC and Voltage also plays a critical role, while other interactions and the square term for EC are less significant.

(xii) From ANOVA table of Width of Groove (WG), EC (wt%) is the most influential factor on WG, followed by rotational speed of workpiece (RPM) and Voltage (V). The square terms for rotational speed of workpiece (RPM) and EC also play an important role, while the interaction terms and the square term for Voltage are less significant.

(xiii) From the ANOVA table of Depth of Groove (DG), the most significant linear effect comes from EC (wt%) while voltage and rotational speed of workpiece exhibit both significant linear and nonlinear effects. The model effectively explains the variations in groove depth, with EC (wt%) which is the most influential factor during electrochemical discharge micro-grooving on cylindrical surface of glass.

(xiv) The single-objective optimization using desirability function analysis for micro-grooving on a cylindrical shows that the optimal process variable settings for achieving a maximum MRR of 95.31 µg/s are 30 wt% EC, 12.83 RPM rotational speed of workpiece and voltage of 55V. Similar way, to attain the target value width of groove and depth of groove (500 µm), optimal input variable settings are 29.82 wt% EC, 50 RPM rotational speed of workpiece, 53.79 V voltage and 27.42 wt% EC, 10 RPM rotational speed of workpiece, 50.74 V voltage respectively.

(xv) The multi-objective optimization reveals that a maximum MRR of 58.04 µg/s is achieved with a perfect desirability score of 1.0000. Additionally, width of groove of 493.99 µm and depth of groove of 498.74 µm are obtained with desirability scores of 0.9701 and 0.9972, respectively both very close to the ideal value of 1. The optimal settings for this multi objective optimization plot of input parameters are 28.70% for EC, 30.20 RPM for rotational speed of workpiece and 50.56V for voltage.

6.2 FUTURE SCOPE OF RESEARCH:

The research outcomes will obviously provide valuable guidance to researchers and manufacturing experts for establishing a unique framework for glass micro-machining, focusing on desired machining rates, precision, and other characteristics. Also, there is lot of areas in glass micro-machining require further investigation. Theoretical modeling and simulations can provide deeper understanding into spark formation and material removal mechanisms, leading to better process control. Progress in these areas will expand the applications of micro-machined glass across various industrial applications. The future scopes of present research are as follows:

(i) **The design and development of a microprocessor-controlled tool-feeding system**: An advanced tool-feeding system can be developed to automatically adjust the tool's movement based on real-time conditions such as spark stability, material removal rate, tool wear etc. This will help maintain consistent machining performance and improve accuracy.

(ii) **Approaches of Hybrid Machining for Better Process Performance**: Combining μ-ECDG process with other advanced machining methods like ultrasonic vibration or electrochemical jet-assisted discharge micro-machining can improve control over material removal in specific areas, increasing process accuracy and efficiency.

(iii) **Complex 3D Microstructure Fabrication on Nonconductive Materials:** Integrating new electrode shapes like helical and conical designs on tool holding system can improve control over spark discharge and heat distribution. This will help in creating more accurate micro components. High resolution cameras and plasma diagnostics may be used to study how bubbles form and break down during the process, which plays a key role in micro-machining process.

(iv) **Implementation of AI and ML:** The implementation of artificial intelligence and machine learning algorithms could help predict machining outcomes, thereby ensuring process reliability. Furthermore, Finite Element Analysis (FEA) and Molecular Dynamics (MD) simulations can be employed to examine micro-machining performance and operational conditions in greater detail.

REFERENCES

[1] Basak, I., Ghosh, A., *Mechanism of spark generation during electrochemical discharge machining: a theoretical model and experimental verification*, Journal of Materials Processing Technology, 62, 46-53, 1996.

[2] Ghosh, A., *Electrochemical Discharge Machining: Principle & Possibilities*, Sadhana 22(3), 435-447, 1997.

[3] Bhattacharyya, B., Doloi, B., Sorkhel, S.K., *Experimental investigations into electrochemical discharge machining (ECDM) of non-conductive ceramic materials* Journal of Materials Processing Technology, 95, 145-154, 1999.

[4] Jain, V.K., Dixit, P.M., Pandey, P.M., *On the analysis of the electrochemical spark machining process*, International Journal of Machine Tools & Manufacture, 39, 165–186, 1999.

[5] Kulkarni, A, Sharan, R., Lal, G. K., *An experimental study of discharge mechanism in electro-chemical discharge machining*, International Journal of Machine Tools & Manufacture, 42, 1121–1127, 2002.

[6] Skrabalak, G., Zybura, M,, Skrabalak, Ruszaj A, *Building of rules base for fuzzy-logic control of the ECDM process*, Journal of Materials Processing Technology, 149, 530–535, 2004.

[7] Peng, W.Y. and Liao, Y.S., *Study of electrochemical discharge machining technology for slicing non-conductive brittle materials*, Journal of Materials Processing Technology, 149, 363–369, 2004

[8] Kozak, J., Rajkumar K.P., Makkar,Y., "Study of Pulse Electrochemical Micromachining", Journal of Manufacturing Processes 6-1,pp 7-14,2004.

[9]Mediliyegedara, T.K.K.R., De Silva, A.K.M., Harrison, D.K., McGeough, J.A., *New developments in the process control of the hybrid electro chemical discharge machining (ECDM) process*, Journal of Materials Processing Technology, 167, 338–343, 2005.

[10] Wu¨thrich, R. and Fascio, V., *Machining of non-conducting materials using electrochemical discharge phenomenon—an overview*, International Journal of Machine Tools & Manufacture, 45, 1095–1108, 2005.

[11] Bhondwe, K. L., Yadava, V., Kathiresan, G., *Finite element prediction of material removal rate due to electro-chemical spark machining*, International Journal of Machine Tools & Manufacture. 46, 1699–1706, 2006.

[12] Sarkar, B.R., Doloi, B., Bhattacharyya, B., *Parametric analysis on electrochemical discharge machining of silicon nitride ceramic,* International Journal Advanced Manufacturing Technology, 28, 873-881, 2006.

[13] Kim, D.J., Ahn, Y., Lee, S.H. and Kim, Y.K., *Voltage pulse frequency and duty ratio effects in an electrochemical discharge micro-drilling process of Pyrex glass*, International Journal of Machine Tools & Manufacture, 46, 1064-1067, 2006.

[14] Maillard,P., Despont, B., Bleuler,H., Wuthrich, R., "Geometrical characterization of micro-holes drilled in glass by gravity-feed with spark assisted chemical engraving (SACE)", Journal of micromechanics and microengineering 17, 1343–1349, 2007

[15] Zheng, Z. P., Su, H. C., Huang, F. Y. and Yan, B. H., *The tool geometrical shape and pulse- off time of pulse voltage effects in a Pyrex glass electrochemical discharge microdrilling process*, Journal of Micromechanics & Microengg., 17, 265–272, 2007.

[16] Han, M. S., Min, B. K., Lee, S. J., *Improvement of surface integrity of electro-chemical discharge machining process using powder-mixed electrolyte*, Journal of Materials Processing Technology, 191, 224–227, 2007.

[17] Jain, V. K., Adhikary, S., *On the mechanism of material removal in electrochemical spark machining of quartz under different polarity conditions*, Journal of Materials Processing Technology, 200, 460–470, 2008.

[18] Coteata, M., Slitineanu, L., Dodun, O., Ciofu, C., *Electrochemical discharge machining of small diameter holes*, Int J Mater Form Suppl 1,1327 –1330, 2008.

[19] Chak, S. K. and Rao, P. V., *The drilling of Al2O3 using a pulsed DC supply with a rotary abrasive electrode by the electrochemical discharge process*, International Journal Advanced Manufacturing Technology, 39,633–641, 2008.

[20] Furutani, K. and Maeda, H., *Machining a glass rod with a lathe-type electro-chemical discharge machine*, Journal of Micromechanics & Microengg., 18, 065006 (8pp), 2008.

[21] Han, M. S., Min, B. K. and Lee, S. J., *Geometric improvement of electrochemical discharge micro-drilling using an ultrasonic-vibrated electrolyte*, Journal of Micromechanics & Microengineering, 19, 065004 (8pp), 2009.

[22] Coteaţă, M., Ciofu, C., Slătineanu, L., Munteanu, A. and Dodun, O., *Establishing the electrical discharge weight in electrochemical discharge drilling*, Int J Mater Form, Vol. 2 Suppl 1:673–676, 2009.

[23] Liu, J. W., Yue, T. M., Guo, Z. N., *An analysis of the discharge mechanism in electro chemical discharge machining of particulate reinforced metal matrix composites*, International Journal of Machine Tools & Manufacture, 50, 86–96, 2010.

[24] Yang, C.-K., Cheng, C.-P., Mai, C.-C., Wang, A. C., Hung, J.-C., Yan, B.-H., *Effect of surface roughness of tool electrode materials in ECDM performance*, International Journal of Machine Tools & Manufacture, 50 , 1088–1096, 2010

[25] Cheng C. P., Wu, K. L, Mai, C. C., Yang, C. K., Hsu, Y. S., Yan, B. H., *Study of gas film quality in electro-chemical discharge machining*, International Journal of Machine Tools & Manufacture, 50, 689–697, 2010

[26] Wüthrich, R., Allagui, A., *Building micro and nanosystems with electrochemical discharges*, Electrochimica Acta, 55, 8189–8196, 2010

[27] Yang, C.K., Cheng, C.P., Mai, C.C., Wang, A.C., Hung J.C., Yan, B.H., "Effect of surface roughness of tool electrode materials in ECDM performance", International Journal of Machine Tools & Manufacture 50, 1088–1096,2010

[28] Sankar, A. R., Bindu, V.S.S, Das, S., "*Coupled effects of gold electroplating and electrochemical discharge machining processes on the performance improvement of a capacitive accelerometer"*, Microsyst. Technol, 17, 1661–1670, 2011

[29] Yang, C. K., Wu, K. L., Hung, J. C., Lee, S. M., Lin, J. C., Yan, B. H., *Enhancement of ECDM efficiency and accuracy by spherical tool electrode,* International Journal of Machine Tools & Manufacture, 51, 528–535, 2011

[30] Wei, C., Xu, K., Ni. J., Brzezinski, A. J., Hu, D., *A finite element based model for electrochemical discharge machining in discharge regime*, International Journal Advanced Manufacturing Technology, 54, 987–995, 2011

[31] Wei, C., Hu, D., Xu, K., Ni, J., *Electro-chemical discharge dressing of metal bond micro-grinding tools,* Inter. Journal of Machine Tools & Manuf., 51, 165–168, 2011

[32] Ziki, J.D., Didar, T.F, Wuthrich, R., *Micro-texturing channel surfaces on glass with spark assisted chemical engraving*, International Journal of Machine Tools & Manufacture, 57, 66-72, 2012

[33] Cao, X. D., Kim, B. Y. and Chu, C. N., *Hybrid Micromachining of Glass using ECDM and Micro Grinding*, International Journal of Precision Engineering and Manufacturing, 14 (1), 5-10, 2013

[34] Jiang, B., Lan, S., Ni, J., Zhang, Z., *Experimental investigation of spark generation in electrochemical discharge machining of non-conducting materials,* Journal of Materials Processing Technology, 214, 892– 898, 2014

[35] Huang, S. F., Liu, Y., Li, J., Hu, H. X., Sun, L. Y., *Electrochemical Discharge Machining Micro-Hole in Stainless Steel with Tool Electrode High-Speed Rotating*, Materials and Manufacturing Processes, 29, 634–637, 2014

[36] Singh T., Dvivedi A., *Developments in electrochemical discharge machining. A review on electrochemical discharge emachining process variants and their hybrid methods,* International Journal of Machine Tools & Manufacture 105, 1–13, 2016

[37] Furutania K., Kojimaa S., *Prototyping of Acceleration Sensor by Using Lathe-type Electro-chemical Discharge Machine*, Procedia CIRP, 42, 772 – 777, 2016

[38] Guo D, Wu X., Lei J., Xu B., Kometani R., and Luo F., *Fabrication of micro/nanoelectrode using focused-ion-beam chemical vapor deposition, and its application to micro-ECDM*, Procedia CIRP ,42, 733 – 736, 2016

[39] Liu Y., Wei Z., Wang M., Zhan J., *Experimental investigation of micro wire electrochemical discharge machining by using a rotating helical tool*, Journal of Manufacturing Processes 29, 265–271,2017

[40] Mehrabia F., Farahnakiana M., Elhamib S., Razfarb M. R., *Application of electrolyte injection to the electro-chemical discharge machining (ECDM) on the optical glass,* Journal of Materials Processing Tech. 255, 665–672, 2018

[41] Xu Y., Chen J., Jiang B., Liu Y., Ni J., *Experimental investigation of magnetohydrodynamic effect in electrochemical discharge machining*, International Journal of Mechanical Sciences 142–143, 86–96,2018

[42] Arya R. K., Dvivedi A., Investigations on quantification and replenishment of vaporized electrolyte during deep micro-holes drilling using pressurized flow-ECDM process, Journal of Materials Processing Tech.,266,217–229,2019

[43] Arab J., Mishra, D. K., Kannojia, H. K., Adhale, P., & Dixit, P., *Fabrication of multiple through-holes in non-conductive materials by Electrochemical Discharge Machining for RF MEMS Packaging.* Journal of Materials Processing Technology, 271, 542-553, 2019

[44] Singh,T., Dvivedi,A., Arya, *R.K., "Fabrication of micro-slits using W-ECDM process with textured wire surface: An experimental investigation on kerf overcut reduction and straightness improvement",* Precision Engineering, 59, 211-223, 2019

[45] Ji, B., Tonga H., Li,J., Li, Y., Xu, M., *"Scanning process of spark assisted chemical engraving (SACE) on ZrO2 ceramics by constraining discharges to tool electrode end",* Ceramics International, 46,1433-1441, 2020

[46] Singh,T., Dvivedi, A., "*Fabrication of micro holes in Yttria-stabilized zirconia (Y-SZ) by hybrid process of electrochemical discharge machining (ECDM)",* Ceramics International, 47, 23677–23681,2021

[47] Kang, X., Tang,W.,Zhao,W., Qian,J., Lauwers,B., *"Experimental and numerical investigations of material removal process in electrochemical discharge machining of glass in discharge regime",* Precision Engineering, 72, 706–716,2021

[48] Arab, J., Mishra, D.K., Dixit,P., *"Measurement and analysis of the geometric characteristics of microholes and tool wear for varying tool-workpiece gaps in electrochemical discharge drilling"* Measurement, 168, 108463, 2021

[49] Bhargav, K.V.J., Shanthan, P., Balaji, P.S., Sahu, R.K., Sahoo, S.K., *"Generation of microholes on GFRP composite using ES-μ-ECDM system"*, CIRP Journal of Manufacturing Science and Technology, 38, 695-705,2022

[50] Appalanaidu,B., Dvivedi,A., *"On the use of sacrificial layer in ECDM process for form accuracy",* Journal of Manufacturing Processes, 79, 219–232, 2022

[51] Santra, S., Sarkar, B.R., Doloi, B., *"Investigation on electrochemical discharge milling by side feeding technique",* Materials Today: Proceedings, 62, Part 12, 6438-6444, 2022

[52] Nawaz, S.A., Cao, P., Tong, H., Li,Y., *"Micro ECDM scanning process with feedback control of flexible contact force",* Journal of Manufacturing Processes, 94, 266–277,2023

[53] Mandal, N., Kumar, N., Das, A.K.,*"Powder mixed electrochemical discharge process for micro machining of C103 niobium alloy",* Defence Technology, 26, 84-101,2023

[54] Lu, J., Guan, J., Dong, B., Zhao,Y., *"Control principle of anodic discharge for enhanced performance in jet-electrochemical discharge machining of semiconductor 4H-SiC"* Journal of Manufacturing Processes, 92, 435–452, 2023

[55] Wang,T., Liu,Y., Wang,K., Lv,Z., "*Investigation on a sustainable composite method of glass microstructures fabrication—Electrochemical discharge milling and grinding (ECDM-G)",* Journal of Cleaner Production, 387,135788, 2023

[56] Chen, Z.,, Liu,Y., Wang,T., Wang,K., "*Ultrasonic assisted electrochemical discharge milling of complex glass microstructure with high-quality*", Journal of Manufacturing Processes, 94, pp. 94-106, 2023

[57] Zou,Z., Chan,K., Qiao,S.,Zhanga,K., Yueb,T., Guo, Z., Liu,J., 2023, *"Electrochemical discharge machining of a high-precision micro-holes array in a glass wafer using a damping and confinement technique"*, Journal of Manufacturing Processes, 99,152–167, 2023

[58] Kong, H., Qu, N., Chen, J., *"Machining behaviour modulation of electrochemical milling via manipulation of inter-electrode gap: From electrochemical machining to electrochemical discharge machining",*Journal of Materials Processing Tech.,333, 118584, 2024

[59] Mhahe, F.B., Zhang,Y., Chen,C., Umoren,W.I.,*"Investigation of the influence of different types of electrolytes on the performance of the Electrochemical Discharge Machining process during micromachining of molybdenum",* International Journal of Electrochemical Science,19, 100647, 2024

[60] Li,Q., Yu,J., Zhao, C., Dai,W., Zhang,J., Guo,C., Yue ,H., *"Experimental and numerical investigations into the fabrication of alumina ceramic surface microchannel by electrochemical discharge machining",* Ceramics International, 50, 19202–19216, 2024

[61] Shen,J., Zeng,Y., Zhang,R., Kong,W., *"Effect of discharge thermal action in ECDM on electrochemical behaviours of matrix material and its recast layer in glycol-based solution"* Corrosion Science, 241,112525,2024.

[62] Bahar,D., Dvivedi,A., Kumar,P., "*Optimizing the quality characteristics of glass composite vias for RF-MEMS using central composite design, metaheuristics, and bayesian regularization-based machine learning"* Measurement; 243, 116323, 2025

[63] Masuzawa, T., and Toenshoff, K.K., "*Three-dimensional micromachining by machine tools*", Annals of the CIRP-Manufacturing Technology, 46, 621-628,1997

[64] Masuzawa, T., "*State of the art of micromachining*", Annals of the CIRP-Manufacturing Technology, 49(2), 473-488, 2020

[65] Chatti, S., and Tolio, T., *CIRP Encyclopedia of Production Engineering*, Springer Berlin, Heidelberg, 2022

[66] Rawal, S., Sidpara A.M., Paul, J., "*A review on micro machining of polymer composites*, Journal of Manufacturing Processes"*,* 77, 87-113, 2022

[67] Sarkar, B. R., Doloi, B., and Bhattacharyya, B., "*Investigation into the Influences of the Power Circuit on the Micro-Electrochemical Discharge Machining Process,*" Proc. Inst. Mech. Eng. Part B, 223(2), 133–144, 2009

[68] Jain, V.K., and Adhikary, S., *On the mechanism of material removal in electrochemical spark machining of quartz under different polarity conditions,* Journal of Materials Processing Technology, 200, 460–470, 2008.

[69] Sarkar, B.R., Doloi B., Bhattacharyya, B., *Experimental investigation into electrochemical discharge micro drilling on advanced ceramics.* Int. J. Manufacturing Technology and Management, 13(2/3/4), 214–225.2008.

[70] Goud, M., Sharma, A.K., "*A three-dimensional finite element simulation approach to analyze material removal in electrochemical discharge machining",* Proceedings of the

Institution of Mechanical Engineers Part C Journal of Mechanical Engineering Science 1989-1996 (vols 203-210) 231(13), 2016

[71] Yadav,R.N, *"Electro-chemical spark machining–based hybrid machining processes: Research trends and opportunities*", Proceedings of the Institution of Mechanical Engineers, Part B: Journal of Engineering Manufacture,233 (4), 1037-1061, 2018

ASME Journal of Micro- and Nano-Manufacturing
Online journal at:
https://asmedigitalcollection.asme.org/micronanomanufacturing

Micro-Channel Cutting on Glass in Electrochemical Discharge Machining Process Using Different Electrolytes and Tool Polarity

M. N. Ali
Production Engineering Department,
Jadavpur University,
Kolkata 700032, India
e-mail: mnali.jupe@gmail.com

B. R. Sarkar
Production Engineering Department,
Jadavpur University,
Kolkata 700032, India
e-mail: sarkarbiplab_s@rediffmail.com

B. Doloi
Production Engineering Department,
Jadavpur University,
Kolkata 700032, India
e-mail: bdoloionline@rediffmail.com

B. Bhattacharyya
Production Engineering Department,
Jadavpur University,
Kolkata 700032, India
e-mail: bb13@rediffmail.com

Microchannel cutting on electrically nonconducting materials with electrochemical discharge machining (ECDM) process has drawn a momentous attention in manufacturing field as compared to other existing nontraditional machining processes. In the present research work, an effort has been accomplished to investigate the effects of process parameters, namely, applied voltage (V), electrolyte concentrations(wt%), pulse frequency, and duty ratio on different performance characteristics of ECDM viz., material removal rate (MRR), overcut (OC) and heat-affected zone (HAZ) area during microchannel cutting on glass. Also, the comparative performance studies during microchannel cutting have been done by using mixed electrolyte of NaOH and KOH and different tool polarities. Overcut is measured as lower (42.26 μm) when aqueous KOH electrolyte is used and as higher (133.44 μm) for aqueous NaOH electrolyte. HAZ enlarges with enrichment in concentration for both types of electrolyte. It is observed that polarity has a vital role on various machining characteristics. As compared to direct polarity, MRR is found very low (3.2 mg/h) in reverse polarity of tool. Overcut is found low in KOH electrolyte for both types of tool polarity (i.e., 64.68 μm for direct polarity and 42.27 μm for reverse polarity). The process parameters influence on the surface texture of microchannels. Microcrack is noticed for direct polarity of tool. [DOI: 10.1115/1.4065326]

Keywords: ECDM, micro-channel, mixed electrolyte, polarity, MRR, overcut, HAZ, glass

1 Introduction

Recent changes in society lead to the usage of highly sophisticated manufacturing materials like composites, polymers, fiber-glasses, metallic-glasses, and biomaterials. Advanced machining processes are also necessary to produce the products with these materials due to their favorable characteristics. But, there are limitations of the available processes. For example, micro-ultrasonic machining has certain intrinsic disadvantages such as tool wear, high investment cost, and bending of tool. Micro-laser beam machining is another advanced process, which involves high investment cost and creation of very wide unwanted heat affected zone. Microcutting with abrasive water jet machining is also dangerous and troublesome because of its traverse cutting speed. Then micro-electrochemical discharge machining (micro-ECDM) appears as the contemporary alternative machining method that works on thermo-chemical phenomena and is used to create microhole and microchannel on various electrically conducting and nonconducting materials like composites, polymers, fiber-glass, metallic-glass, and biomaterials.

The basic mechanism of removing materials in micro-ECDM process is entirely similar to ECDM or ECSM or SACE [1–5]. In this process, two electrodes of different size and shape along with workpiece material are submerged normally in an aqueous alkaline electrolyte. Here, the tool is connected as positive electrode and another electrode (auxiliary electrode) is connected as anode to complete the electrical circuit since the workpiece material is an electrically nonconducting. These electrodes get power supply from a DC source. ECDM process works on the principle of electrode effects. The gas film isolates one electrode from its adjacent electrolyte. This type of gas film is formed whenever the current starts to flow in the electrolyte solution. When DC power is switched on, the electrolysis begins and if the imposed voltage exceeds its threshold value, the gas bubbles begin to combine to form an insulating film layer nearby cathode electrode. As a result, a high electric field grows across the film layer. Then spark discharge is initiated across the gas film near the tool-electrode. If the workpiece material is kept very near to the cathode, unwanted material is removed from the workpiece material due to melting and vaporization.

Sarkar et al. [6] developed a nonlinear model of second-order based on response surface methodology to analyze the effects of different input parameters on various response characteristics associated with ECDM process. West and Jadhav [7] documented

Contributed by the Manufacturing Engineering Division of ASME for publication in the Journal of Micro- and Nano-Manufacturing. Manuscript received August 13, 2023; final manuscript received January 31, 2024; published online May 31, 2024. Assoc. Editor: Sylvie Castagne.

Electrochemical Discharge Machining Technology Applied for Turning Operation

M N Ali[1], B Doloi[2], B R Sarkar[3]

[1] Mechanical Engineering Department, Netaji Subhash Engineering College, Kolkata-152, India
[2-3] Production Engineering Department, Jadavpur University, Kolkata-32, India

Email: mnali.jupe@gmail.com

Abstract. In hybrid electrochemical discharge machining (ECDM) process machining of electrically conducting and non-conducting materials takes place in an alkaline electrolyte with the introduction of a tool electrode and an auxiliary electrode. In this paper an alternative of ECDM process, Electrochemical Discharge Turning (ECDT), is proposed to machine a cylindrical job which rotates continuously against a stationary or moving tool electrode. The material removal mechanism of ECDT process is similar to ECDM process, but ECDT employs ECDM components with rotary cylindrical workpiece immersed in an electrolytic solution. The present paper highlights the design and development of ECDT set-up which can be applied for turning operation. The proposed ECDT set up can also be utilized for making grooves of different shapes and sizes on cylindrical parts of electrically non-conducting materials.

1. Introduction

The limitations of conventional machining process in the area of complex shapes, miniature sizes, three dimensional (3D) complex parts and the need of machining of brittle harder and newer materials lead to the development and establishment of non-conventional machining processes in the industry as efficient and economic alternatives to conventional machining processes. Demand and need of research in these areas are also growing to develop precise understanding and knowledge of different aspects. Electrochemical Discharge Turning (ECDT), an alternative process of ECDM process, can be used to machine a cylindrical job in which job rotates continuously. The material removal mechanism of ECDT process is similar to ECDM process but ECDT employs ECDM components with rotary cylindrical workpiece immersed in an electrolytic solution. Sarkar *et al*. [4] studied the parametric analysis of ECDM process on silicon nitride ceramics. Furutani *et al*. [5] studied the performance of lathe type ECDM process for machining of glass rod revolving in an electrolyte as a working fluid. Singh *et al.* [9] developed ECDM based triplex hybrid methods and presented machined features with its com-

Md. Niamat Ali

Presented and accepted for publication in the Proceedings of 13th International Conference on Precision, Micro, Meso and Nano Engineering (COPEN 13), NIT Calicut, December 13-15, 2024.

Experimental Investigation on Electrochemical Discharge Micro-Grooving of Glass

Md Niamot Ali [a], Biplab Ranjan Sarkar[b], Biswanath Doloi[c] ,Bijoy Bhattacharyya[d]

[a b c d]Jadavpur University, Production Engineering Department, Kolkata-700032, India

* Corresponding author e-*mail address:* mnali.jupe@gmail.com

Abstract: Electrochemical Discharge Micro-Grooving (µ-ECDG) is an advanced hybrid machining process capable of producing micro-grooves and profiles on any cylindrical workpiece, regardless of its hardness or toughness. An experimental setup of µ-ECDG was first designed and developed to conduct all the experiments. This research study aims to investigate the impact of different input process variables, including electrolyte concentration, rotational speed of workpiece and voltage on various machining responses, such as Material Removal Rate (MRR) and Width of Groove (WG). All the experiments were conducted using a direct polarity in a KOH electrolyte solution. The micro-groove was produced on a cylindrical glass workpiece by rotating it against a stationary µ-tool electrode of 280 µm diameter. Microscopic views of micro-grooves were measured and analysed to study the impact of above mentioned variables. High spark discharge intensity was observed when voltage and electrolyte concentration exceeded 50 V and 20 wt% respectively. As the electrolyte concentration and voltage increased, both MRR and WG raised, but these values decreased significantly with a higher rotational speed of the workpiece.

Keywords: µ-ECDG, Micro-Groove, MRR, Width of Groove, Glass

1. Introduction

The fast-paced development of advanced manufacturing technology requires the creation of innovative machining processes that can satisfy the high precision and efficiency requirements of numerous industries. Electrochemical Discharge micro-Grooving (µ-ECDG) is a newly developed machining process that can be used for grooving and micro-profile generation of any hard and brittle, electrically non-conducting material of cylindrical shape. µ-ECDG is a triplex hybrid machining process that effectively combines the fundamentals of ECM (Electrochemical Machining), EDM (Electrical Discharge Machining) and grooving process to achieve precise and excellent surface quality. In µ-ECDG process, workpiece is rotated with an angular speed against a micro-tool which is fitted to a XZ stage. Both longitudinal and cross feed can be given to tool by means of a spring feed mechanism. Basak [1] et al. studied the mechanism of spark in ECDM process and tried to improve the process capability with the help of mathematical model. Ghosh [2] documented that spark in ECDM process was mainly because of switching phenomenon. Bhattacharyya et al. [3] investigated the material removal mechanism in ECDM process and successfully machined electrically non-conducting ceramic like Al_2O_3. Sarkar *et al.* [5] developed a mathematical

Md. Niamot Ali

Presented and accepted for publication in AIMTDR 2023 Proceedings Volume3: Advances and Futuristic Trends in Machining Volume I, Proceedings of 9th International and 30th All India Manufacturing Technology, Design and Research Conference (AIMTDR 2023), IIT BHU, Varanasi, India, December 08-10, 2023.

Experimental Investigation into Electrochemical Discharge Turning of Cylindrical Glass

Sudip Santra[1*], Dwarika Pratap Singh[2], M.N. Ali[3], Biswanath Doloi[4], Biplab Ranjan Sarkar[5]
Jadavpur University, Production Engineering Department, Kolkata-700032
sudip16santra@gmail.com

Abstract. Electrochemical Discharge Turning (ECDT) represents a cutting-edge machining technique that synergizes the fundamentals of electrochemical machining and electrical discharge machining. This innovative method offers a distinctive avenue for precisely machining hard and brittle materials, such as ceramics, glass, and composites, which pose considerable challenges when employing conventional machining approaches. This study delves into the feasibility of employing Electrochemical Discharge Turning (ECDT) for both grooving and turning of glass rods. ECDT exhibits the potential for attaining exceptional precision and accuracy while crafting cylindrical geometries across diverse materials. The applied voltage, electrolyte concentration and revolution of the workpiece were altered during the experimentation using a cylindrical tool electrode. The overarching goal of this research endeavour is to find out better ECDT process parameters to achieve a commendable material removal rate (MRR) while simultaneously enhancing groove width.

Keywords: ECDM, ECDT, Cylindrical Glass, MRR, Groove.

1 Introduction

Electrochemical Discharge Turning (ECDT) is a proficient machining technology to remove materials from electrically non-conductive materials. The machining process consists of two electrodes separated by a distance and immersed into an electrolyte. Following the application of voltage across two electrodes, the electrolysis process commences, leading to the formation of gas bubbles that gather around the tool electrode, resulting in the creation of an insulating gas film. Beyond a specific voltage threshold, this gas film destabilizes and triggers spark discharge, effectively removing material from the workpiece situated close to the spark discharge zone. Basak et al. **[1]** developed a theoretical model for electrochemical discharge accurately estimating critical voltage and current. The simplified idealistic mechanism provided reasonably accurate discharge onset conditions, supported by experimental data. Bhattacharyya et al. **[2]** investigated the machining of ceramics and analyzed the electrochemical process during the process. Wuthrich et al. **[3]** developed an experimental method to measure gas film thickness using current-voltage characteristics, improving machining reproducibility. They found that changing tool electrode wettability and adding liquid soap to the electrolyte enhanced machining precision to better than 5µm. Thinner gas films led to less variation and more consistent machining, accompanied by a lower critical voltage requirement. Jain et al. **[4]** compared two Electrochemical Spark Machining (ECSM) methods for cutting quartz. ECSM with reverse polarity cut faster but had drawbacks like overcut, increased tool wear, and rougher surfaces. They also noted the dissolution of quartz into NaOH solution and the importance of electrode

Md. Nizamat Ali

Presented in International Conference on Advances in Materials and Manufacturing Engineering (ICAMME 2019), organised by KIIT, Bhubaneshwar during March 15- 17, 2019.

Electrochemical Discharge Machining Technology Applied for Turning Operation

M.N. Ali[1], B. Doloi[2][0000-0003-3601-2452], B. R.Sarkar[3][0000-0002-8965-9893]

[1]Mechanical Engineering Department, Netaji Subhash Engineering College, Kolkata-152
[2-3]Production Engineering Department, Jadavpur University, Kolkata-32

[1]*mnali.jupe@gmail.com*,[2]*bdoloionline@rediffmail.com*,[3]*sarkarbiplab_s@rediffmail.com*

Abstract. In conventional electrochemical discharge machining (ECDM) process machining of electrically non-conducting materials takes place in an alkaline electrolyte, with the introduction of a tool electrode and a counter electrode. In this paper an alternative of ECDM process, Electrochemical Discharge Turning (ECDT), is proposed to machine a cylindrical job which rotates continuously against a stationary or moving tool electrode. The material removal mechanism of ECDT process is similar to ECDM process but ECDT employs ECDM components with rotary cylindrical workpiece immersed in an electrolytic solution. The present paper highlights the design and development of ECDT set-up which can be applied for turning operation. The proposed ECDT set up can also be utilized for making grooves of different shapes and sizes on cylindrical parts of electrically non-conducting materials.

Keywords: ECDM, Electrochemical Discharge Turning

1 Introduction

The limitations of conventional machining process in the area of complex shapes, miniature sizes, three dimensional (3D) complex parts and the need of machining of brittle harder and newer materials lead to the development and establishment of non-conventional machining processes in the industry as efficient and economic alternatives to conventional machining processes. Demand and need of research in these areas are also growing to develop precise understanding and knowledge of different aspects. Electrochemical Discharge Turning (ECDT), an alternative process of ECDM process, can be used to machine a cylindrical job in which job rotates continuously. The material removal mechanism of ECDT process is similar to ECDM process but ECDT employs ECDM components with rotary cylindrical workpiece immersed in an electrolytic solution. Sarkar *et al. (2006)* studied the parametric analysis of ECDM process on silicon nitride ceramics. Furutani *et al. (2008)* studied the performance of lathe type ECDM process for machining of glass rod revolving in an electrolyte as a working fluid. Singh *et al. (2016)* developed ECDM based triplex hybrid methods and presented machined features with its complexity and accuracy level. Furutani *et al. (2016)* constructed the control method of the electrode feeding for machining of a thin rod with the lathe-type ECDM process and showed the application to a fine part fabrication. Sabahi *et al. (2017)* showed that the presence of surfactant in electrolyte helped in improvement of the material removal rate (MRR), accuracy, heat affected

Md. Niamat Ali.

22/07/2025

Professor
Production Engineering Department
Jadavpur University
Kolkata - 700 032

22/07/25

Professor
Production Engineering Department
Jadavpur University
Kolkata - 700 032